ISSMGE Technical Committee TC 209
Offshore Geotechnics

Proceedings of TC 209 workshop

19th ICSMGE - Seoul, 20 September 2017

Foundation Design of Offshore Wind Structures

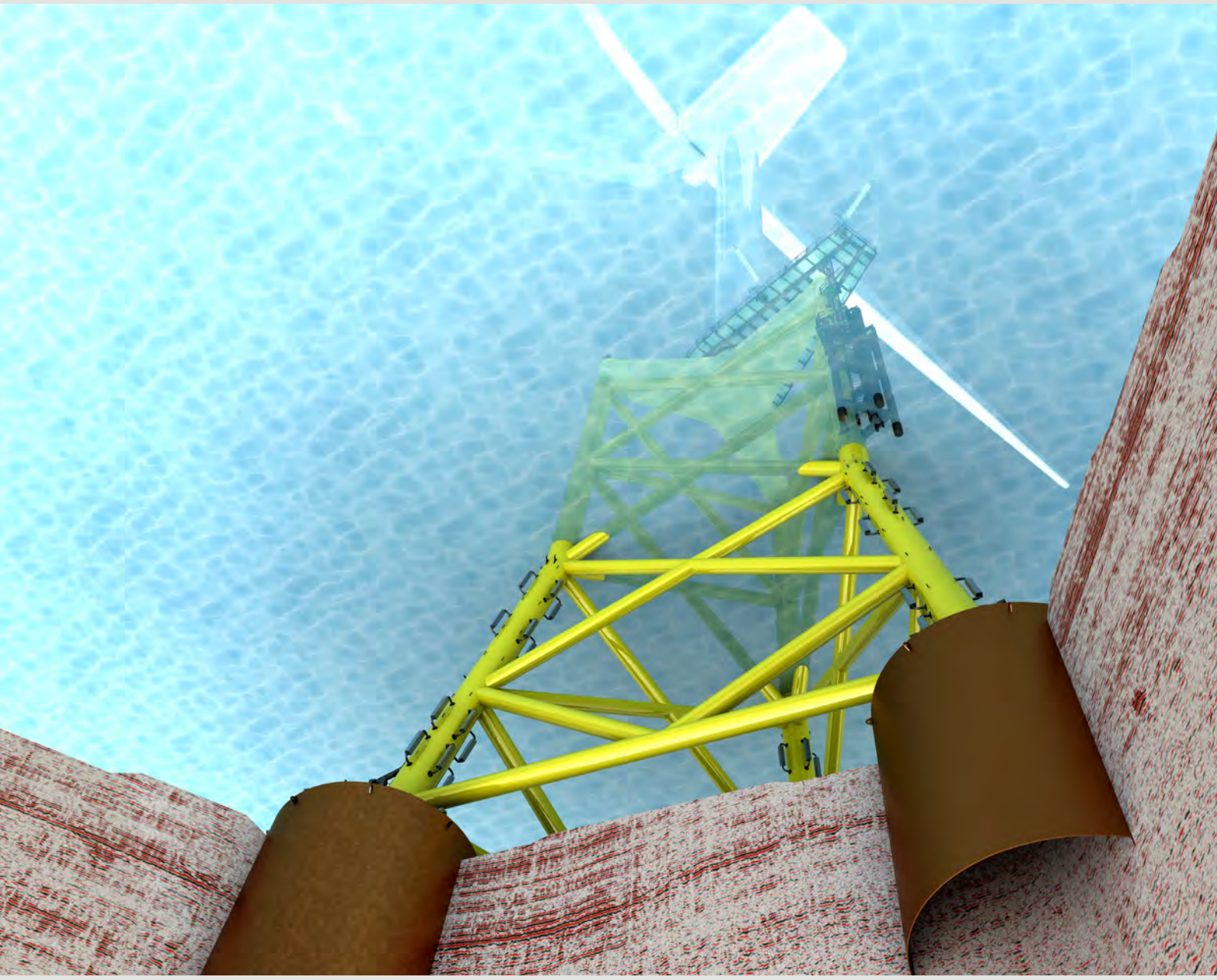

Edited by: Yunsup Shin

ISSMGE Technical Committee TC 209
Offshore Geotechnics

Proceedings of TC 209 workshop

19th ICSMGE - Seoul, 20 September 2017

Foundation Design of Offshore Wind Structures

Edited by: Yunsup Shin

NGI

SIMSG ISSMGE

NGI

ON SAFE GROUND | NGI.NO

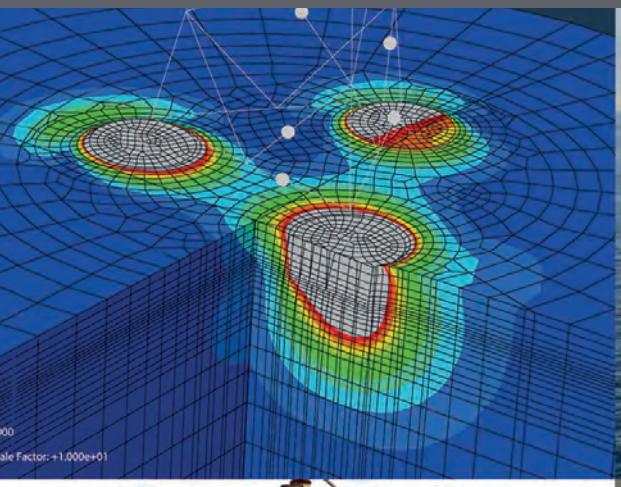

Integrated Geotechnical Services

We research and develop solutions for both industry and society, ensuring that we live, build and travel on safe ground. NGI has more than 60 years experience in geotechnical engineering, both onshore and offshore, including:

- Site characterization including advanced laboratory testing of soil and rock
- Advanced numerical modelling and finite element analysis
- Instrumentation and monitoring for complex geotechnical and structural applications
- Foundations for long-span bridges and strait crossings
- Deep excavations for infrastructure and buildings
- Offshore foundations and anchoring solutions, including suction caissons for offshore wind
- Natural hazards, including slope stability, debris flow, earthquakes and tsuanmis

NGI | Oslo

PO Box 3930 Ullevaal Stadion,
N-0806 Oslo
Sognsvn. 72, N-0855 Oslo
Norway

+47 22 02 30 00
ngi@ngi.no

NGI | Houston

10615 Shadow Wood Dr,
Suite 100,
Houston TX 77043
USA

+1 281 752 4667
houston@ngi.no

NGI | Perth

PO Box 5667,
Perth, WA 6831
Level 7, 40 St Georges Terrace,
Perth, WA 6000

+61 8 6141 3141
perth@ngi.no

NGI present at ICSMGE conference in Seoul:
www.ngi.no/ICSMGE2017

#onsafeground

Foreword

The International Society for Soil Mechanics and Geotechnical Engineering (ISSMGE) and its Technical Committee 209 (TC209) on Offshore Geotechnics are proud to support this workshop and the publication of this volume.

The theme for this workshop is "*Foundation design of offshore wind structures*".

The offshore wind industry is expanding rapidly throughout Asia. Projects are currently being developed in China, Taiwan and South Korea, with many other countries aggressively pursuing opportunities in this market sector. Cost reductions driven by a mature European market and local pricing, combined with the social benefits of generating power offshore and away from densely populated areas, makes offshore wind an attractive economic prospect for meeting national renewable energy targets.

It is with the market situation in mind that TC209 decided to make offshore wind the focus of this workshop. The workshop comprises a series of carefully selected papers, each representing different subjects – and all addressing aspects of foundation design.

First is a review of the offshore wind market in Korea, honouring our hosts for this workshop, and providing an interesting backdrop to past and future developments. The second paper provides an overview of the need for high quality site characterisation in support of efficient foundation design. The third and fourth papers present technical summaries of the key design challenges for monopile and suction caisson foundations, when used to support wind turbines. Finally, results from an instrumented jacket supported on suction buckets are presented in detail – adding valuable observations of actual performance, to enhance future design.

I trust that you will find the workshop both interesting and of strong technical merit.

ISSMGE TC209 is grateful to Norwegian Geotechnical Institute (NGI) for funding the publication of this volume; to all the authors for sharing their passion, knowledge and experience; and to the team who coordinated the preparation of this workshop, especially Dr Yunsup Shin.

Phil Watson
Incoming Chair, ISSMGE TC-209 on Offshore Geotechnics

Editorial address

This Technical Committee 209 workshop at 19th International Conference on Soil Mechanics and Geotechnical Engineering (ICSMGE) follows the success of the previous workshop in Paris 2013.

Offshore wind farms are constructed in many parts of the world, and many more are being planned, inlcuding in Korea. Foundation design is an essential part of the design of the offshore wind structures, and this TC209 workshop has placed focus on several of the important foundation design aspects, i.e. marine site characterization, foundation design and installation considerations for various foundation types (such as monopiles and suction caisson foundations), and case histories of already installed structures. The offshore wind plan and strategy in Korea is also presented.

NGI is proud to sponsor this edition of the TC 209 Workshop Proceedings which includes:

- "Geotechnical perspective on offshore wind plan, strategy, projects and research in Korea" prepared by Bae K.T. (DAEWOO E&C), Choo Y.W. (Kongju National University), Youn H.J. (Hongik University), Kim J.Y., Choi C.H. (KICT), and Kwon O.S. (KIOT) on behalf of Energy Plant Technical Committee in Korea Geotechnical Society;
- "Marine site characterisation and its role in wind turbine geotechnical engineering" prepared by Rattley M., Salisbury R., Carrington T., Erbrich C., and Li G. (Fugro);
- "Design aspects for monopile foundations" prepared by Burd H. J., Byrne B. W., McAdan R. A., Houlsby G. T., Marten C. M., Beuckelaers W. J.A.P. (Oxford University), Zdravković L., Taborda D.M.G., Potts D. M., Jardine R. J. (Imperial College), Gavin K., Doherty P., Igoe D. (Formerly University College Dublin), Gretlund J. S., Andrade M. P., and Wood A. M. (DONG Energy) on behalf of PISA team;
- "Design Aspects of Suction Caissons for Offshore Wind Turbine Foundations" prepared by Sturm H. (NGI);
- "Suction bucket jackets for offshore wind turbines: applications from in situ observations" prepared by Shonberg A., Harte M., Aghakouchak A., Brown C. S. D., Andrade M. P., and Liingaard M. A. (DONG Energy)

We believe that the papers collected in a single publication will provide the offshore geotechnical engineers with unique and useful information and recommendations for designing offshore wind foundations.

We thank Marit Støvne (NGI) for her editorial assistance, Maren Kristine Johnsen (NGI) and Kjell Hauge (NGI) with graphical design and webpage development. We are also grateful for the helpful advice from Philippe Jeanjean (BP), Phil Watson (Fugro), Knut Andersen (NGI), Thomas Langford (NGI), and Hendrik Sturm (NGI) with respect to planning of the workshop.

Yunsup Shin

Norwegian Geotechnical Institute

September 2017

Table of contents

Geotechnical perspective on offshore wind plan, strategy, projects, and research in Korea

Le plan, la stratégie, les projets, et la recherche des éoliennes en mer en Corée, d'un point de vue géotechnique

Kyung-Tae Bae
Chair of Energy Plant Technical Committee, Korean Geotechnical Society
Daewoo Institute of Construction Technology, DAEWOO E&C, Republic of Korea

Yun Wook Choo
Secretary of Energy Plant Technical Committee, Korean Geotechnical Society
Dept. Civil & Env. Eng., Kongju National University, Republic of Korea, ywchoo@kongju.ac.kr

Heejung Youn
School of Urban and Civil Eng., Hongik University, Republic of Korea

Jin Young Kim & Changho Choi
Korea Institute of Construction Technology, Geotechnical Engineering Research Institute, Republic of Korea

Osoon Kwon
Coastal Disaster Prevention Research Center, Korea Institute of Ocean and Technology, Republic of Korea

ABSTRACT: This paper introduces the results and current status of the Korean offshore wind technology development from the viewpoint of geotechnical engineering. First, Korea's offshore wind resources and geographical/geotechnical conditions are introduced, followed by construction records for offshore wind farms development, and the research and development projects of the substructure for offshore wind turbine installation.

RÉSUMÉ : Cet article présente les résultats et l'état actuel du développement de la technologie éolienne en mer coréenne du point de vue de l'ingénierie géotechnique. En premier lieu, les ressources éoliennes en mer en Corée et les conditions géographiques/géotechniques sont présentées, suivies des archives de construction pour le développement de parcs éoliens en mer et des projets de recherche et développement de la sous-structure pour l'installation d'éoliennes en mer.

KEYWORDS: Korea, wind energy resource, geological conditions, construction records, research and development.

1 INTRODUCTION

Along with the greenhouse gas mandatory reduction goals set forth in the Kyoto Protocol in 1997, Korean government has established a new and renewable energy policy and, in addition, conducted research and development projects as well as pilot projects led by the public sector.

Among various renewable energy sources, wind power is known as an energy source that meets the geographical/ geotechnical conditions of the Korean Peninsula (MOTI and KEA, 2016). From a geographical point of view, onshore wind power has a very great advantage in the mountainous region where the northwest wind develops, and offshore wind power has a great advantage in terms of the effective transportation and utilization of production power, since the three sides of the Korean Peninsula are surrounded by the sea and the mega-cities (Seoul, Busan, Incheon etc.), which are major energy consumers, are located at the coastal line of Korea.

Heavy Industries already have great technological capabilities and infrastructure for the design, manufacture, and installation of wind power generation facilities and support structures. It is attributed to the abundant technological capabilities of the shipbuilding/marine industry and the established supply chains for production of the wind power plant. However, because the environmental damage caused by installing onshore wind power generator is rising and there are local limitations on generator installations in such a small country, interest in offshore wind power has been increasing, and the relevant research, development, and projects have been carried out.

In this paper, the past records, progress and current status of the offshore wind technology development in Korea is presented from the geotechnical engineering perspective. The structure of this paper is as follows: Section 2 introduces Korea's offshore wind resources and geographical/geotechnical conditions. Section 3 introduces the construction performance of the offshore wind farms development. Finally, Section 4 introduces the research and development projects of sub-structure technologies for offshore wind turbine installation.

2 WIND ENERGY RESOURCE AND GEOLOGICAL CONDITIONS

2.1 *Wind energy resources*

Domestic offshore wind potential capacity is estimated to be 426 GW and technically feasible capacity is estimated to be 33.2 GW (MOTI and KEA, 2016). This corresponds to 17.8% of the total power generation in Korea. Although Korea is a peninsula surrounded by sea with abundant offshore wind resources, all resources cannot be utilized due to economic and technological limitations; furthermore, the offshore wind farms

are constructed considering wind speed, wind density and water depth.

Figure 1 shows the domestic weather map provided by the meteorological resources map (www.greenmap.go.kr). The wind speed measured at 80 m above the ground is about 7.0-7.5 m/s near the Western coast, mostly 7.5 m/s or above at the coasts of Jeju Island, and 8.5 m/s or above in other areas.

Since the offshore wind farm becomes economically inferior at 30 m sea level or above, the East Sea, where the water depth drastically deepens as it gets farther from the coast, is considered to be inappropriate despite its satisfactory wind speed, and the Southwest Sea and Jeju Island coastal areas with moderate changes in water depth are evaluated as suitable sites for offshore wind farms. Typical water depths for the developing or soon-to-be-developed offshore wind farms are 10-20 m.

As shown in Figure 2, the main wind direction in the area considered as potential sites for offshore wind farm power, is the northwest. This major northwest wind is mixed with the northeast wind in the waters near Jeju Island and southwest coast. The wind turbine power generation efficiency is improved when the wind speed of 5 m/s or more is maintained, and the number of days with wind speed of 5 m/s or more is measured to be approximately 55% of the year in the west coast and 65% or more in the coastal area near Jeju Island.

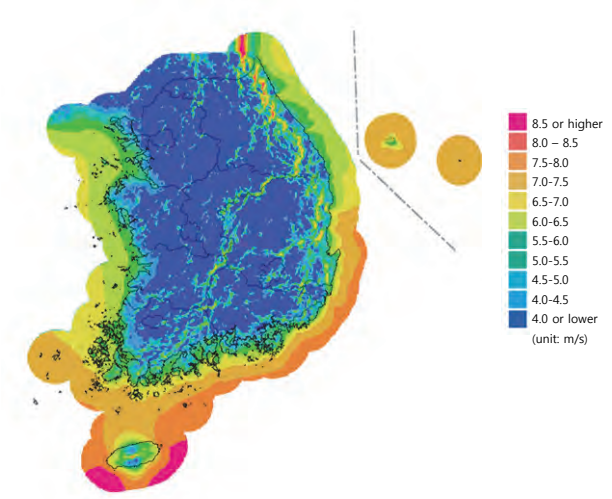

Figure 1. Wind speed map at the elevation of 100 m from sea level (modified from www.greenmap.go.kr).

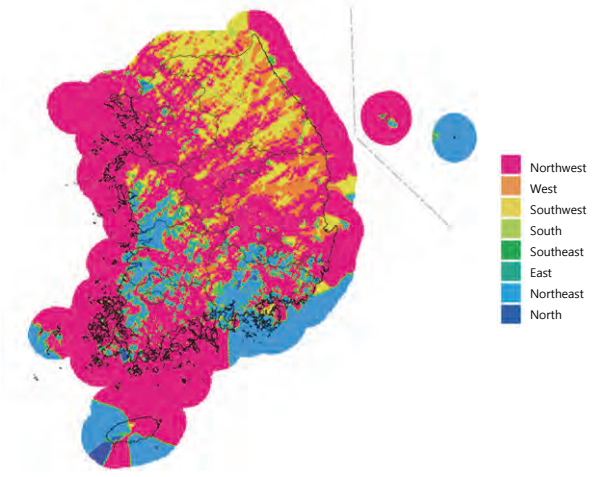

Figure 2. Main wind direction distribution (modified from www. greenmap.go.kr)

Figure 3 shows the locations of the offshore wind farms in the west coast, HeMOSU-1 Met mast, and the ground investigation locations. HeMOSU-1 has measured the weather information for three years, showing the monthly average wind speed of 7.0 m/s from winter to early spring and less than 5.0 m/s (which is the effective limit wind speed) in May and June, and then increases again in July (Figure 4). The average annual wind speed is 6.97 m/s at 97 m from sea level and 6.71 m/s at 76 m and does not drastically change with height.

The mean wind speed distribution per year for the past 30 years, back-estimated from the observations of HeMOSU 1, is shown in Figure 5, and it is expected that the average wind distribution per month is 6.5–7.0 m/s per month according to this estimation.

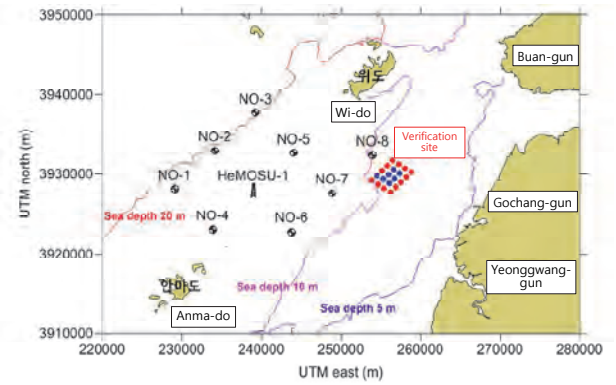

Figure 3. Locations of offshore wind farm, HeMOSU-1 met mast tower, and site investigation (modified from KEPRI, 2014).

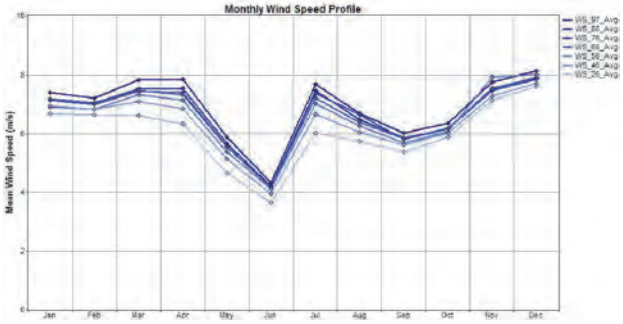

Figure 4. Mean wind speed measured at HeMOSU-1 met mast tower (KEPRI, 2014).

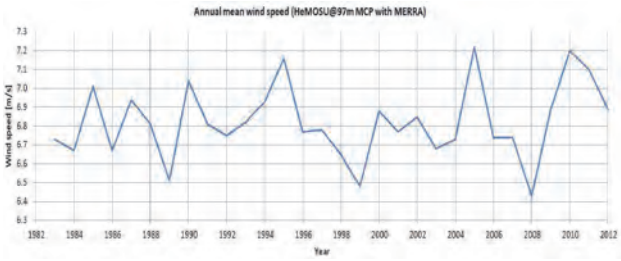

Figure 5. Annual wind speed for 30 years estimated by MCP method using HeMOSU-1 data (KEPRI, 2014).

2.2 *Site investigation*

This section explains the ground conditions of the Southwest offshore wind farm (verification phase) whose construction inaugurated in early 2017, and the Jeju Tamra offshore wind farm (30 MW) which has been producing electricity since 2016. A total of 11 boreholes were drilled in the west coast of Korea (8 holes around HeMOSU-1 and 3 holes in the farm area for the verification phase (as shown in the Figure 3) and the stratigraphy of the site was constructed using the results of Standard Penetration Test (SPT).

According to Yoon et al. (2014), there is a marine sedimentary layer composed of marine clay (ML, CL) and marine sandy soil (SM, SP, SW-SM, GP) near the seabed, and weathered residual soils, weathered rocks, and bedrocks are followed in order underneath. The thickness of the marine sediments above the bedrocks is about 24.3–62.5 m and tends to thicken toward the outer sea. The undrained shear strengths were derived from the Cone Penetration Tests (CPT) performed near the verification wind farm, displaying 10 kPa or below near the seabed, yet increasing as it gets deeper, with the average value of 33.9 kPa.

On the other hand, the results from the drilling investigation near HeMOSU-1, where the offshore wind farm will be constructed, are somewhat different. Figure 6 shows the results of holes Nos. 7 and 8 among the 8 holes, with similar results from the other boreholes. There is a silt-mixed sand of approximately 4 m from the seabed, and the N value in the layer is about 40. Below the layer, there is approximately 25 m thick very soft silty clay with the N value of less than 10, followed by a very dense sand layer with the N value of over 50 at depth of 30 m or deeper, and a layer of soft rock is located at a depth of 40 - 50 m. Therefore, the stratigraphic near the HeMOSU-1 is very different from the verification wind farm. Foundation types of offshore wind farm near HeMOSU-1 seem to be greatly affected by the soil layer with a soft clay of thickness of 20 m or more.

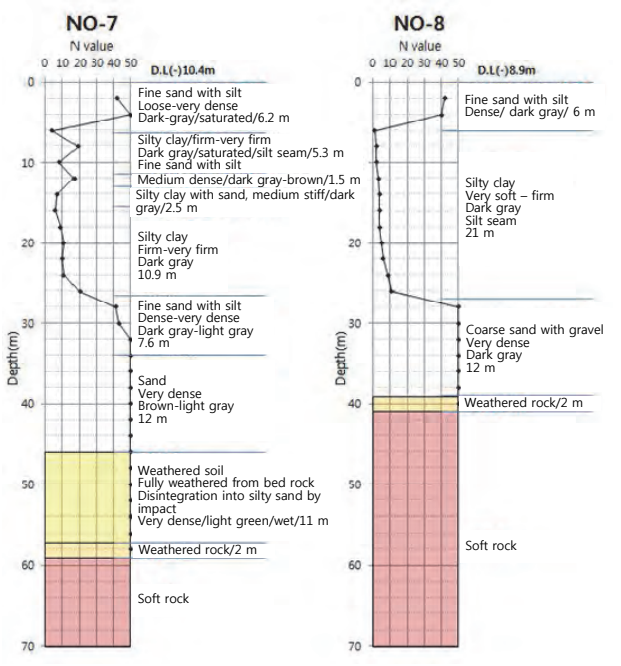

Figure 6. Boring log at Nos. 7 and 8 of southwest sea offshore wind farm (modified from KEPRI, 2014).

The Jeju Tamra offshore wind Farm located on the northwestern coast of Jeju Island has a soft rock layer at shallow depth, which is different from that of the southwest wind farm site, and thus, a supporting structure type is selected by this soft rock layer. Because Jeju Island is an island formed by volcanic activity, the geological structure near Jeju Island is almost identical.

Figure 7 shows the stratigraphy of the Jeju Tamra offshore wind farm area. It was confirmed with five boreholes that there is 0–0.3 m thin marine sediments (classified as SP) on the seabed and basaltic soft rock or caustic rock layer underneath. The water content of marine sediments was 24.1% with the specific gravity of 2.73, the fine contents passing #200 sieve was 4.26%, and the N value was 4. However, since the layer is thin, the physical properties of the soil layer do not seem to affect the underlying foundation design. The degree of weathering and joint spacing of the soft rock layer with basalts as parent rocks was widely distributed with the RQD of 54-80%, and a hard rock layer. The monopile was designed to penetrate into the soft rock layer whose uniaxial compressive strength ranges from 24.7 to 26.9 MPa and the deformation modulus is 2,552 MPa.

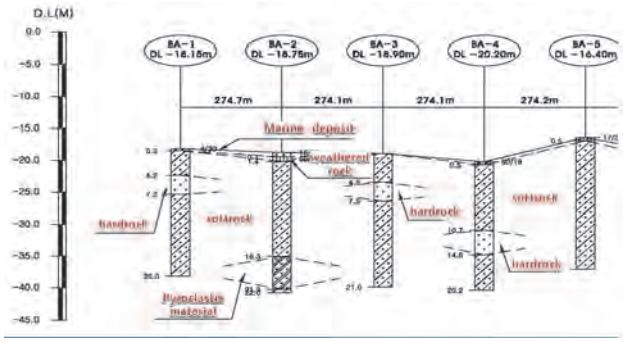

Figure 7. Stratigraphy of Jeju Tamra offshore wind farm (Choi et al., 2014).

3 CONSTRUCTION RECORDS

3.1 *Present conditions of wind farms*

The current status of the Korean offshore wind farms is shown in Figure 8 and Table 1. Currently, a total of 38 MW is in operation with 35 MW in Jeju Island and 3 MW in Gunsan. About 2,500 MW in the Southwest Sea is under construction and 4,686 MW is being prepared.

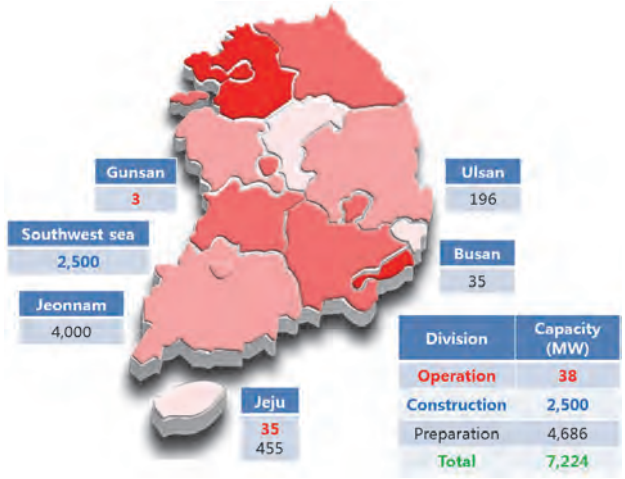

Figure 8. Performance and plan of offshore wind farms.

Table 1. Present and planned wind farms.

Locations	*Capa -city (MW)*	*Owner*	*Substru- cture*	*Installation Year*
Jeju Island (Woljeong)	5	Korea Institute of Energy Research, Doosan Heavy Industries & Construction Co., Ltd.	Jacket	2011
Jeju Island (Tamra)	30	Korea Southern Power Co., Ltd. Doosan Heavy Industries & Construction Co., Ltd.	Jacket	2016
Gunsan	3	KEPCO Research Institute	Suction	2016
Southwest Sea	2,500	Korean Offshore Wind Power Co., Ltd.	Jacket, Suction	2017~
Jeju Island (Dae-jeong)	200	Korea Southern Power Co., Ltd.	NA	Under preparation
Jeju Island (Hanrim)	150	KEPCO Engineering & Construction Co., Inc.	NA	Under preparation
Jeju Island (East)	105	Halla Wind Energy Co., Ltd.	NA	Under preparation
Busan (Mokdo)	35	Korea Southern Power Co., Ltd.	NA	Under preparation
Ulsan	196	SK Construction Co., Ltd.	NA	Under preparation
Jeonam	4,000	Jeollanam-do	NA	Under preparation

3.2 *Jeju Woljeong*

Jeju Woljeong offshore wind test site was completed in 2011 using jacket substructures. A total of 5 MW is in operation including a single unit of 2 MW of the Korea Institute of Energy Research and a single unit of 3 MW of Doosan Heavy Industries & Construction. The turbine installed at 2 MW is HARAKOSAN's Z72 with the tower length of 51 m and weight of 170 ton. Meanwhile, the turbine installed in 3 MW is Doosan Heavy Industries & Construction's WinDS3000 with the tower length of 61 m and weight of 190 ton.

Figure 9. Jeju Woljeong offshore wind test site.

3.3 *Jeju Tamra*

Jeju Tamra offshore wind farm was commissioned by Korea Southern Power Co., Ltd. and Doosan Heavy Industries & Construction consortium completed installation in 2016. As shown in Figures 10 and 11, ten units of 3 MW of Doosan Heavy Industries & Construction's WinDS3000 are in operation and the tower length is 65.1 m. The depth of the water is about 20 m and the upper structure is designed to be supported by the jacket substructure through a pin pile to the shallow depth of about 15 m of Jeju Island area basalt rock.

Figure 10. Jeju Tamra offshore wind farm.

Figure 11. Jeju Tamra offshore wind farm monitoring center.

3.4 *Gunsan*

Gunsan suction foundation test site was commissioned by KEPCO Research Institute, and the installation was completed in 2016 (Figure 12). A 3 MW WinDS3000 by Doosan Heavy Industries & Construction is in operation and its tower length is 58.5 m. The water depth is about 20 m, and the upper structure with a total weight of 342 ton was designed to be supported by the tripod suction foundation in the sandy soil; the tower weight is 155.8 ton, nacelle weight is 128 ton, hub weight is 28 ton, and each blade weighs 10 ton. As shown in Figure 13, the suction foundation is composed of three steel suction bases with a diameter of 6 m, a height of 12 m, and a weight of 148 ton. It is inclined up to 0.33° during installation as shown in Figure 14, but by controlling the output of the suction pump, the verticality is secured up to 0.02° after completion of installation.

Figure 12. Gunsan suction foundation test site.

Figure 13. Panoramic view of tripod suction foundation.

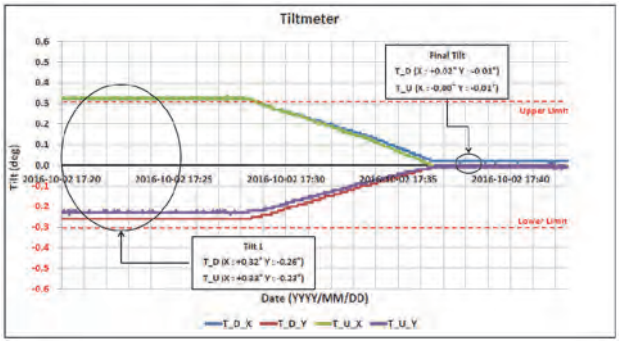

Figure 14. Verticality control using suction pump.

3.5 *Southwest Sea wind farm*

The Southwest Sea offshore wind farm is located between Wi-do and Anma-do in Jeollanam-do province and was commissioned by the Korean Offshore Wind Power Co., Ltd. (Figure 15). As tabulated in Table 2, a total of 2,500 MW are planned to be constructed with 60 MW in the first phase, 440 MW in the second phase, and 2,000 MW in the last phase using the integrated SCADA system developed by the KEPCO Research Institute for management.

As of July 2017, the first jacket substructure is under construction as the first phase (Figure 16). The first verification phase was designed such that Doosan Heavy Industries & Construction's WinDS3000 Turbines would be supported by 19 jacket substructures and one tripod suction foundation. The water depth is about 10 m, and the supporting rock bed appears at 40 m or deeper.

Figure 15. Location of the Southwest Sea wind farm

Table 2. Construction plan of Southwest Sea wind farm.

Phases	Phase 1 (Verification)	Phase 2 (Demon-stration)	Phase 3 (Large scale)	Total
Capacity (MW)	60	440	2,000	2,500
Substructure	Jacket, Suction	NA	NA	
Installation Period	2017～2019	2020～2022	2023～2024	

Figure 16. Panoramic view of the pin pile rock excavation for the jacket substructure.

4 RESEARCH AND DEVELOPMENT OF SUB-STRUCTURE IN KOREA

In Korea, research related to wind power generation have been continued since 1988, and the focus was on domestic wind turbine technology development including development of core parts with investing about 271 billion Korean Won (KRW) by 2010, wind resource evaluation, power plant design and power grid. In recent years, an interest in offshore wind power has increased, and research on the development of offshore wind substructure has been conducted by companies and research institutes (KGS 2014). This session introduces the status of research and development related to offshore wind power substructure.

4.1 *Monopile*

A project of "Development of Offshore Wind Energy Foundation Systems for Large Diameter (more than 5m) and Deep Sea (less than 60m)" was conducted to develop a large-diameter, excavation-type monopile system with a diameter of 5 m or more, capable of efficiently supporting large capacity generators of 3 MW or more in marine ground conditions of 30 m depth or more, where the ground is composed of rock mass (KICT and KIOST et al. 2015).

In detail, a rock drilling rig that excavates a rock by using a number of small hammers was developed to improve the rock excavation speed as shown in Figure 17. The optimal design guideline for offshore wind power generation monopiles in line with LRFD-based international design standards was developed, as well as the platform design/work tip stability technology and the optimal form of TP (Transition Piece) for fast and precise marine construction.

In addition, a single and tripod bucket foundation system that can be applied economically in thick soil depth (50 - 60 m) was developed with design guidelines for bucket foundation. The system evolves the limit-state design method based on the development of intrusion device and construction system capable of maintaining the accuracy of vertical angle within 1°.

The developed large-diameter monopile technology was adopted in a detailed design for the Jeju Tamra offshore wind farm project, and the bucket foundation technology was applied and constructed for the supporting structure of the offshore wind turbine in Jeollanam-do Province.

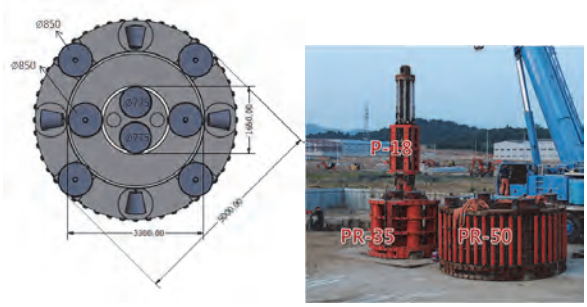

Figure 17. Rock drilling rig with multiple hammers (KICT and KIOST et al. 2015)

4.2 *Jacket substructure*

In order to support the Southwest Sea offshore wind farm project sponsored by the Korean government, a project of “Development of Substructure Systems for Offshore Wind Power in Shallow Sea Water (Less than 40 m)” funded by MOTIE (Ministry of Trade, Industry and Energy) developed a substructure technology for 5 MW wind turbine of less than the depth of 40 m installed on the South-western coast of Korea, as shown in Figure 18, and developed the new concept of fixed substructure system and advanced design technology, high durability materials for marine structure and utilization technology, technology for securing bearing capacity of foundation, and finally, verified the technology by applying to a test bed.

With regard to the technology for securing support capacity of the foundation structure, the analytical technique and the support capacity evaluation system of the offshore wind structure were developed through the laboratory model test, the centrifugal model test, and the numerical analysis, and the domestic submarine ground modeling technique necessary for the analysis of the offshore wind turbine response. As of 2017, the development technology is being applied to the Southwest Sea offshore wind farm (verification phase) in the southwestern coast.

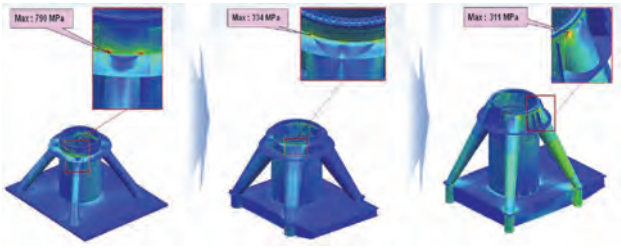

Figure 18. 5 MW jacket substructure TP design (POSCO et al. 2017).

4.3 *Hybrid foundation*

A project titled "Development of Hybrid Substructure System for Offshore Wind Turbine" has been developing a new type hybrid support structure system suitable and economical for the Southwest coast of Korea (KICT et al. 2013). In detail, as shown in Figure 19, research topics include development of economical hybrid support structure system technology through efficient combination of structural materials (steel and concrete) and foundation type, development of foundation/support structure/tower connection technology, foundation type and development of scour prevention technology for hybrid support structure system, development of response analysis technology of hybrid support structure considering fluid-soil-structure interaction, and rapid installation method and maintenance technology development of hybrid supporting structure.

Consultations are underway to apply the new hybrid support structures in this R&D project to the construction of offshore wind farms in the Southwest Sea. By solving the technical problems to secure the support structure in the soft ground, the cost reduction for constructing the support structure is expected to be more than 15%.

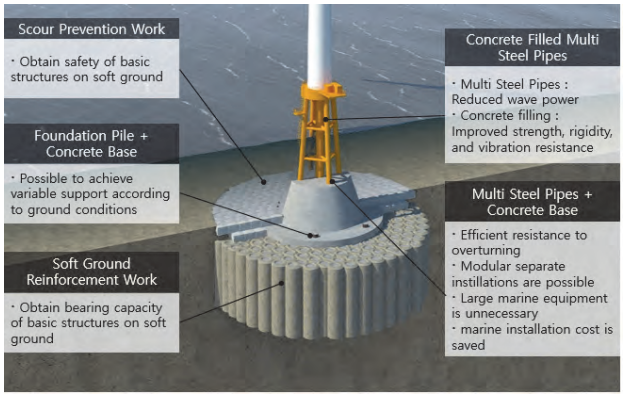

Figure 19. Offshore wind power hybrid foundation and characteristics (modified from KICT et al. 2013)

4.4 *Monopod concrete suction foundation*

A research and development project titled "Development of design basis and concrete technologies for offshore wind turbine support structures" funded by MOF (Ministry of Oceans and Fisheries) is aiming at the development of the design standards for Korea's offshore wind support structure as well as the design/construction guidelines for the new type of concrete support structure applicable to the HS-139, 5 MW offshore wind turbine by Hyosung (KR and DAEWOO E&C et al. 2017). In the case of steel structures, the top generator is sensitive to deformation and fatigue due to vibration, wind, and wave load, and is less resistant to corrosion.

To overcome this, the study proposed a new type of concrete support structure combined with a suction foundation, which is currently being actively reviewed as one of the alternative of offshore wind support structures due to its quick and easy installation and economic advantages (Figure 20).

Furthermore, in this study, three compartments are implemented inside the suction foundation and the suction pressure can be individually controlled for each compartment so that vertical control during construction and operation is possible (Kim et al. 2015, Kim et al. 2016).

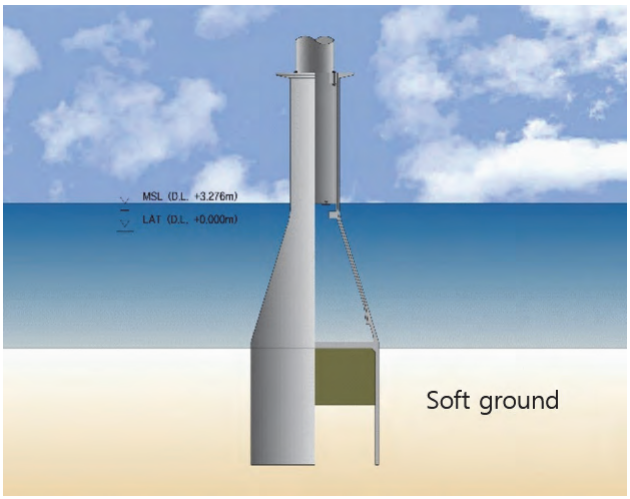

Figure 20. Concrete monopod suction foundation (KR and DAEWOO E&C et al. 2017).

4.5 *Tripod steel suction foundation*

A project titled "Seashore wind turbine construction & commercialization embedded suction bucket support structure (SuCCESS)" has been carried out on the detailed design of support structure and the transfer/installation of prototype (Rye et al. 2017).

As shown in Figure 21, a reduced-scale model was constructed and tested to verify its applicability. The study focused on the development of support structures suitable for mid-water depth and soft seabed of the Southwest coast of Korea, to achieve economic efficiency by reducing the installation cost of offshore wind support structures and to reduce the business risk by shortening the marine operation period.

Figure 21. Steel tripod suction foundation scale model (Ryu et al. 2017).

4.6 *Deep-sea floating substructure*

A project "Development of Floating Substructure/Platform for Offshore Wind Power in Deep Water" aimed to develop the core technology for the floating substructure and its platform design/drying/installation/evaluation/verification as well as the technology for mooring gear that overcomes harsh marine environment and regarding material/method technology (PNU et al. 2013).

Its goals are to develop the market-oriented source technologies in Stage 1 (2011-2013), the competitive core design skills in Stage 2 (2011-2013), and the practical applications and monitoring, and the commercialization technology of the developed technology in Stage 3 (2011-2013). This study includes the development of anchor system for deep sea considering ground characteristics which is core technology of the floating wind power system and development of the floating wind platform technology.

5 SUMMARY

In this paper, the trends related to offshore wind power generation in Korea since the 2000s were introduced; in particular, we discussed geological and wind-resources-related characteristics and the present state of research and development related to the supporting structures in near shore area of the Korean peninsula.

In Korea, the three boundary sides are surrounded by the sea, and as pointed in this paper, the offshore wind power projects are being promoted mostly on the western and southern coast, and Jeju Island. This is because the depth of the East Sea is relatively deep, which makes it difficult to install a fixed support structure. In the future, when the technology on floating support structures would be accumulated, the project is expected to proceed.

This paper, prepared for the TC209 Offshore Geotechnics workshop of the International Conference of Soil Mechanics and Geotechnical Engineering (ICSMGE), is expected to contribute to the understanding and role of the geotechnical field for the revitalization of the offshore wind power industry in Korea.

6 REFERENCES

Choi C.H., Kim W.K, and Cho S.D. 2014. Detailed design on monopile foundation used in offshore wind energy test bed, *The 2nd KICT-YU-CBNU Joint Workshop*.

KEPRI. 2014. *Test bed for 2.5 GW offshore wind farm at Yellow sea interim design basis report*, KEPRI report.

Korea Institute of Civil Engineering and Building Technology (KICT) et al. 2013. *Development of hybrid substructure systems for offshore wind power*. 1st year research report. Ministry of Land, Infrastructure, and Transport. Korea.

Korea Institute of Civil Engineering and Building Technology (KICT) and Korea Institute of Ocean Science and Technology (KIOST) et al. 2015. Development of offshore wind energy foundation systems for large diameter (more than 5m) and deep sea (less than 60m). Registration number: 11-1613000-001295-01. Ministry of Land, Infrastructure, and Transport. Korea.

Korean Geotechnical Society (KGS). 2014. *Geotechnical Design of Offshore Wind Foundation for Geotechnical Engineers*. CIR, Seoul.

Kim B.W., Kim Y.S., Jin B.M., Bae K.T. and Youn H.J. 2016. Numerical analysis on tilting control of suction pile for offshore wind power. *Journal of the Korean Geo-Environmental Society* 17(9), 5-12.

Kim Y.S., Bae K.T., Lee J.P., Joung J.W. and Choo Y.W. 2015. Model tests for tilting control of suction bucket foundation for offshore wind turbine. *Journal of Korean Society of Hazard Mitigation* 17(2), 207-218.

Korean Register (KR) and DAEWOO E&C et al. 2017. *Development of design basis and concrete technologies for offshore wind turbine support structures*. No.20120093. Ministry of Oceans and Fisheries.

MOTI and KEA. 2016. *New & renewable energy white paper*. Registration number: 11-1410000-001321-11, Ministry of Trade, Industry and Energy, and Korea Energy Agency.

POSCO et al. 2017. *Development of substructure systems for offshore wind power in shallow sea water (less than 40 m)*. Ministry of Trade, Industry and Energy.

Pusan National University (PNU) et al. 2013. *Development of Floating Substructure/Platform for Offshore Wind Power in Deep Water*. Ministry of Trade, Industry and Energy, Korea.

Ryu M., Lee J., Kwag D., Bang S. 2017. Design, construction, and installation of offshore wind turbine with tripod suction bucket foundation. *Proc. of the ASME 36th Int. Conf. on Ocean, Offshore, and Arctic Engineering*, OMAE 2017. Trondheim, Norway.

Yoon G.L., Kim S.B., Kwon O.S., and Yoo M.S. 2014. Partial safety factor of offshore wind turbine pile foundation in West-South Mainland sea. *Journal of the Korean Society of Civil Engineers KSCE* 34(5), 1489-1504.

Marine site characterisation and its role in wind turbine geotechnical engineering

Caractérisation du site maritime et son rôle dans l'ingénierie géotechnique des éoliennes

Michael Rattley, Richard Salisbury, Timothy Carrington**,** Carl Erbrich & Gary Li
Fugro, m.rattley@fugro.com

ABSTRACT: The compartmentalised approach of separate geophysical and geotechnical investigations, followed by independent engineering design that has typified offshore site developments over most of the past 50 years is changing. Offshore wind farms (OWFs) have large spatial extents and the potential to encounter variable soil conditions at numerous turbine locations may lead to adoption of multiple substructure concepts with differing design considerations. At the data analysis stage it is therefore common to construct a fully informed ground model to develop the requisite understanding of the OWF site. This paper describes how integration should be extended to include all the technical aspects of marine site characterisation, but with specific focus on the geotechnical phases of the process. It will demonstrate the benefits of considering all aspects under a single direction over the lifetime of an investigation, focussed on close collaboration between different specialists and end users. By this means design can be optimised, risks can be managed and costs controlled.

RÉSUMÉ : L'approche compartimentée d'enquêtes géophysiques et géotechniques séparées, suivie d'une conception d'ingénierie indépendante qui a typifié les développements de sites offshore au cours de la plupart des 50 dernières années, change. Les parcs éoliens offshore (OWF) ont de vastes étendues spatiales et le potentiel de rencontrer des conditions variables du sol dans de nombreux endroits de la turbine peut conduire à l'adoption de multiples concepts de sous-structure avec des considérations de conception différentes. À l'étape de l'analyse des données, il est donc commun de construire un modèle de terrain pleinement éclairé pour développer la compréhension requise du site OWF. Cet article décrit comment l'intégration doit être étendue pour inclure tous les aspects techniques de la caractérisation des sites marins, mais en mettant l'accent sur les phases géotechniques du processus. Il démontrera les avantages de considérer tous les aspects sous une seule direction tout au long de la vie d'une enquête, axée sur une collaboration étroite entre différents spécialistes et utilisateurs finaux. Par ce moyen, la conception peut être optimisée, les risques peuvent être gérés et les coûts contrôlés.

KEYWORDS: site characterisation; ground model; geotechnical engineering

1 INTRODUCTION.

Marine site characterisation is the understanding of geological, geotechnical, environmental and metocean conditions in relation to the planned development of a site. In concept, it is designed to provide the right information at the right project stage to allow optimal location, design and installation of subsea infrastructure. Large offshore sites are required to be characterised to develop offshore wind farms (OWFs) and interconnector cables; the site characterisation process is a critical component of the project development cycle.

The processes associated with the planning and execution of geophysical and geotechnical site characterisation for OWFs are outlined in guidance notes presented by the SUT (2014). This paper describes how an integrated site characterisation should include all technical aspects, including: desk study, fieldwork planning, data collection, ground model construction, and geotechnical parameterisation. In that sense the paper builds on the approach presented by Thomas (2017), but with a specific focus on the impact of the wind turbine generator (WTG) and offshore substation (OSS) geotechnical engineering design requirements on the process. Similar discussion was presented by Evans (2011) with regard to the development of economic and safe offshore oil and gas facilities in geotechnically challenging areas.

2 MARINE SITE CHARACTERISATION

2.1 *Integrated Ground Model Approach*

Thomas (2017) presents a phased approach for integrated marine site characterisation, with specific reference to large deepwater oil and gas developments. While not all analytical studies incorporated within that approach may be relevant for an OWF development, the general framework can still be successfully implemented. The resulting early project stage benefits are therefore unchanged from those noted by Thomas:

- An **evolutionary ground model** to characterise site conditions for a range of analyses;
- A compiled **site characterisation inventory** to document and monitor project data acquisition and analysis requirements;
- Early identification of potential **constraints and geohazards**;
- Early identification of potential **implications of site conditions** on project schedule and cost;
- Early identification of **data acquisition and interpretation** requirements;
- Early identification of requirements for **specialist analytical studies**;
- **Prevention of surprises** otherwise impacting on overall project schedule and cost; and
- Provision of a tool to **manage and communicate** the development to project stakeholders.

The integrated approach is also analogous to the risk management process described by SUT (2014) with a key message: *"…the level of (residual) risk is inversely proportional to the level of knowledge and, ideally, the risk assigned to any development will decrease with increased knowledge of the development area prior to the development design being finalised"*.

In terms of the specific geotechnical engineering design risk management and foundation optimisation process, the benefits listed above become keenest once the outline requirements of the geotechnical design process are known, or can be reasonably established, and can therefore be anticipated as part of the data acquisition planning. Given recent developments in geotechnical design (Byrne et al. 2015) for WTG foundations, early consultation on the geotechnical design process is key to delivering the full benefit of the integrated marine site characterisation approach for an OWF development.

Several areas of investigation and specialist study are outside of the main focus of this paper (that being the ground

model and geotechnical characterisation process), but are no less important in the overall OWF site characterisation process. These areas are considered briefly in the sections below.

2.2 *Unexploded Ordnance*

Unexploded ordnance (UXO) refers to explosive devices that have not fully detonated, and includes mines, air-dropped bombs, mortars anti-aircraft projectiles and grenades (Figure 1). These items can be lying on the seafloor or buried at shallow depth by mobile sediments and carry a risk of detonation from impact or movement. At risk areas include historic war zones, firing ranges and dumping grounds. There is an implied risk to equipment and personnel during the intervention activities at OWFs including soil testing, turbine installation cable laying and operation.

Figure 1. A WW2 mine discovered during survey at the Horns Rev 3 offshore windfarm in 2015. The mine was detonated in 2016 (Vattenfall, 2016)

The risk is higher for OWFs than for most other marine developments such as oil & gas fields, because of the extensive areas of sea floor involved and the large number of structures. In Europe, many wind farms are located in the Southern North Sea where past conflicts have left a significant UXO legacy.

The process normally starts with a desk study, based on available information, to assess the potential threat of UXO being present in the area and assess the risk to the planned works. Elements to consider include the type of UXO that might be encountered, the local marine environment, the type of works to be carried out and the overall development schedule. The result of the desk study will normally be a recommendation to carry out a geophysical survey to detect UXO followed by a detailed survey specification.

The most common geophysical technique used to detect UXO is magnetometry. Over the past 10 years this has developed from using a single magnetometer to multiple gradiometer systems that measure the magnetic gradient and provide more accurate, detailed directional information. Figure 2 shows Fugro's Geowing which deploys multiple magnetometers on a fixed frame towed behind the survey vessel using a remotely operated towed vehicle (ROTV) that offers depth control and steerability.

Data processing and interpretation is a two stage process. First the data were processed to identify any anomalies, which are then correlated with any acoustic information available from bathymetry and side scan sonar surveys. In the second stage the interpreted data is analysed by UXO specialists who will assess the risk of the anomalies representing UXO.

The UXO investigation will need to be completed early in the overall site investigation process so that locations can be cleared before the first intervention work takes place. This will often be geotechnical drilling, testing and sampling

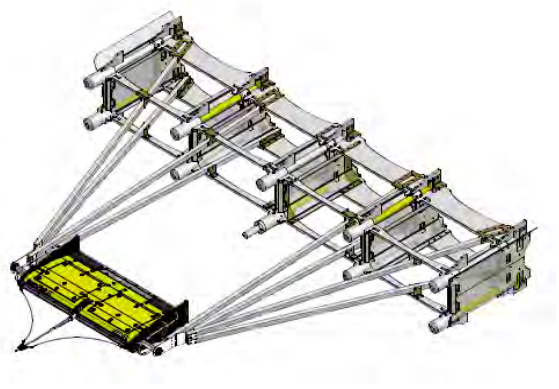

Figure 2. The Geowing gradiometer; consisting of five fixed magnetometers in a rigid, steerable frame. Operated by Fugro

2.3 *Metocean Data*

As part of the site characterisation it is essential to define the meteorological and oceanographic (metocean) conditions prevailing at the location. The winds, waves, current speeds and water levels will determine the loading on the WTG structure and hence on the foundations. The metocean requirements for WTGs are given in standards such as BS EN 61400-3:2009.

The metocean criteria include wind speeds and direction (Figure 3) at a series of heights above mean sea level, for a range of averaging times (e.g. 1 hourly mean, 10 minute mean, 3 second gust); significant and maximum wave heights and associated wave periods and directions; profiles of current speeds and directions though the water column; and water levels caused by tides and surge.

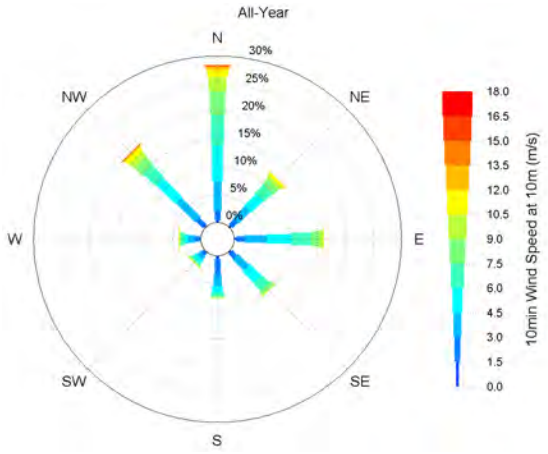

Figure 3. Wind rose showing joint occurrence of wind speed and direction

Metocean design criteria are typically derived using hindcast model data as such models can provide a long enough time series to allow extreme conditions to be determined with confidence. Usually at least 20 years of data are used, and an Extreme Value Analysis is performed to extrapolate the data to the required return periods (e.g. 50 years). Ideally the models

would be validated against site-specific measured data, and calibrated if necessary. This is particularly important for currents, whose complexity makes numerical modelling more challenging. Site-specific small-scale models can be set up to accurately account for the local bathymetry at the wind farm location. These models are nested within global-scale models that provide conditions at the model boundary.

In addition to design criteria, operational statistics are required to assist with operational planning during the installation phase. Knowledge of the seasonal variation in conditions means that weather-sensitive operations are planned for times when conditions are most likely to be suitable.

2.4 *Environmental study*

An environmental study will be needed to address a number of points that may include habitats, existing infrastructure such as cables and pipelines, meteorological conditions, oceanography, fishing, shipping movements, recreational issues, military exercise areas, dumping grounds and possibly many others. Precise requirements will vary depending on the regulatory and licensing regulations and the local conditions.

The environmental study will often be a major undertaking involving a number of different specialists and not directly related to the investigation of foundation conditions. However, there is benefit in maintaining liaison between the environmental study and the foundation study so that data collection programmes can be coordinated, relevant information shared and a consistent approach made to the analysis and presentation of data common to both. For example, an environmental baseline or habitat investigation will normally involve sampling and photographing the seafloor producing information that will be useful in building the initial ground model. Data analysis for environmental purposes may consider sediment distribution (Figure 4) and seafloor processes, both of which are also relevant in an engineering context and will be relevant to refining the ground model and site characterisation.

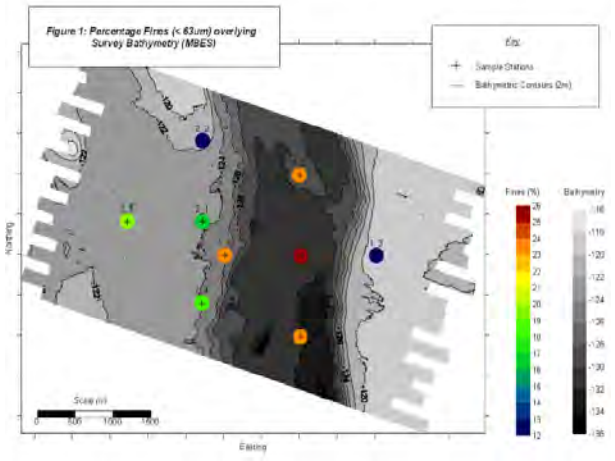

Figure 4. Example of a seafloor map produced for environmental study purposes

3 ENGINEERING DESIGN REQUIREMENTS

Early design of foundations for offshore WTGs and OSSs drew upon the significant volume of experience existing within the offshore oil and gas industry. It is therefore unsurprising that a large number of the early offshore WTGs and OSSs in the North Sea were founded on piled jacket substructures. With greater understanding of the critical WTG load cases and development of integrated structural and geotechnical design processes, the monopile eventually became the prevailing foundation concept for WTGs, although jacket solutions are still popular in deeper waters (Figure 5) and for OSS structures. Monopiles now make up over 70% of foundations for WTGs (Kallehave et al., 2015) and current market trends indicate that monopiles will continue to be the preferred foundation concept for WTGs in Europe in the next 10 years. The single-pile foundation is attractive due to its simplicity and robustness, allowing costs to be reduced through mass fabrication and quicker installation.

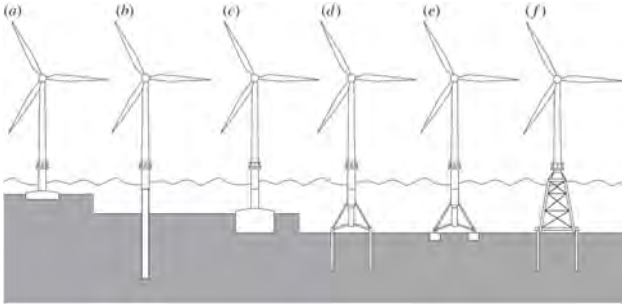

Figure 5. WTG foundation concepts (a) gravity-based foundation (b) monopile foundation (c) caisson foundation (d) multipile foundation (e) multi caisson foundation and (f) jacket foundation (Kallehave et al., 2015)

The requirement for increased global OWF capacity has led to consideration of bigger WTGs and larger OWFs in the North Sea and new rounds of development worldwide. New developments coincide with a focus on reducing the cost of wind energy, for which the foundation is a significant contributing factor. These requirements give rise to design challenges for optimisation of WTG foundation solutions, since the planning, design and execution of an OWF is governed by the seabed conditions. Efficient geotechnical engineering design may be restricted where challenging or uncertain soil conditions are encountered, as they often are. Soil and rock conditions display an extremely broad spectrum of classification and mechanical response, and 'local' variability can be amplified across large OWF sites. Seabed conditions could vary from high strength volcanic and igneous rocks to normally consolidated, very soft marine sediment.

Nevertheless, optimisation is required and the boundaries of current geotechnical design practice must be tested in order to deliver reducing costs for OWF development. Recent industry driven research has focussed in this area (Byrne et al. 2015) and new or relatively unproven (for WTGs) foundation concepts, such as suction bucket jackets (SBJs), are being considered along with WTG substructure concepts, such as floating turbine concepts, which will permit OWF development in deeper water sites. Such methods essentially necessitate the engineering design strategy for "New Design Solutions" outlined by Evans (2011). As the complexity of the geotechnical design challenges increase, so too will the input data requirements associated with ever more complex geotechnical analyses (Zdrakovic et al, 2015). In order to optimise the marine site characterisation process, and ensure that the likelihood of unforeseen data input requirements arising at a later stage of the project is minimised, these input data requirements should be considered and communicated at an early project stage. However, different foundation design concepts will require different input data and geotechnical parameterisation requirements, due to the varying nature of the geotechnical analyses required.

Considering monopiles for example, advanced lateral design methods (e.g. Peralta, et. al. 2017) require information on soil stiffness encompassing small to large strain, detailed information on cyclic degradation and parameters to define the consolidation rate of the soil (i.e. to define the drainage

conditions around the piles). This information is mostly obtained from carefully conducted laboratory tests.

The pioneering SBJs in sandy soils (see Bye. et. al., 1995) for oil and gas infrastructure were heavy and the foundations were only occasionally subject to tensile loads. However, OWF SBJ's are much lighter and hence tensile loading is a more frequent occurrence. With the wind load comprising a much larger component of the total environmental load compared to a traditional oil and gas platform, large static load offsets lead to sustained tensile loads which must be resisted. To address this design challenge advanced numerical modelling is essential with detailed and precise geotechnical parameterisation, particularly of the soil dilational response and the notoriously variable soil permeability (e.g. see Whyte et. al., 2017). Such properties can only be obtained in practice through comprehensive laboratory testing programmes.

A number of recent OWF's where weak rocks (calcarenites and/or chalk) are prevalent have encountered different but no lesser challenges. Once again specialised laboratory testing is required for optimised design; for example constant normal stiffness (CNS) testing for assessing axial response in soft rocks provides critical input into state-of-the-art design methods (e.g. Erbrich, et. al., 2010a and Augustesen et al., 2015). Lateral pile design for such geotechnical conditions also requires specialised tools and laboratory inputs (e.g. Erbrich, 2004 and Muir Wood et al. 2015) and the envelope is being pushed in terms of pile driving into such soil conditions, with accompanying threats of premature refusal and pile buckling (see Erbrich, et. al, 2010b). The advanced analyses which should be conducted to appropriately assess these issues require comprehensive and detailed field information (e.g. cone penetration testing (CPT) for profiling, seismic CPT for in situ small strain stiffness) and extensive laboratory testing for measurement of representative strength and stiffness parameters.

To date, most OWFs have been located in areas with low seismic activity but as interest increases worldwide, plans for OWFs in seismically active areas such as North America and Asia are starting to appear. Seismic engineering will prove a major new challenge for some of these cases and the foundation response under seismic loading, and in particular the threat of soil liquefaction, will need to be carefully evaluated from early stages of development in order to demonstrate project feasibility. Conventional simplified design approaches for assessing seismic liquefaction are not likely to be sufficient for WTG foundations and advanced analyses are anticipated to be essential to capture response in soils that exhibit softening under cyclic loading and/or liquefaction. Giannokou, et. al. (2016) and Erbrich et. al. (2016) discuss similar design scenarios within oil and gas infrastructure. These will invariably require detailed information on soil stress-strain response and cyclic degradation/liquefaction all of which are derived from, or calibrated to comprehensive laboratory testing.

The above discussion highlights the critical link between the advanced analyses required for optimised foundation design and the geotechnical input parameters required for these models, which are derived from the field and laboratory testing. The best outcomes will invariably be obtained when the site characterisation process is advanced with full knowledge of the design method input requirements. Hence wherever possible the required geotechnical investigation programmes should be developed jointly between the engineering designers and the characterisation team.

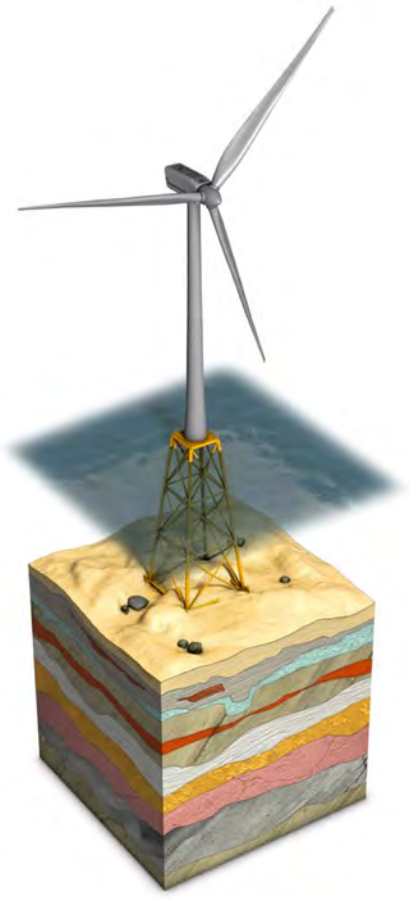

Figure 6. The ultimate design objective is an optimised WTG location and design, installed on time and operating reliably (conceptual jacket substructure shown)

4 EVOLUTIONARY GROUND MODEL DEVELOPMENT

4.1 *Overview*

OWF sites cover increasingly large areas of the seafloor as the number of turbines continues to grow and some developments plan for over 100 turbines. One OWF site can include multiple geological formations (both laterally and with depth), a range of water depths, seafloor gradients, seafloor processes, other constraints and geohazards, all of which can impact on development planning. A combination of these factors at any given site requires a coordinated strategy of environmental baseline or habitat sampling, metocean acquisition, geophysical survey, geological and geotechnical sampling, in-situ testing and laboratory testing. Integrating and interpreting these datasets efficiently is essential to assess the engineering significance of the seabed conditions. The development of a parameterised (engineering) ground model is the key to this process (Figure 7)

A successful OWF ground model can identify, map and assess geotechnical constraints and geohazards and provide input parameters to facilitate WTG and OSS foundation design, development layout and cable routing. Campbell (1984) first discussed the ground model method in relation to prediction of seabed conditions for a large offshore development site. Fookes (1997) describes numerous example onshore projects where ground models were used as a powerful communication tool to explain the diversity of the anticipated ground conditions. Campbell et al (2008) describe the use of a ground model to develop an optimised site investigation programme and budget. Successful application of ground models was further

demonstrated by Power et al. (2011), Evans (2011) and Hill (2011) as a means to reduce uncertainty in ground condition across large scale marine developments. Mason and Smith (2016) discuss integration of data for power cable routing. In the context of an OWF, the ground model is described by SUT (2014) as an industry standard approach to collating site information as part of the geotechnical risk management process.

Thomas (2017) further defines an evolutionary ground model, which is the concept adopted here, in the sense that it is necessary to understand the operation through time of the formative or active processes at a site to understand and explain the physical attributes of the site. The terminology also invokes a useful inference regarding the construction of the ground model itself, over the course of a site development.

The components of a preliminary evolutionary ground model are discussed in the following sections, which represent the site characterisation process up to the point where a detailed geotechnical site investigation is initiated. It is during the course of this preliminary ground model development that the potential requirements of the geotechnical design process should be considered in as much detail as the available information allows.

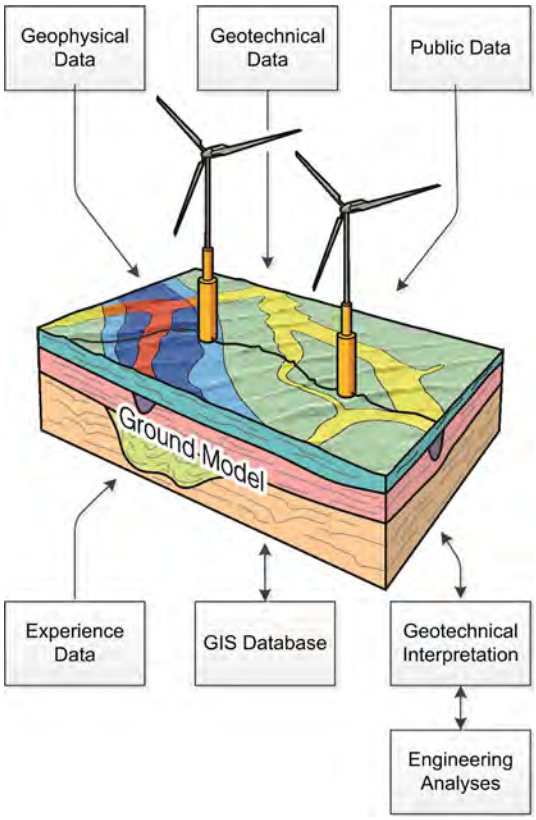

Figure 7. The OWF Ground Model

4.2 *Desk study*

The first stage in characterising the geological and environmental conditions in an area where an OWF is to be built is to carry out a desk study. The objective is to make maximum use of existing data and knowledge, by generating a preliminary evolutionary, engineering geological ground model. This can be upgraded and refined as the project progresses, new data becomes available and further integration and analysis takes place. Provided that suitable geophysical, geological and geotechnical data is collected and integrated, the logical conclusion is that the ground model will evolve into an engineering ground model suitable to form the basis for foundation design, for example by establishing critical subsurface features (Figure 8).

The process of carrying out a desk study for an OWF is described by the SUT (2014) which contains a detailed list of items to be addressed including typical sources of information. A great deal of relevant information is typically available in the public domain including nautical charts, research papers and local experience and knowledge. In addition, there may be geophysical and geotechnical site investigations and installation records from existing infrastructure, and although this is likely to be proprietary information, will be a valuable input to the desk study if permission for its use can be secured or it can otherwise be drawn upon as background experience.

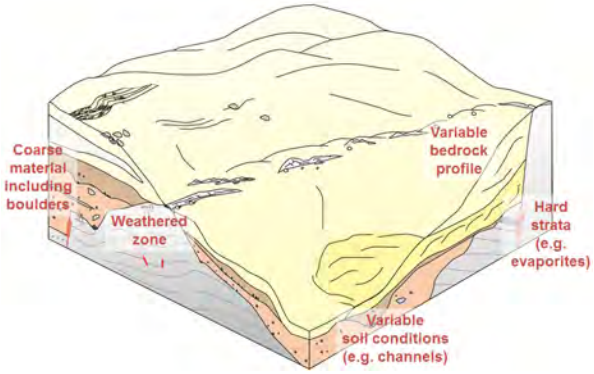

Figure 8. Example of subsurface features as identified during desk study for an offshore site

4.3 *Geophysical Investigation*

In general geophysical investigations precede geotechnical investigations with their results used both to update the ground model, and aid selection of geotechnical investigation locations. The geophysical survey thus provides the initial site specific dataset from which the preliminary ground model formed during the desk study is developed. As described by SUT (2014), geophysical surveys are often carried out in two phases. A reconnaissance survey over a coarse survey grid with a line spacing of perhaps several hundred metres, using both seafloor mapping and sub-seafloor mapping tools, will be designed to gain a regional understanding of shallow geological conditions. It should also identify any obvious geohazards and areas likely to be problematic for installing turbines. Depending on the licensing system, the reconnaissance survey may be carried out before the final investment decision has been made.

There are a number of good references that describe the equipment and techniques for marine geophysical investigations and their application to studies such as offshore wind farms. SUT (2014) contains information on this subject and more detail can be found in the Conduct of Offshore Drilling Hazard Site Surveys - Technical Notes, IOGP (2015), which although produced for the oil & gas industry contains much relevant information.

Detailed geophysical surveys are conducted to investigate more closely any potentially problematic conditions identified at an earlier stage, to refine the ground model and investigate planned turbine locations and cable route alignments. In order to gain maximum value from the detailed geophysical survey it should be carefully planned, and timing within the overall site characterisation process will be critical. Integration of all reconnaissance geophysical and geotechnical site investigation data should have been completed and the ground model

updated. The survey should be designed to define the engineering geological units identified and to tie these into the proposed turbine locations which should have already been selected (Figure 9). Survey line spacing will typically be reduced compared to the reconnaissance survey and the choice of equipment directed by the desired resolution that may be higher than for the reconnaissance survey.

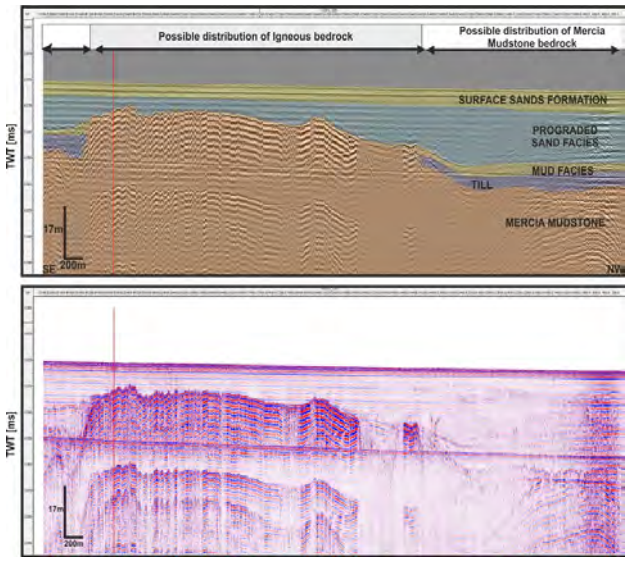

Figure 9. Example interpretation of geological soil units from a geophysical section

Once the detailed geophysical survey is complete the results are used to update the ground model. In some circumstances there may be sufficient confidence in the ground model derived from detailed geophysical and reconnaissance geotechnical data, that foundations can be designed on the basis of the parameters assigned to well defined stratigraphical units. In this case the detailed geotechnical survey would be directed at characterising these units and may be limited in its extent perhaps to the point where a borehole or CPT is not required at every turbine location. This is considered further by the SUT (2014) and later in this paper.

4.4 *Reconnaissance Geotechnical Investigation*

Generally the geotechnical data acquisition for a new development is best performed as a staged process with one or more preliminary investigations undertaken to develop the ground model as an iterative process, and to aid conceptual design and turbine layout. More information on geotechnical data acquisition techniques are given in Section 5.

Early reconnaissance geotechnical data feeds into the ground model development, aids interpretation of the geophysical data and allows foundation concept review and selection. It can also be used as a trial of different site investigation techniques to confirm that the best techniques are being used to obtain the required geotechnical data given the site ground conditions. It is also an opportunity to obtain preliminary data to characterise the stiffness and cyclic response of key geotechnical units within the ground model, as identified during the desk study and following geotechnical design review.

Together with seafloor maps produced during the geophysical investigation and the environmental study, the geotechnical data will inform the ground model of areas of potential seafloor mobility and scour potential, which are common geohazards for OWF developments.

4.5 *Geotechnical Design Evaluation*

In terms of the framework described by Thomas (2017), a relatively detailed consideration of the geotechnical design requirements for an OWF development should ideally occur during the "System Definition" project stage where the geotechnical evaluation of the site is first considered (Figure 10). This coincides with the development of a preliminary geotechnical model for the site based on information gathered during the desk study and (early) reconnaissance geotechnical investigation stages of the ground model development.

At this stage it is not necessary to be able to anticipate the final foundation design solution; however, it is likely that the foundation concept could be reasonably narrowed to consideration of one or two primary concepts based on prior review and foundation constraints (Figure 11). The potential geotechnical design requirements associated with each concept can then be developed, considering the critical geological formations as relevant for each foundation type. Even a high level review which identifies the potential need for advanced numerical analyses and associated input data requirements is beneficial at an early stage in order to refine the scope of future geotechnical investigations, as necessary

The above process should then be subject to review and iteration as further geotechnical data becomes available and further geotechnical analyses are performed.

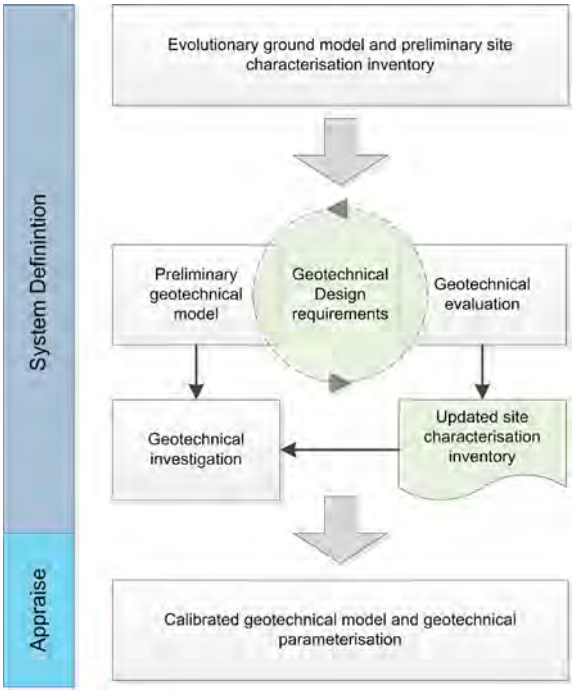

Figure 10. Expansion of process flow presented by Thomas (2017) to include consideration of geotechnical design requirements

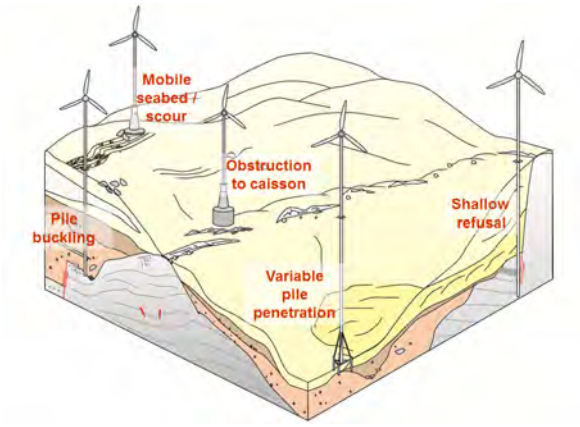

Figure 11. Example WTG foundation constraints related to identified subsurface features (Figure 8)

5 DETAILED GEOTECHNICAL INVESTIGATION

5.1 *Overview*

As noted earlier, the geotechnical data acquisition for a new development is best performed as a staged process with one or more preliminary investigations undertaken to feed into and develop the ground model as an iterative process and to aid conceptual design and selection of foundation concept and turbine layout. There is usually then a final phase of geotechnical data acquisition focussed on filling gaps in the ground model and finalising key geotechnical design parameters for each structure location.

The selection of site investigation plant is dictated by water depth, environmental conditions, availability, and cost (day rate and mobilisation), and the geotechnical data that is required. Many wind farm developments, especially those in shallower waters, are in areas of relatively high tidal currents and this can affect the choice and workability of the site investigation plant. If the water depth and seabed conditions permit, jack-ups are generally the most cost effective solution, and permit standard onshore equipment and site investigation approaches to be used. If the water depth precludes the use of a cost effective jack up, then barges or ships will be required (Figure 12). The cross over is typically in the 15 m to 20 m water depth range.

Figure 12. Geotechnical drilling vessels working at an OWF site in the North Sea

In areas of high current, anchored vessels are a good solution, but generally dynamically positioned ships are used. Use of floating vessels then requires incorporation of heave motion compensators for vessel mounted equipment or the use of seabed mounted equipment. SUT (2014) provide further discussion on the advantages and disadvantages of various vessel and drill platform types, with regard to geotechnical investigation at OWF sites.

In general, seabed founded cone penetration testing (CPT) systems and vessel mounted drilling systems are adopted. Seabed founded drilling systems have not been an economic option to date and are technically limited for these types of investigations. However, new innovative systems (Figure 13) mean that future investigations can now consider hybrid drilling techniques, such as the SEADEVIL™ system (Looijen & Peuchen, 2017), which can offer improved drilling for difficult ground conditions and deployment of a full suite of investigation tools.

Each stage of geotechnical site investigation will normally comprise predominantly seabed founded in situ testing to refusal with a number of locations continued to greater depth with down-the-hole in situ testing. This is usually complimented at a select number of locations with high quality sampling to enable characterisation of the significant soil units, especially regarding strength, stiffness at various strain levels, and how these vary under cyclic loading. Some in situ measurement of small strain stiffness, either P-S suspension logging or seismic cone testing should be considered. SUT (2014) provide recommendations for best practice geotechnical work scope, based on foundation type. Kort et al. (2015) present a more detailed summary of geotechnical investigation planning for GBS foundation design.

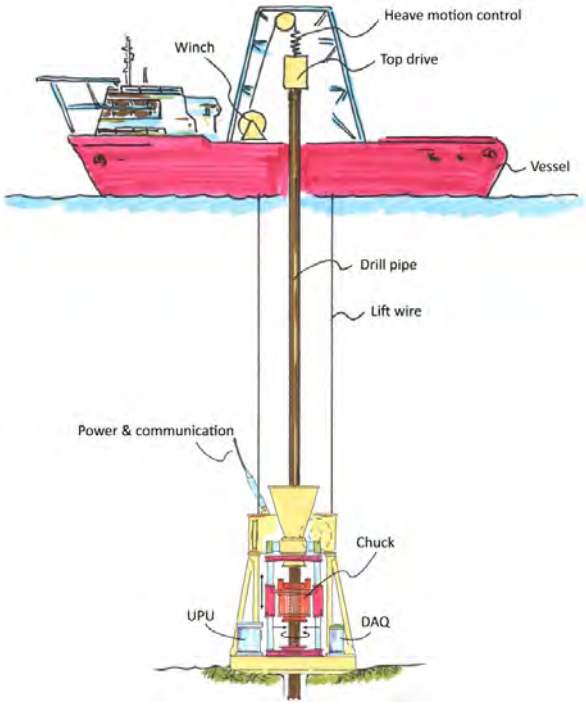

Figure 13. The SEADEVIL™ hybrid vessel-seafloor drilling (Looijen & Peuchen, 2017)

5.2 *Coverage of Investigation*

It has previously been mentioned that a typical OWF site will generally cover a large area of the seafloor, encountering a

range of geological formations (both laterally and with depth). Clearly then, acquiring detailed geotechnical data at all structure locations within the OWF area may not appear warranted, especially where a well-developed ground model is in place; however the requirement for location specific investigation should be considered in the context of the geotechnical risk assessment for the site. This consideration should be informed by the outcomes of the desk study and the information contained within the preliminary ground model, but also taking into account the geotechnical design requirements and track record of the proposed foundation concept(s). High levels of lateral and vertical variability may necessitate structure location specific investigation, or indeed several investigation points across a single foundation footprint, in order to reduce the foundation design and installation risks as low as reasonably practicable for the project.

The subject of data coverage for different foundation concepts is discussed by SUT (2014) and is not restated here, except to note that ultimately the extent of the geotechnical investigation may be governed by the national design code requirements applicable for the OWF site under consideration.

5.3 *In situ testing*

In situ testing is predominantly static CPT and this is a good way of getting high quality geotechnical data at many locations in a cost effective manner. If conditions are suitable, seabed testing units, which are available with up to 20t thrust, can test up to 40m below seafloor, or beyond. Even if hard ground conditions restrict the achievable penetration to an average of, say, 14m, it is usually cost effective to undertake seabed founded testing and then to progress with down-the-hole CPTs in drilled boreholes to cover the full depth of interest for the foundations. This is normally done at least c. 30% of locations providing near continuous data for soil profiling (Figure 14).

It is also possible to extend the measurement potential of the standard CPT cone to include additional sleeves. For example, the dual sleeve cone (Figure 15) measures not only initial soil:sleeve frictional resistance, but also the resistance measured after a degree of further relative soil:steel movement (approximately 0.5 m for the example dual sleeve cone shown in Figure 12). This yields valuable data regarding the degradation or 'friction-fatigue' of soil resistance with relative soil:steel movement, which is a key input into assessing skirt penetration resistance for suction bucket foundations and soil resistance to driving (SRD) for driven piles.

Performing seismic cone penetration tests (SCPT) at a number of locations, typically 10 to 20%, is a small increment in time and cost over standard CPTs and gives valuable information on in situ small strain stiffness. SCPT is not always possible due to limited cone penetration, in which case seismic wave velocity (P-S) suspension logging can be used in the unsupported open borehole, so long as borehole stability is sufficient. Often P-S suspension logging is performed at the end of a sampling or CPT borehole and the borehole quality is not very good. Consideration should be given to undertaking the logging in a bespoke borehole, or to undertake it at intermediate stages during the drilling of a borehole for other purposes so that the logging is undertaken in a fresher, better quality hole. In practice a combination of SCPT and P-S logging is undertaken to cover the full depth of the foundation. High pressure dilatometer or pressuremeter testing can also be undertaken to gain insight in soil stiffness and strength at a rage of strain levels. However this testing is rather slow, and hence expensive, and only produces discrete data points. The test is also often difficult to interpret and therefore may provide limited resolution in strong to hard soils. Only a few number of tests therefore are generally undertaken and the data extrapolated by correlation with other data, e.g. CPT.

Future advances are expected to include wider use of recently developed fibre optic cone technology, which offers significantly improved accuracy of cone resistance and pore pressure measurements compared to existing strain gauge technology (Fugro, 2017). Other in situ characterisation tools, such as the SEADART^{TM} free fall penetrometer, may provide cost-effective shallow geotechnical data in very soft clays for the purpose of cable route investigation, where seafloor detection may be of concern (Peuchen et al., 2017). Further developments are expected to include cyclic CPT measurements under increasing accuracy of control.

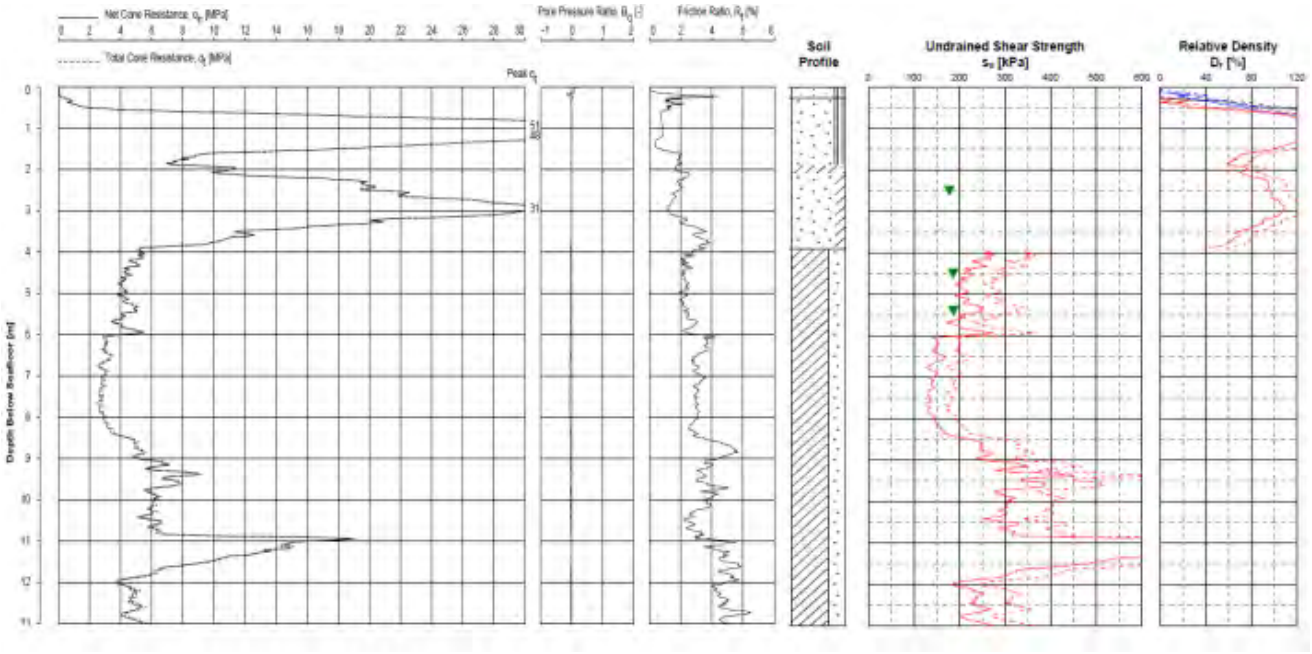

Figure 14. Example measured and interpreted CPT data

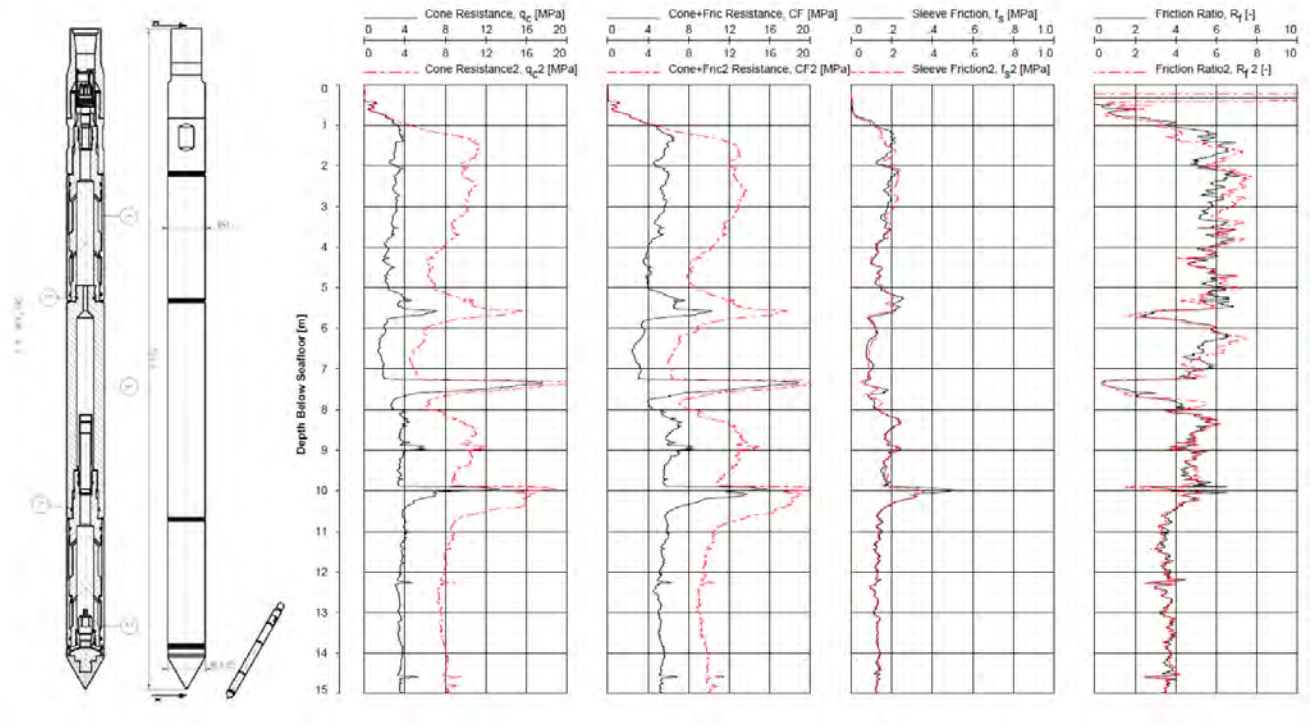

Figure 15. The dual sleeve cone and example cone resistance and sleeve friction data. Operated by Fugro

5.4 *Sampling*

Sampling boreholes will typically be undertaken at 10% of the WTG locations and at each OSS location to obtain samples (Figure 16) in the significant soil layers to feed into the design. The data obtained from the soil samples is then extrapolated across the site by correlation with the in situ test data via the calibrated ground model. Sampling boreholes should be taken in the direct vicinity of CPT boreholes to allow best correlation between CPT and laboratory datasets.

The SUT (2014) provide a summary of seabed sampling equipment suitability by soil type. For the majority of the equipment types considered by the SUT, two types of samples are obtained during marine geotechnical investigation: 'undisturbed' and disturbed samples. The sample type describes whether or not the soil is recovered in an intact state, with regard to the in situ condition. Obtaining undisturbed sand samples is not practicable offshore and therefore laboratory testing on cohesionless soils is by necessity on reconstituted samples, as discussed later. Clayton et al. (1995) provide a comprehensive discussion on sampling and sample disturbance effects for onshore site investigations, which is equally valid for use of sampler and coring methods offshore. Similar discussion is presented for very soft to soft clays by Ladd and DeGroot (2003). Sample disturbance has a significant impact on laboratory element testing, as considered later in this paper.

The soil samples from geotechnical investigation ground truth the in situ testing data and also enable the measurement of the soil properties needed for efficient turbine foundation design, such as the variation of soil stiffness and strength at different strain levels and during cyclic loading. If rock is encountered in the foundation zone, then triple barrel rotary coring can be undertaken. This can also be used to obtain high quality samples in more competent soils. To obtain good quality core recovery requires very good heave compensation when working from a floating vessel. Even from a jack-up platform, high quality coring can be challenging as there is a large unsupported length of coring string compared to onshore coring operations.

As with the selection of in situ methods and for the reasons highlighted earlier in this paper, soil sampling for OWF characterisation is subject to the recommendation proposed by Clayton et al (1995): *"…there is a need to match the sophistication of sampling to the sophistication of the analysis and design of the project… the constitutive modelling of soil behaviour via finite element or finite difference analyses, will require high-quality sampling and testing methods."*

5.5 *Laboratory testing*

SUT (2014) recommend the following geotechnical data requirements for foundation and cable installation design:

- Description and index classification
- Strength parameters (for different failure modes, monotonic and cyclic)
- Soil modulus and damping parameters
- Permeability and consolidation parameters
- Liquefaction potential
- Thermal conductivity
- Chemical composition

In situ measurements alone are not able to meet the data requirements for geotechnical analyses since these do not provide information across the full stress-strain range to be investigated for design and cannot cover a full range of foundation loading conditions. Laboratory testing is therefore required to provide information on soil and rock classification and mechanical response under monotonic and cyclic loading for foundation design, and chemical and thermal properties for cable assessments.

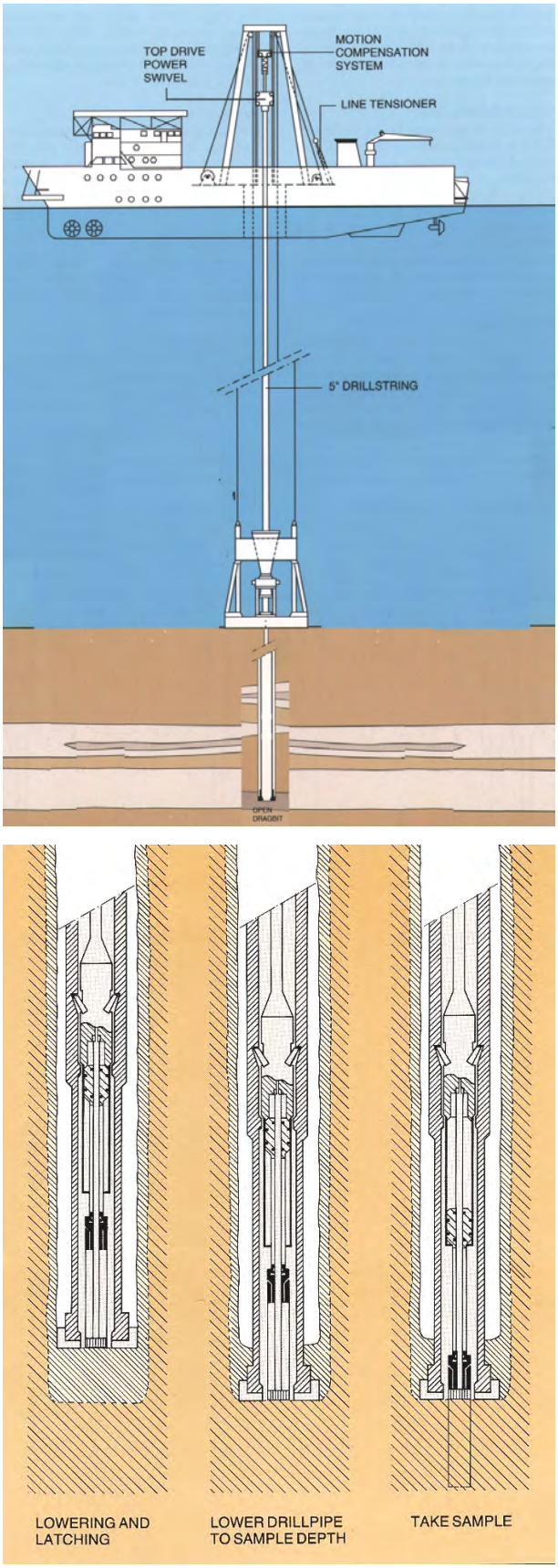

Figure 16. Conceptual illustration of the (API drilling mode) downhole sampling process

SUT (2014) provide guidance on the applicability of various conventional laboratory testing methods for measurement of different soil parameters in several soil types, including sand, clay, carbonate/calcareous soils and weak rock. These guidelines provide a useful point of reference for planning of laboratory testing programmes, but they should not be considered as (and are not intended as) blanket recommendations across all foundation and geotechnical analysis types. For example, any geotechnical design process including consideration of advanced numerical analysis is likely to generate input data requirements outside of the scope of guidance provided by SUT.

It is common to make a distinction between 'routine' and 'advanced' testing, where the latter are subject to a higher degree of interpretation and require an increasingly careful and detailed specification. Rather than make an arbitrary distinction based on apparatus type, 'routine' laboratory testing should be considered as all tests scheduled for general soil unit identification, ground model calibration, basic engineering classification and parameter profiling, regardless of test type. 'Advanced' testing is then defined as those tests from which detailed and specific soil behavioural models will be developed for application in advanced geotechnical analyses (e.g. FEA or similar, site response analysis (SRA) or other state-of-the-art design methods for monotonic or cyclic foundation response analysis).

5.5.1 *Laboratory Specimens*

Scheduling, specification and interpretation of laboratory testing should always consider the methods employed to obtain and prepare the geotechnical samples being tested. As discussed previously, sample disturbance has a significant impact on the laboratory measured response of both soft clays (Lunne et al., 2006) and overconsolidated clays (Berre, 2014). Disturbance can also be introduced during preparation of intact soil specimens. X-ray examination of sample cores can be considered ahead of testing, to ensure samples are of suitable quality and free of inclusions which may otherwise compromise the quality of the test data.

The soil fabric created during soil deposition and subsequent processes in situ contributes to mechanical response to the extent that the effect of structure can be of equal importance to those of soil state (void ratio) or effective stress (Mitchell and Soga, 2005). Given the range of depositional and post-depositional processes acting on soils offshore, laboratory reconstitution is unlikely to result in test specimens which are fully representative of the in situ soil state. The laboratory measured response of reconstituted soil specimens will then depend on the preparation method employed (Ishihara, 1993). The effect on drained strength is less significant due to rapid changes in fabric during shearing and tends to diminish with increasing relative density. However, the effect on undrained response of sand is particularly pronounced and has been investigated extensively in relation to the liquefaction potential of cohesionless soils (Vaid et al. 1999; Sze and Yang, 2014).

The procedures necessary to minimise the impact of disturbance and specimen preparation should therefore be carefully considered during specification of laboratory testing. In addition the designer's interpretation of the laboratory data should also be carefully considered. For example, the specification of direct simple shear (DSS) testing as input to pile design should consider the boundary conditions of the problem as replicated during testing. Application of normal stresses representing in situ effective vertical stress would be relevant for lateral pile design (Erbrich et al., 2010). For axial pile design it may be necessary to consider a normal stress which is representative of the effective horizontal stress

condition, imposed on a test specimen cut at 90 to vertical from a sample core (Figure 17, Rattley et al., 2017; Sim et al., 2013).

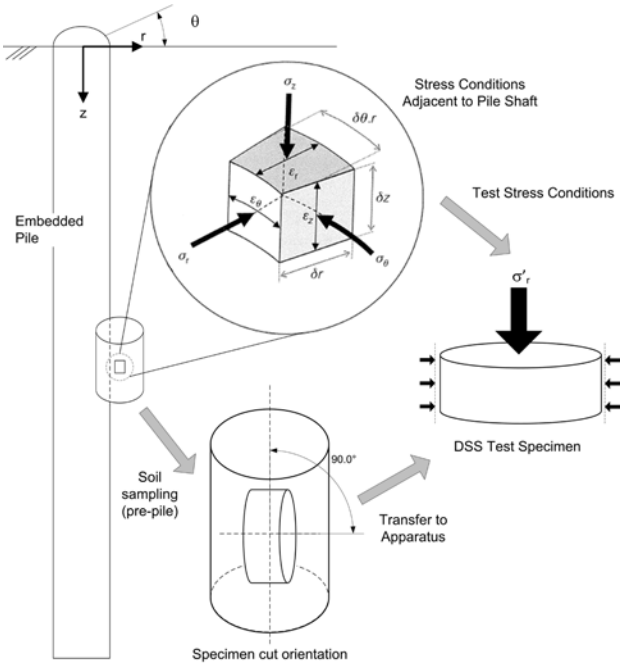

Figure 17. Schematic of stress conditions in a soil element adjacent to a pile shaft as translated in the DSS test for axial pile design (see also Sim et al., 2013)

5.5.2 *Routine Laboratory Testing*

Laboratory test schedules for routine testing should be assigned by an experienced engineer based on the soil conditions sampled during geotechnical investigation and considering the evolutionary ground model developed for the site. The latter is essential for a coherent site characterisation process. A laboratory testing schedule should contain sufficient testing to allow classification of the soils general engineering characteristics and to enable soil unit identification for calibration of the ground model. Laboratory testing should therefore be scheduled on a soil unit basis. Where the same soil unit is encountered at a range of depths at a number of borehole locations, it is recommended to schedule tests at different depths to provide a composite, near-continuous data profile across the soil unit. More frequent testing, including thermal conductivity tests, may be required on soil near the seafloor for cable route assessments. In addition to index testing, tests should be scheduled for derivation of general design parameter profiling with depth, at each sampled location, for input to foundation design.

For cohesionless material, minimum and maximum density (min/max) tests are typically undertaken to define the approximate limits of the void ratio which may be present in-situ. Results from these tests are used to calculate target densities for laboratory reconstituted soil specimens, based on relative density values determined from the CPT data. While this method is generally considered standard practice for offshore site characterisation, it should be noted that the approach is subject to some known limitations surrounding determination of maximum in situ density (Blaker et al ,2015). Consolidated drained (CD) triaxial compression tests are typically performed for determination of drained shear strength (friction angle).

Undrained shear strength is measured offshore using index test methods. More accurate test methods, where effective stresses can be controlled (to varying degrees), such as consolidated undrained (CU) triaxial compression and extension tests and DSS tests, can be performed onshore on undisturbed and reconstituted soil specimens. For routine (profiling) effective stress triaxial testing (Figure 18), the specimen is tested under conditions that replicate as closely as possible the (pre-sampling) in situ stress conditions at the sample depth. Performing a range of strength testing enables undrained strength to be measured under different failure modes, providing an indication of strength anisotropy of the soil. From these measurements the variance in the cone factor (N_{kt}) can be estimated for each mode of failure, allowing near-continuous undrained shear strength profiling from CPT cone resistance data. Note that it is a common oversight not to perform undrained strength testing on cohesionless soil samples. While this data may not be required for jacket pile design, a drained soil response assumption is unlikely to be valid for the majority of large diameter monopile and suction bucket design cases. For these foundations response may be at least partially drained under environmental loading, even for relatively uniform sand profiles (Peralta et al., 2017; Whyte et al., 2017) and the undrained strength of sands soils is of practical interest for design. For the same reason, laboratory measurements of soil permeability may also be required.

As a part of the 'routine' triaxial test, bender elements can be included in the platens of the apparatus to measure (vertically propagating) shear wave velocity for determination of shear modulus at very small strain (G_{max}). This parameter is a key input for geotechnical design of WTG foundations and frequent laboratory measurement allows reliable correlation with in situ data for parameter profiling. The measurements can also be used to assess the reliability of laboratory reconstituted specimens by comparison to in situ data.

Figure 18. 'Routine' triaxial testing systems. Operated by Fugro

Consolidation tests (i.e. constant rate of strain (CRS) or incremental oedometer tests) are undertaken to assess the one-dimensional compression response of the soil. The tests are particularly important for soils with a variable geological stress history. In the North Sea, for example, many soil formations have experienced significant variation in past stress levels due to geological processes including: desiccation and glacial advancement and retreat, and other process such as creep (ageing) and physicochemical actions. Geological history therefore has an important influence on the mechanical response of marine soils. Evans (2011) describes how the framework proposed by Burland (1990), Chandler (2000) and Cotecchia and Chandler (2000) can provide an essential interpretation basis for understanding the influence of soil structure on the response of clay soils, allowing for sedimentation structure and post-sedimentation effects. Both intact and reconstituted tests are therefore recommended.

Understanding stress history in clay soil units can also provide valuable insight into the past loading of underlying sand units, since the variation of stress conditions in situ (i.e. evolution of in situ K_0) cannot be assessed by direct measurements on disturbed sand samples.

5.5.3 *Advanced Laboratory Testing*

Jardine (2014) provides an overview of advanced laboratory testing which focusses on the application of highly instrumented testing to increase understanding of foundation response. Jardine illustrates the practical value of such testing, but also demonstrates that the aims of the foundation analysis must be well understood in order that the laboratory testing is carefully specified and controlled to maximise the applicability of the resulting data. Jardine ends his discussion with an observation which is now fundamental to the WTG foundation design process: *"Advanced laboratory testing is vital to advancing all difficult geotechnical engineering problems where the outcomes depend critically on the detailed constitutive behaviour of the ground."*

The complexity of geotechnical analysis being routinely applied for WTG foundation design is increasing. To achieve foundation optimisation under complex loading it is necessary to perform advanced analysis (FEA or similar) and such analysis requires careful calibration of a suitable constitutive model to predict soil response. Advanced laboratory test programmes are therefore required to evaluate specific aspects of soil response as considered critical for detailed geotechnical analysis. These generally include, but are not limited to:

- Cyclic behaviour
- Nonlinear stiffness (stress/strain dependent)
- Rate dependency and creep
- Anisotropy
- Critical states
- Yield surface and plastic potential

The laboratory testing required to investigate the above includes dynamic testing such as the cyclic triaxial (CTXL) (Figure 19), cyclic direct simple shear (CSS) (Figure 20) and resonant column (RC) tests. However it can also include carefully planned series of tests performed on routine testing apparatus such as the triaxial and oedometer apparatus, with variations in test specification lying outside of those that would be considered for routine (profiling) testing. Triaxial testing may also include non-standard measurements, such as high resolution local strain measurements, vertical and horizontal BE determinations and mid-height pore water pressure measurements to increase the scope of the test data for constitutive model calibration.

Figure 19. Cyclic triaxial testing systems. Operated by Fugro

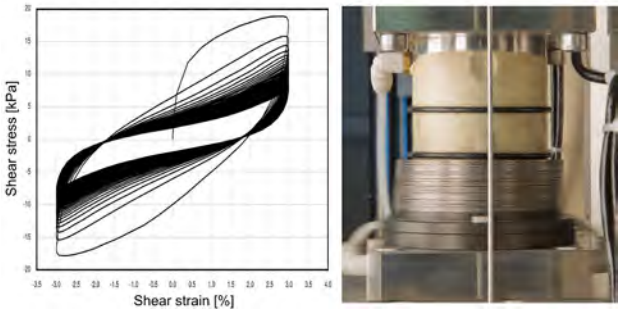

Figure 20. Clay specimen during cyclic shearing in the CSS apparatus and resulting stress-strain data. Operated by Fugro

The soil response measured in any stress or strain controlled laboratory test is a direct function of the boundary conditions applied by the test apparatus and the processes that preceded the shearing stage of the test and the application of such processes should be carefully considered. For example, the following are just a small subset of considerations which may be pertinent to specification of advanced (or routine) laboratory testing:

- Specimen reconstitution method
- Saturation of heavily overconsolidated (swelling) clays
- Preconsolidation regime
- Consolidation stress paths
- Consolidation creep intervals
- Pre-shearing stages
- Cyclic loading ratios, etc.

The above discussion reinforces the requirement for the advanced laboratory testing programme for an OWF development to be considered with full understanding of the laboratory testing methods and knowledge of the design method input requirements. It is therefore recommended that a clear distinction is made between the routine testing and advanced testing programmes (although scheduling is interdependent), with the former being developed jointly between the engineering designers and the site characterisation team. It is of limited value to schedule a generic suite of 'advanced' laboratory testing simply to satisfy a general preconception of applicability to design. To ensure project value advanced laboratory testing must be coordinated with a clear design strategy and ideally based on knowledge gained from preliminary geotechnical analyses using soils data generated from the preliminary ground model. This approach will ensure adequate opportunity for a thorough gap analysis approach to test scheduling.

6 GEOTECHNICAL INTERPRETATION

Geotechnical interpretation and parameterisation forms the link between the ground model and the engineering design process (Figure 5) and is interrelated to each. As part of the geotechnical interpretation it is necessary to define soil unitisation and design parameter profiling with depth for each WTG and OSS structure location. Soil behavioural models, considering aspects of response as discussed earlier, are developed. If required, constitutive model calibration will also be performed as input to engineering analyses (Figure 21).

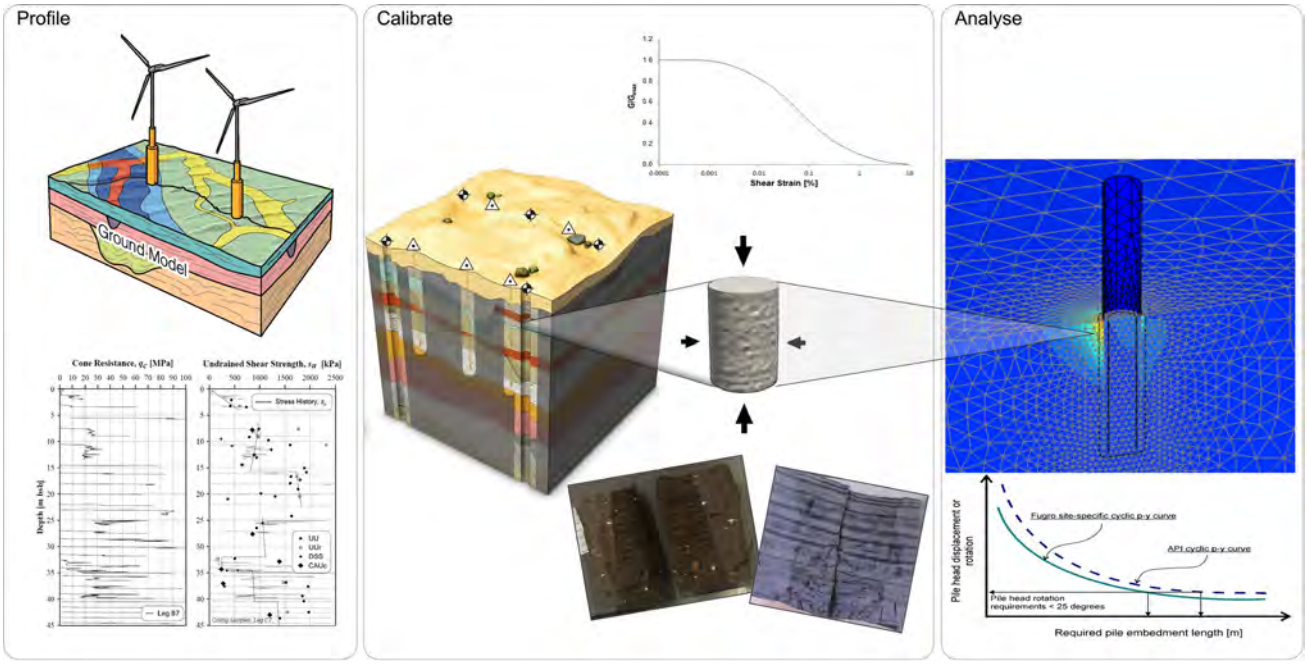

Figure 21. Schematic example of the geotechnical interpretation and analysis process for WTG monopile analysis (up to FEA)

If the integrated site characterisation process has been well coordinated, taking input from all parties, then the geotechnical interpretation will proceed successfully without highlighting data gaps which lead to: excessive conservatism in parameter selection, extended parametric analyses, or a requirement for further geotechnical investigation. Ultimately it is likely that some extrapolation of data is required as part of the geotechnical interpretation; this should be performed with care and taking due consideration of all available published and proprietary experience available. Common with development of geotechnical investigation programmes, geotechnical interpretation should be progressed jointly between the engineering designers and the characterisation team.

7 CONCLUDING REMARKS

The large spatial extents of offshore wind farms mean that an effective site characterisation is essential to achieving optimised geotechnical design. A compartmentalised approach of separate geophysical and geotechnical investigations followed by independent engineering design can lead to undesirable project surprises which impact on overall project schedule and cost. The solution is a phased approach to integrated marine site characterisation where all technical aspects are considered. The benefits of this approach become keenest when the requirements of the geotechnical design process are considered at an early stage of the characterisation process. The best outcomes will invariably be obtained when the site characterisation process is advanced with full knowledge of the design method input requirements.

To ensure project value, detailed geotechnical investigation must be coordinated with a clear design strategy, ideally based on knowledge gained from preliminary geotechnical analyses using soils data generated from the preliminary ground model. This approach will ensure adequate opportunity for a thorough gap analysis approach to investigation planning. Wherever possible the required geotechnical investigation programmes should be developed jointly between the engineering designers and the characterisation team.

8 REFERENCES

Augustesen A., Leth C., Ostergaard M., Moller M., Duhrkop J. and Barbosa P. 2015. *Design methodology for cyclically and axially loaded piles in chalk for Wikinger OWF*. Proc. Int. Symp. on Frontiers in Offshore Geotechnics, Oslo, Norway.

Berre T. 2014. Effect of sample disturbance on triaxial and oedometer behaviour of a stiff and heavily overconsolidated clay. *Canadian Geotechnical Journal*, 51(8), 896-910.

Blaker O., Lunne T., Vestgarden T., Krogh L., Thomsen N., Powell J. and Wallace C. 2015. *Method dependency of determining maximum and minimum dry unit weights of sands.* Proc. Int. Symp. on Frontiers in Offshore Geotechnics, Oslo, Norway.

Burland J.B. 1990. On the compressibility and shear strength of natural clays. *Geotechnique*, 40(3), 327-378.

Bye A., Erbrich C., Rognlien B. and Tjelta T. 1995. *Geotechnical Design of Bucket Foundations*. Proc. Offshore Technology Conference Houston, USA. OTC 7793.

Byrne B.W., Mcadam R., Burd H. and Skov Gretlund J. 2015. *New design methods for large diameter piles under lateral loading for off-shore wind applications.* Proc. Int. Symp. on Frontiers in Offshore Geotechnics, Oslo, Norway.

Campbell K. 1984. *Predicting offshore soil conditions*. Proc. Offshore Technology Conference Houston, Texas. OTC 4692.

Chandler R.J. 2000. Clay sediments in depositional basins: the geotechnical cycle. *Q. J. Eng. Geology*, 33, 7-39.

Clayton C., Matthews M. and Simons N. 1995. *Site Investigation*. Blackwell Science, Oxford.

Cotecchia F. and Chandler R.J. 2000. A general framework for the mechanical behaviour of clays. *Geotechnique*, 50(4), 431-447

Erbrich C. 2004. *A New Method for the Design of Laterally Loaded Anchor Piles in Soft Rock*. Proc. Offshore Technology Conference, Houston, USA. OTC 16441.

Erbrich C., O'Neill M., Clancy P. and Randolph M. 2010a. *Axial and Lateral Pile Design in Carbonate Soils*. Proc. Proc. Int. Symp. on Frontiers in Offshore Geotechnics, Perth, Australia.

Erbrich C., Barbosa-Cruz E., and Barbour R. 2010b. *Soil-Pile Interaction During Extrusion of an Initially Deformed Pile*. Proc. Int. Symp. on Frontiers in Offshore Geotechnics, Perth, Australia.

Erbrich C., Wallbridge P. and Yamamoto N. 2016. *Numerical Modelling of Seismically Induced Settlement for Ichthys Riser Support Structure*. Proc. Offshore Technology Conference OTC Asia 2016. OTC-26778-MS.

Evans T. 2011. *A systematic approach to offshore engineering for multiple-project developments in geohazardous areas*. Proc. Int. Symp. on Frontiers in Offshore Geotechnics, Perth, Australia.

Fookes P. 1997. Geology for engineers: the geological model, prediction and performance. The First Glossop Lecture. *Q. J. Engineering Geology*, 30, 293-424.

Giannakou A., Makra A., Chacko J. and Poudens O. 2016. *Evaluation of Kinematically Induced Demands on Offshore Platform Foundations due to Liquefaction*. Proc. Int. Conf. on Natural Hazards & Infrastructure, Chania, Greece.

Ishihara K. 1993 Liquefaction and flow failure during earthquakes. *Geotechnique*, 43(3), 351-451.

Jardine R.J.J. 2014. Advanced laboratory testing in research and practice. *Geotechnical Research*, 1(1), 2-31.

Kallehave D, Byrne B., Thilsted C., Mikkelsen K.K. 2015. Optimization of monopiles for offshore wind turbines. *Phil. Transactions*, Royal Society Publishing.

Kort D., Pederstad H. and Nowaki F. 2015. *Planning of soil investigation for GBS foundation design*. Proc. Int. Symp. on Frontiers in Offshore Geotechnics, Oslo, Norway.

Ladd C.C. and DeGroot D.J. 2003. *Recommended practice for soft ground site characterization*. Proc. PanAmerican Conf. Soil and Rock America, USA

Lunne T., T Berre and S Strandvik. 1997. *Sample disturbance effects in soft low plasticity Norwegian clay*. Proc. Conf. on Recent Developments in Soil and Pavement Mechanics, Rio de Janeiro, Brazil.

Lunne T., Berre T., Andersen K.H., Strandvik S. and Sjursen M. 2006. Effects of sample disturbance and consolidation procedures on measured shear strength of soft marine Norwegian clays. *Canadian Geotechnical Journal*, 43(7), 726-750.

Mason A. and Smith C. 2016. Integration of geophysical and geotechnical data for the routing of power cables. Conf. Applied Shallow Marine Geophysics. Near Survey Geosciences, Barcelona, Spain.

Mitchell J.K. and Soga K. 2005. *Fundamentals of soil behaviour*. Wiley & Sons, USA.

Muir Wood A., Mackenzie B., Burbury, D., Rattley M., Clayton C., Mygind M. and Liingaard M.A. 2015. *Design of large diameter monopiles in chalk at Westermost Rough offshore wind farm*. Proc. Int. Symp. on Frontiers in Offshore Geotechnics, Oslo, Norway.

Perelta P., Ballard J.C., Rattley M. and Erbrich C. 2017. *Dynamic and Cyclic Pile Soil Response Curves for Monopile Design*. Proc. Int. Conf. Offshore Site Investigation and Geotechnics, London, UK.

Looijen P. and Peuchen J. 2017. *Seabed investigation by a novel hybrid of vessel-based and seafloor-based drilling techniques*. Proc. Int. Conf. Offshore Site Investigation and Geotechnics, London, UK.

Peuchen J., Looijen P. and Stark N. 2017. *Offshore characterisation of extremely soft sediments by free fall penetrometer*. Proc. Int. Conf. Offshore Site Investigation and Geotechnics, London, UK.

Power P., Clare M., Rushton D. and Rattley M. 2011. *Reducing Geo-risk for Offshore Development*. Int. Symp. on Geotechnical Risk and Safety.

Rattley M., Costa L., Jardine R. and Cleverly W. 2017. *Laboratory test predictions of the cyclic axial resistance of a pile driven in North Sea soils*. Proc. Int. Conf. Offshore Site Investigation and Geotechnics, London, UK.

Sim W., Aghakouchak A. and Jardine R.J. 2013. Cyclic Triaxial Tests to Aid Offshore Pile Analysis and Design. *Geotechnical Engineering*, 166 (2), 111-121.

Society for Underwater Technology (SUT). 2014. *Offshore Site Investigation Committee, 2014, Guidance Notes for the Planning and Execution of Geophysical and Geotechnical Ground Investigations for Offshore Renewable Energy Developments*. SUT, London.

Sze H. and Yang J. 2014. Failure Modes of Sand in Undrained Cyclic Loading: Impact of Sample Preparation. *Journal of Geotechnical and Geoenvironmental Engineering*, 140(1), 152-169.

Thomas S. 2017. *A Phased and Integrated Data Interpretation Approach to Site Characterisation*. Proc. Int. Conf. Offshore Site Investigation and Geotechnics, London, UK.

Vaid Y.P., Sivathayalan S. and Stedman D. 1999. Influence of specimen reconstituting method on the undrained response of sand. *Geotechnical Testing Journal*, 22(3), 187–195.

Vattenfall. 2016. Mines found at Horns Rev 3 site [online] http://news.vattenfall.com/en/article/mines-found-horns-rev-3-site

Whyte S., Rattley M., Erbrich C.E., Burd H.J. and Martin C.M. 2017. *A practical constitutive model for soil structure interaction problems involving dense sands*. Proc. Int. Conf. Offshore Site Investigation and Geotechnics, London, UK.

Zdravkovic L., Taborda D.M.G., Potts D.M., Jardine R.J. and Sideri M. 2015. *Numerical modelling of large diameter piles under lateral loading for offshore wind applications*. Proc. Int. Symp. on Frontiers in Offshore Geotechnics, Oslo, Norway.

Design aspects for monopile foundations

Aspects du dimensionnement pour les fondations monopieux

Harvey J. Burd, Byron W. Byrne, Ross A. McAdam, Guy T. Houlsby, Chris M. Martin, William J.A.P. Beuckelaers

Department of Engineering Science, Oxford University, UK, email: harvey.burd@eng.ox.ac.uk

Lidija Zdravković, David M.G. Taborda, David M. Potts, Richard J. Jardine

Department of Civil and Environmental Engineering, Imperial College London, UK

Ken Gavin, Paul Doherty, David Igoe

Formerly University College Dublin, Ireland

Jesper Skov Gretlund, Miguel Pacheco Andrade

DONG Energy Wind Power

Alastair Muir Wood

Formerly DONG Energy Wind Power

ABSTRACT: This paper describes the outcome of a recently completed research project – known as PISA – on the development of a new process for the design of monopile foundations for offshore wind turbine support structures. The PISA research was concerned with the use of field testing and three-dimensional (3D) finite element analysis to develop and calibrate a new one-dimensional (1D) design model. The resulting 1D design model is based on the same basic assumptions and principles that underlie the current *p-y* method, but the method is extended to include additional components of soil reaction acting on the pile, and enhanced to provide an improved representation of the soil-pile interaction behaviour. Mathematical functions – termed 'soil reaction curves' – are employed to represent the individual soil reaction components in the 1D design model. Values of the parameters needed to specify the soil reaction curves for a particular design scenario are determined using a set of 3D finite element calibration analyses. The PISA research was focused on two particular soil types (overconsolidated clay till and dense sand) that commonly occur in north European coastal waters. The current paper provides an overview of the field testing and 3D modelling aspects of the project, and then focuses on the development, calibration and application of the PISA design approach for monopiles in dense sand.

RESUME : Ce papier décrit les résultats d'un projet de recherche terminé récemment – connu sous le nom de PISA – portant sur le développement d'une nouvelle procédure pour le dimensionnement des fondations monopieux pour les structures support des éoliennes offshore. La recherche PISA s'est intéressée à l'utilisation d'essais in-situ sur pieux et d'analyse (3D) par éléments finis afin de développer et de calibrer un nouveau modèle de dimensionnement unidimensionnel (1D). Le modèle de dimensionnement 1D obtenu est basé sur les mêmes hypothèses et principes fondamentaux à la base de la méthode p-y actuelle. Cependant, la méthode est étendue afin d'inclure des composants supplémentaires à la réaction du sol sur le pieu, et améliorée afin de fournir une meilleure représentation du comportement de l'interaction sol-pieu. Des fonctions mathématiques – appelées 'soil reaction curves' (courbes de réaction du sol) – sont utilisées afin de représenter les composants individuels de la réaction du sol dans le modèle de dimensionnement 1D. Les valeurs des paramètres requis pour spécifier les courbes de réaction du sol pour un scenario de dimensionnement donné, sont déterminés au moyen d'un ensemble d'analyses de calibration 3D par éléments finis. La recherche PISA s'est concentrée sur deux types de sols spécifiques (argile glaciaire surconsolidée et sable dense) communément présents dans les eaux côtières du nord de l'Europe. Le présent papier offre une vue d'ensemble des caractéristiques des essais in-situ sur pieux et des modélisations 3D du projet, et se concentre ensuite sur le développement, la calibration et l'application de l'approche de dimensionnement PISA pour les monopieux dans du sable dense.

KEYWORDS: monopile design, 1D model, soil reaction curves

1 INTRODUCTION

The monopile is the dominant foundation system for current and planned offshore wind farm developments in shallow coastal waters, particularly in Europe. Monopile foundations in this application are typically designed with the aid of simplified analysis approaches, such as the '*p-y*' method and its variants, in which the foundation is modelled as an embedded beam, with the lateral load-displacement interaction between the soil and pile represented by non-linear functions known as *p-y* curves. Simplified computational models of this sort facilitate the development of multiscale optimisation procedures in which models of the performance of individual wind turbine structures are employed within a computational framework to optimise an entire windfarm. For a wind turbine foundation model to be useful in this context, it must be fast to compute and sufficiently accurate and reliable for design purposes. Analyses based on the *p-y* method can be computed rapidly, but current forms of the *p-y* method – which have their origins in the design of long, relatively flexible piles – are widely regarded as being unreliable for the design of monopiles with relatively small values of L/D (where L is embedded length and D is pile diameter), see e.g. Doherty and Gavin 2011.

A recent project – known as PISA (**PI**le **S**oil **A**nalysis) – employed field testing and computational modelling to develop a new design approach for monopile foundations for offshore wind turbine applications. In this new approach, the underlying simplicity of the *p-y* method – in which the pile is modelled as an embedded beam – is retained, but additional components of soil reaction are incorporated within the design model to improve its performance.

The PISA project was conducted, between 2013 and 2016, as a joint industry/university study. The scientific programme was developed by an Academic Working Group (AWG) with members drawn from Oxford University, Imperial College and University College Dublin. The research was supported by the project partners listed in the Acknowledgements section of this paper; Dong Energy acted as the lead partner and main contractor. PISA consisted of three related research strands: (i) reduced-scale field testing of monopile foundations (with associated site investigation and laboratory soil testing) (ii) three-dimensional (3D) finite element modelling and (iii) the development of a new one-dimensional (1D) modelling approach for design.

The PISA research was focused on monotonic lateral loading, as this was identified to be the area where substantial gains could be achieved. Although it is acknowledged that improved design methods for cyclic loading are needed, it is first necessary to have robust procedures for monotonic loading before addressing more complex cyclic loading issues. The methods developed in PISA are capable of future extensions to cyclic loading, and additional cyclic testing was conducted during the field testing phase to aid such extensions.

To limit the scope of the research the project was concerned specifically with two sets of soil conditions that are commonly encountered in north European coastal waters: (i) a stiff overconsolidated clay till and (ii) a dense to very dense marine sand. At an early stage in the project, potential sites for the field tests were sought, with approximately homogeneous profiles consisting of each of these two soil types. The outcome of this process was that a site at Cowden in the north east of England was selected as the clay site and a site at Dunkirk in northern France was selected as the sand site.

The current paper provides an overview of the design approach that was developed during the PISA project, together with a description of the process that was employed to calibrate the 1D design model for a representative offshore soil profile consisting of dense sand. The development of representative soil conditions and the model calibration process were based on the results of the Dunkirk field tests and associated 3D finite element modelling.

A similar process to calibrate the design model for a representative offshore clay till site (not discussed in the current paper) is described in Byrne et al. 2017.

2 THE PISA DESIGN APPROACH

2.1 *Formulation of the PISA design model*

The components of the PISA design model are illustrated in Figure 1. A monopile foundation is represented in the model as an embedded beam with moment M_G and horizontal force H_G applied to the pile at the ground surface. Four separate components of soil reaction are assumed to act on the embedded monopile. Consistent with the standard *p-y* method, a distributed lateral load, p (units of force / length) acts on the pile. Additionally, a distributed moment, m (units of force×length / length) is applied; this distributed moment is caused by the vertical tractions that are induced at the soil-pile interface when local pile rotations occur, as indicated in Figure

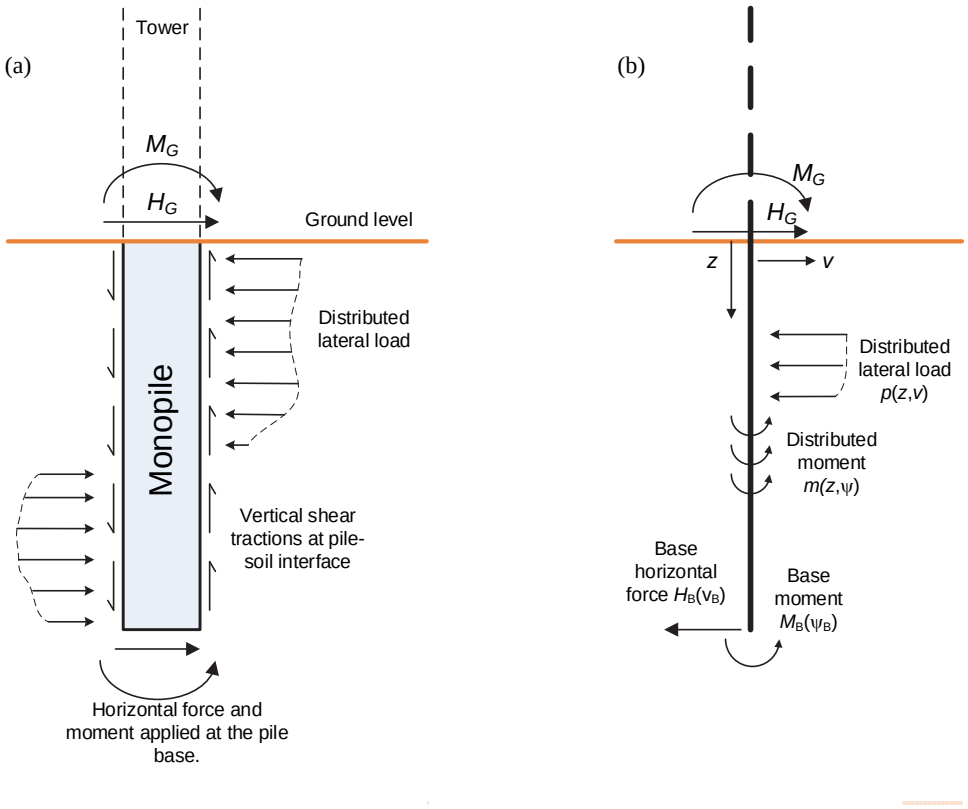

Figure 1. PISA 1D monopile model (a) assumed soil reactions acting on the monopile (b) 1D design model. In the left figure, the soil reactions are shown in the directions that they are likely to act, given the applied loads that are indicated. In the right figure, the indicated directions of the soil reactions are consistent with the cordinate directions shown.

1a and Figure 2.

A horizontal force H_B and a moment M_B acting on the base of the pile are also included in the design model. A four-component model of this sort has previously been employed for the design of drilled shafts for onshore applications (e.g. Lam 2013) and has previously been described in the context of the PISA research by Byrne et al. 2015a.

In the current implementation of the model, the monopile is represented by Timoshenko beam theory, which allows the shear strains in the pile to be incorporated in the analysis in an approximate way. Since the influence of the shear strains on the overall pile deformation is likely to increase as L/D is reduced, the use of Timoshenko theory provides a means of maintaining the robustness of the approach as the embedded length of the monopile reduces (or the diameter is increased).

Consistent with the conventional *p-y* method, the soil reactions are applied to the embedded beam on the basis of the Winkler assumption, i.e. in which the p and H_B components are specified to be functions only of the local pile displacement, v, and m and M_B are specified to be functions only of the local pile cross-section rotation, ψ. Functions relating the soil reactions and the local pile displacements (or rotations) are termed 'soil reaction curves'. Although the Winkler approach neglects the coupling that inevitably occurs between adjacent soil layers, it provides a convenient basis for design calculations, as demonstrated by the widespread adoption of the *p-y* method.

It should be noted, however, that soil reaction curves determined on the basis of the Winkler approach are unlikely to be unique. Appropriate soil reaction curves may depend, for example, on the relative magnitude of the translational and rotational movements of the pile. It is desirable, therefore, to calibrate the soil reaction curves using pile deformation modes that are representative of those that are expected to be experienced by full-scale wind turbine monopile foundations.

The PISA design model reduces to the standard *p-y* approach when m, H_B and M_B are set to zero (and appropriate choices are made on the relationship between p and the local lateral pile displacement, v). Experience has shown, however, that m, H_B and M_B become increasingly important as L/D is reduced (Byrne et al. 2015a). The distributed moment component, for example, depends on the pile diameter; it increases in magnitude as the pile diameter is increased. Similarly the force and moment reactions H_B and M_B at the base of the pile become increasingly significant as L/D is reduced. The four-component model in Figure 1 therefore provides a rational way of addressing a feature of the *p-y* method, that has come to be known as the 'diameter effect', in which the standard *p-y* curves (e.g. API 2010, DNV 2016) are typically found to become increasingly unreliable as the pile diameter is increased, or the pile length is reduced (e.g. Alderlieste et al. 2011, Doherty and Gavin 2011, Lam 2013).

The design model in Figure 1 has been implemented as a 1D finite element model adopting a Galerkin formulation. The implementation is based on standard procedures for non-linear finite element analysis. The functions representing the soil reaction curves are embedded in the 1D model (in much the same was as a constitutive model is embedded in a standard 3D finite element program) with parameters specified by the user.

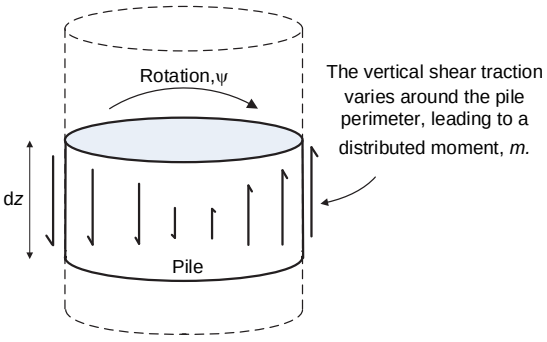

Figure 2. Diagrammatic view of the vertical tractions acting at the soil-pile interface for an elemental length of pile, dz, These tractions are assumed equivalent to a distributed moment reaction, m.

2.2 *Selection and calibration of the soil reaction curves*

The functions selected to represent the soil reaction curves are, to an extent, arbitrary. They should, however, be capable of representing the soil reactions for behaviour ranging from small displacements (needed, for example, to predict the dynamic response and natural frequencies of a wind turbine structure) to the large displacement response (required for the calculation of the Ultimate Limit State, ULS). The conventional cube root function for *p-y* curves in clay (DNV 2016) is unsuitable (unless modifications are introduced) since it implies an infinite initial stiffness. The two-parameter hyperbolic tangent function typically adopted for *p-y* curves in sand (DNV 2016) employs parameters to control both the initial stiffness and the ultimate value of the distributed lateral load. However, it is not possible to tune this function to match the shape of the response between these two limits, or to specify the magnitude of displacement needed to mobilise the ultimate value of distributed load.

In the current work, a four-parameter conic function – described in further detail later – is employed for each of the soil reaction curves in the design model. This four-parameter function appears to provide a reasonable compromise between ability to represent the soil reactions at an appropriate level of detail and the desirability (from a practical perspective) of minimizing the total number of parameters in the model.

Ideally, the soil reaction curves employed in the PISA design model would be calibrated directly, using the results of field testing on full-sized monopiles. However, conducting experiments on full-sized structures would be prohibitively expensive and it would be impractical to devise a test programme that encompasses all of the relevant soil, pile and loading parameters. Also, considerable technical difficulties exist in devising instrumentation systems to determine the various soil reaction components from the measured pile performance.

In PISA, an alternative approach was adopted, in which the calibration of the soil reaction curves in the 1D design model was related, indirectly, to the results of the field testing campaigns conducted during the project, as illustrated in Figure 3. This model calibration process, which employed three separate activities (field testing, 3D finite element modelling and 1D model development) is summarized in general terms below.

Field tests involving lateral loading of monopiles were conducted, at a reduced scale, at the two selected test sites (Cowden and Dunkirk). Bespoke 3D finite element models

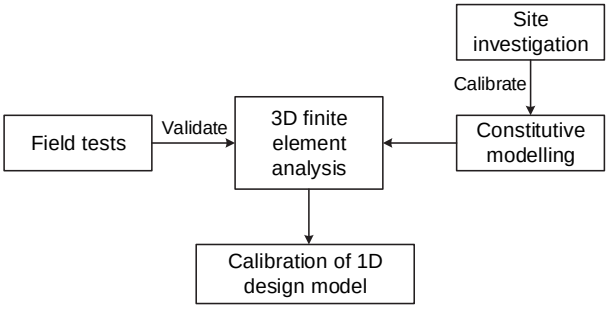

Figure 3. PISA design model development process.

were developed for several of the field test piles. The constitutive models that were selected for the analyses, to reproduce the behaviour of the two soils, were calibrated using the results of advanced site investigations employing pre-existing data combined with intensive new laboratory and field investigations conducted during the PISA project (Zdravković et al. 2015). Data obtained from the field tests were compared with the 3D finite element results to confirm the veracity of the 3D modelling procedures; this process is indicated as 'validate' in Figure 3. A key feature of this validate process is that artificial means of achieving a match between the numerical model and the field tests were rigorously rejected.

Once the 3D finite element simulations of the field tests had been completed, a separate 3D finite element parametric study (referred to below as the 'calibration analyses') was conducted. These calibration analyses adopted homogeneous clay and sand profiles that were based on the soil conditions at each of the two test sites, but adjusted to obtain soil profiles that are representative of offshore conditions. The soil at the onshore Dunkirk test site, for example, was interpreted to have a (small) suction near the surface. Since this is unrepresentative of submerged offshore conditions, a surface layer with negative pore pressures was not included in the 3D finite element calibration analyses employed to develop the PISA sand model. The calibration analyses adopted a range of pile geometries and loading conditions that were judged to span the likely design space for full-sized monopiles.

Numerical data from the 3D finite element calibration analyses were used, directly, to calibrate the soil reaction curves employed in the PISA 1D model. This approach provides an indirect link between the field test data and the 1D model, via the use of 3D finite element modelling procedures. Data processing activities that would be infeasible for the field data (such as extracting the individual soil reaction curves from the soil-pile interface tractions) can be conducted straightforwardly when applied to the 3D finite element results.

The current paper provides a description of the application of this process to calibrate the PISA 1D model for a homogenous sand profile with relative density D_R = 75% based on the Dunkirk field tests, employing the procedures indicated in Figure 3. The paper also demonstrates the application of the 1D model to two design cases with pile parameters that differ from those employed in the 3D finite element calibration process.

3 DUNKIRK FIELD TESTING CAMPAIGN

3.1 *Site details*

The Dunkirk test site is located in a coastal area in northern France, near to the town's Port Ouest. Earlier laboratory and field research described by Chow 1997, Kuwano 1999, Jardine et al. 2006, Ahgakouchak 2015 and Ahgakouchak et al. 2015 showed that the site consists principally of a dense Flandrian sand with a surface layer (about 3m thick) of dense hydraulically-placed sand that has the same geological origin as the deeper Flandrian deposit. New CPTu and seismic cone soundings conducted for PISA and new advanced laboratory tests described by Liu et al. 2017 show that the hydraulic fill and Flandrian sand layers of the soil present relative densities of 100% and 75% respectively, with a critical state friction angle of $\phi'_{cs} = 32^o$. The laboratory tests provide extensive information on the sands stress-dilatancy behaviour and highly non-linear stiffness characteristics.

3.2 *Testing details*

Monopiles with diameter D = 0.273 m, 0.762 m and 2.0 m, and values of L/D between 2 and 10 were installed at the test site. The piles were instrumented with a range of above and below ground instrumentation, including inclinometers, optical fibre Bragg grating strain gauges and extensometer strain gauges. Testing was conducted using the arrangement shown diagrammatically in Figure 4. The test piles were loaded at a height h (termed 'load eccentricity') above ground via a hydraulic ram reacting against a reaction pile. Most of the field tests employed a protocol in which the applied horizontal load, H, was controlled to apply a constant ground-level velocity of D/300 per minute to the pile. At various stages during these constant velocity tests, the applied load was held constant, to allow observations to be made of time-dependent behavior (e.g. due to creep and/or consolidation). A test was considered complete when (i) the ground-level pile displacement exceeded $v_G = D/10$ and (ii) the ground-level pile rotation exceeded 2°. A few tests were conducted at elevated displacement rates and a limited amount of cyclic testing was also conducted. The 3D finite element models of the field tests, however, were validated only with respect to the constant velocity tests. Further details of the field testing campaign are given in Byrne et al. 2015b.

4 3D FINITE ELEMENT MODELLING

4.1 *3D finite element analysis of the Dunkirk tests*

3D finite element models were developed for several of the test piles at the Dunkirk site. Analyses were conducted using the finite element program ICFEP (Potts and Zdravković 1999), adopting the modelling procedures outlined in Zdravković et al. 2015.

The chosen constitutive model was a bounding surface plasticity model (Taborda et al. 2014). This is a critical state model within the state parameter framework, capable of reproducing the stress level- and void ratio-dependent behaviour of sands. The model was calibrated using the earlier research by Imperial College, combined with recent triaxial test data on Dunkirk sand reported in Aghakouchak 2015 and Aghakouchak et al. 2015 as well as the work conducted for PISA described by Liu et al. 2017. The interface between the pile and the soil was represented by an elasto-plastic Mohr-Coulomb model with zero cohesion and a friction angle of 32º.

Detailed consideration of the near-surface ground conditions indicated that the 3 m thick hydraulic fill layer developed higher CPT q_c resistances than had been found in the mid-to-

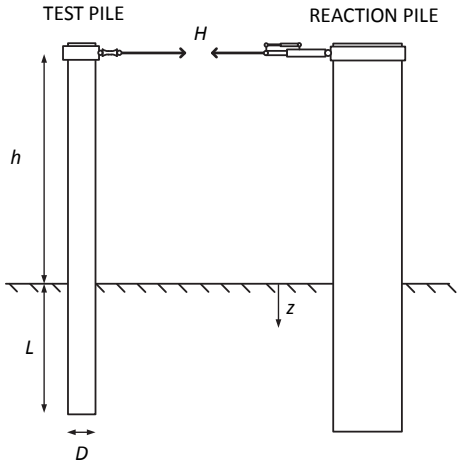

Figure 4. Illustration of the pile testing system employed at the Cowden and Dunkirk sites.

late 1990s investigations described by Chow 1997 and Jardine et al. 2006. It was postulated that the additional shallow resistance was a result of either ageing in the hydraulic fill, local spatial variations, light cementation between the sand grains, or of suctions due to partial saturation. Detailed investigation to fully explain these variations was not feasible. However, piezocone tests did show clear signs of suctions developing at shallow depths and the analyses therefore employed a realistic limited suction (i.e. pore pressures less than hydrostatic) in the soil above the level of the water table (estimated to be at a depth of 5.4 m below ground level). It is noted that the additional complexities involved in modelling unsaturated surface layers are absent from offshore sites, where soils are typically assumed to be fully saturated.

Example field data for a D = 0.762 m, L = 4 m pile (identified as pile DM4) tested at the Dunkirk site, are shown in Figure 5. Figure 5a shows the relationship between the applied lateral load H and the lateral displacement of the pile at ground level, v_G. The constant load steps in the field data indicate the hold periods that were prescribed during the testing process. Also shown in Figure 5a are an unload-reload loop conducted soon after the start of the test, and the unloading response of the pile at the end of the test. The response computed using the 3D finite element analysis is also shown in Figure 5a; this shows good agreement with the field data. Comparisons of a similar quality were obtained for the field test data and the corresponding finite element models for the two large diameter (D = 2 m) piles tested at the site.

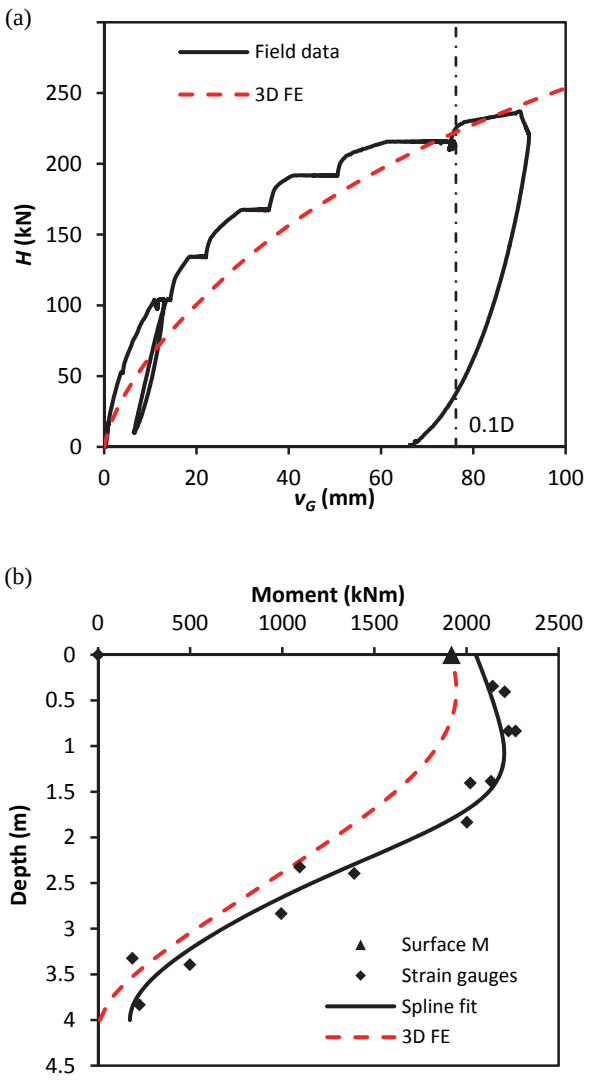

Figure 5. Comparisons between the field measurements and 3D finite element results for pile DM4 (D = 0.762 m, L = 4 m) tested at Dunkirk; (a) horizontal load, H, vs. ground displacement, v_G, response (b) below-ground bending moments at $H = 192$ kN, $v_G = 41$ mm. In (b) 'Surface M' indicates the bending moment determined from the value of the horizontal load, 'Strain gauges' refers to bending moments inferred from the fibre optic Bragg grating strain gauges, 'Spline fit' indicates a spline that has been fitted to the bending moment data.

Figure 5b shows the measured bending moments induced in pile DM4, deduced from the strain gauge instrumentation, at the start of the hold period for $H = 192$ kN. The distribution of bending moments determined from the 3D model at this same value of applied horizontal load is also shown in the figure. The agreement between the two sets of data appears reasonable.

The finite element results were found to be less consistent with the field data for the shortest D = 0.762 m pile (with L = 2.3 m) that was tested at this site. For this relatively short pile, the finite element results are highly dependent on the initial conditions that are assigned to the unsaturated surface layer. Since some uncertainty existed on the appropriate conditions to apply to this surface layer (as a consequence of limitations in the available site investigation data) the finite element results are regarded as being less robust for this particular pile.

The broadly satisfactory comparison between the field test data and the numerical analysis supports the use of the 3D finite element model to calibrate the soil reaction curves in the 1D design model, as described below.

4.2 *3D finite element calibration study*

The calibration analyses were based on the soil conditions at the Dunkirk test site, together with the constitutive model and associated constitutive parameters that were employed in the finite element analyses of the field tests. Certain adjustments to the Dunkirk soil profile were required, however, to ensure that the profile employed in the calibration analyses was representative of an offshore homogeneous sand site. In particular, in the calibration study, hydrostatic pore pressures were assigned to the entire soil profile (noting that a region with a small suction above the water table was adopted to model the Dunkirk field tests). Although the Dunkirk site profile shows variations in sand state with depth, uniform relative density of 75% was assigned to the soil for these calibration analyses.

Eleven calibration analyses were conducted for monopile dimensions and load eccentricities in the range $5\text{m} < D < 10\text{m}$, $2 < L/D < 6$, $5 < h/D < 15$. A typical mesh employed for the

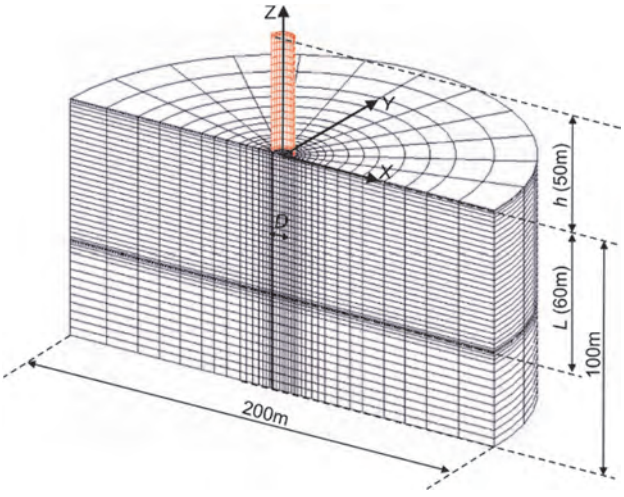

Figure 6. 3D finite element mesh for pile C4 (D = 10 m, L = 60 m, h = 50 m) in the calibration analysis set.

calibration analyses is shown in Figure 6.

5 1D MODEL DEVELOPMENT FOR SAND

5.1 *Soil reaction curves*

Numerical representations of the soil reaction curves (referred to below as 'numerical soil reaction curves') were determined from the 3D finite element calibration analyses using a process in which nodal forces acting at the soil-pile interface, and stresses in the interface elements between the pile and the soil, were extracted. Numerical data on the distributed lateral load, *p*, were determined by integrating the *x*-components (using the coordinate system in Figure 6) of the horizontal tractions acting on the pile at discrete values of depth along the pile. Data on the distributed moment were obtained by integrating the vertical soil-pile tractions, accounting for the distance between the pile neutral axis and the point on the pile perimeter where the traction is applied. The force and moment reactions at the pile base were obtained by integration of the stresses in the layer of soil elements immediately below the pile base.

To proceed, it is necessary to use appropriate non-dimensional parameters to process the numerical results and also to formulate the soil reaction curves. The non-dimensional forms employed for the PISA sand model are listed in Table 1, where σ'_{vi} is the local value of initial vertical effective stress, G is the local value of small-strain shear modulus, v and ψ are the local pile lateral displacement and cross-section rotation respectively. The normalization process for the distributed moment follows a pattern that differs from the other three soil reaction components. It was identified, when reviewing the numerical soil reaction curves, that the distributed moments appeared to scale conveniently with the current value of the local distributed lateral load, *p*. Since the vertical tractions induced on the pile arise as a consequence of friction at the soil-pile interface, it seems plausible that the magnitude of *m* is correlated with the normal tractions applied to the pile. The normal tractions are, themselves, closely associated with the distributed lateral load, *p*; it therefore seemed appropriate in the current modelling to normalize the distributed moment, *m*, with the local value of the distributed load, p. The use of the non-dimensional form $\bar{m}$ in Table 1 implies that the distributed moment *m* is a product of the current value of *p* and a separate function of the local rotation, ψ. Although this adds to the complexity of the 1D model, this form of soil reaction curve is incorporated straightforwardly within the 1D finite element formulation used in the model.

The soil reaction curves employed in the 1D model, referred to below as the 'parametric soil reaction curves' are formulated in terms of the normalized variables listed in Table 1. The four-parameter conic function used to represent the soil reaction curves is illustrated in Figure 7, where $\bar{x}$ signifies a normalized displacement or rotation variable and $\bar{y}$ signifies the corresponding normalized soil reaction component. The conic function is calibrated by the specification of four parameters $(k, n, \bar{x}_u, \bar{y}_u)$, each of which has a straightforward interpretation. The parameter k specifies the initial slope; $\bar{y}_u$ is the ultimate value of the normalized soil reaction and $\bar{x}_u$ is the normalized displacement (or rotation) at which this ultimate value of soil reaction is reached. The parameter n $(0 < n < 1)$ determines the shape of the curve.

Values of the parameters defining the soil reaction curves for each of the soil reaction components were determined via an automatic optimization process conducted over the complete set of eleven 3D finite element calibration analyses. In conducting this optimization, the soil reaction curve parameters for $\bar{p}$ and $\bar{m}$ were assumed to vary linearly with depth along the pile.

Initial values for the model parameters were determined by least-squares fitting of the numerical soil reaction curves, moderated by eye. The calibration was further improved by allowing adjustments to these parameters to optimize the fit between the H vs v_G responses computed using the 3D finite element model and the 1D model for $0 < v_G < 0.1D$.

Table 1. Parameter normalization.

Normalized variable	Non-dimensional form
Distributed lateral load, $\bar{p}$	$\frac{p}{\sigma'_{vi}D}$
Lateral displacement, $\bar{v}$	$\frac{vG}{D\sigma'_{vi}}$
Distributed moment, $\bar{m}$	$\frac{m}{pD}$
Pile rotation, $\bar{\psi}$	$\frac{\psi G}{\sigma'_{vi}}$
Base shear load, $\bar{H}_B$	$\frac{H_B}{\sigma'_{vi}D^2}$
Base moment, $\bar{M}_B$	$\frac{M_B}{\sigma'_{vi}D^3}$

5.2 *Example soil reaction curves*

Two contrasting examples of the process of fitting the four-parameter conic function to the data extracted from the 3D finite element calibration analyses are shown in Figure 8 and Figure 9.

Figure 8 shows example data on normalized distributed lateral load, $\bar{p}$, at various pile depths, *z*, for a calibration calculation (pile C4) with D = 10 m, L = 60 m. At shallow depths, where soil displacements are relatively large, a peak is typically found to occur in the response, followed by post-peak softening. An example of this type of response, for $z/D = 0.23$ is shown in Figure 8a. This behaviour is closely linked to the dilational characteristics of the soil. Since softening behavior cannot be represented with the four-parameter conic function employed in the 1D model, it was necessary to make an arbitrary choice on the ultimate value $\bar{p}_u$ of the normalized distributed load for incorporation in the model. In the current work, when post-peak softening was observed, $\bar{p}_u$ was taken as an intermediate value between the peak and final values determined from the 3D finite element calibration data. The resulting parametric soil reaction curves (determined by optimizing over the complete set of eleven calibration analyses) are plotted for a range of depths, *z*, for the full range of soil displacements developed in the calibration analysis in Figure 8a, and for small displacements in Figure 8b. Differences are shown to exist between the data from the 3D calibration analysis and the resulting calibrated soil reaction curves. As the parametric curves are tailored to provide a representation of the

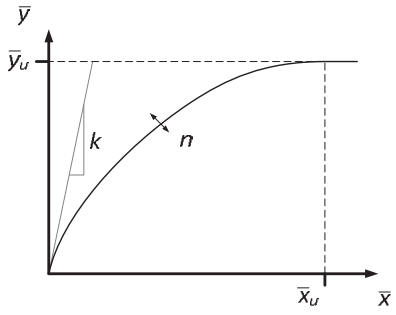

Figure 7. Four-parameter conic function employed to represent the soil reaction curves.

3D finite element data across the complete set of calibration analyses, they therefore can sometimes exhibit the tendency, apparent in Figure 8, to depart significantly from the 3D calibration data for individual piles at a local level.

In contrast, Figure 9 indicates the match between the parametric soil reaction curve and the numerical data for the base moment for pile C4; in case of this component of soil reaction, the two data sets are seen to agree well.

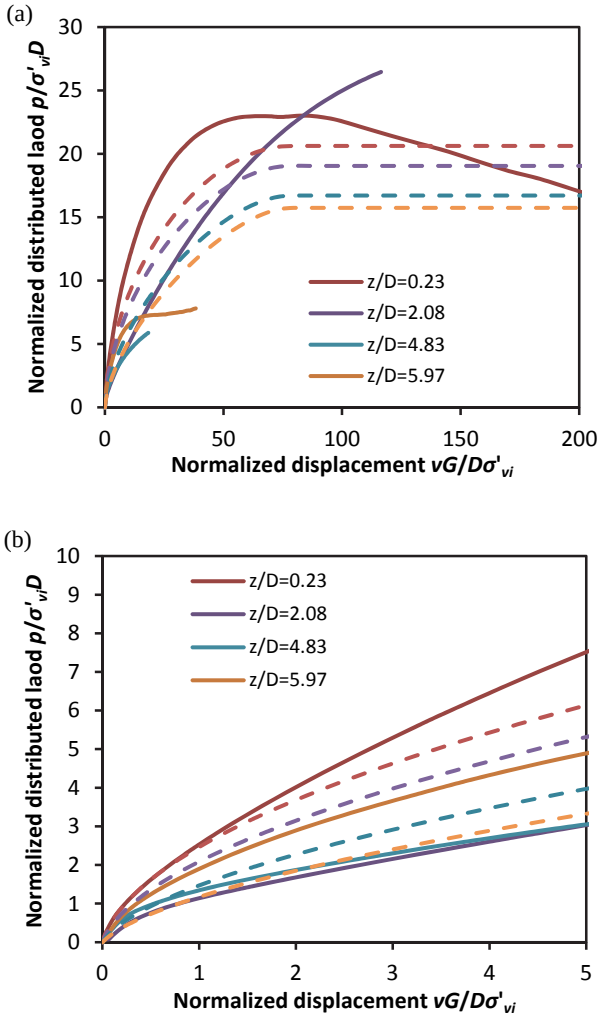

Figure 8. Example soil reaction curves for normalized distributed lateral load for calibration pile C4 (D = 10 m, L = 60 m). Solid line are data from the 3D calibration analysis of the pile, dashed lines are the calibrated soil reaction curves; (a) large displacements, (b) small displacements.

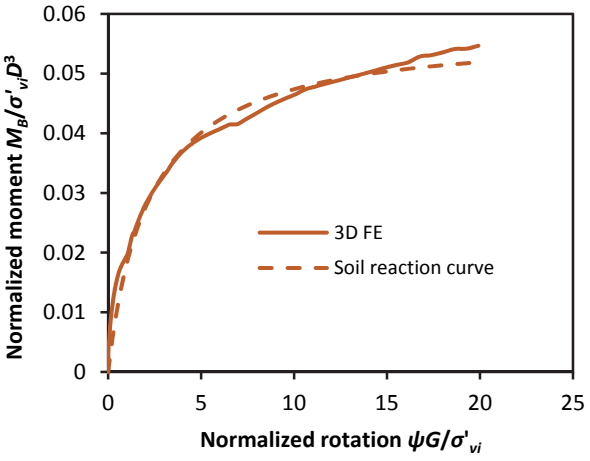

Figure 9. Parametric soil reaction curve (shown as a dashed line) and 3D finite element calibration data (shown as a solid line) for the base moment M_B, for pile C4 (D =10 m, L = 60 m).

5.3 *1D model analysis of the calibration cases*

Example comparisons of the computed H vs v_G response for two of the D = 10 m diameter calibration piles are shown in Figure 10; pile C1 has length 20 m and pile C4 has length 60 m. In spite of the apparently poor performance of the four-parameter function in representing aspects of the computed lateral soil reaction curves for pile C4, as shown in Figure 8, the overall performance of the 1D model – in terms of the extent to which 1D predictions of the H vs v_G response agree with the 3D calibration data for piles C1 and C4 – is seen to be excellent. Similarly close comparisons between the 1D and 3D results were obtained for all of the other calibration analyses.

This exercise indicates that the 1D model is able to reproduce the overall behavior of the calibration piles, although at a local level, significant differences can exist between the calibration data and the parametric soil reaction curves. This well-conditioned aspect of the 1D model is considered to be due to the overall performance being obtained by integrating the soil reaction curves along the entire length of the foundation.

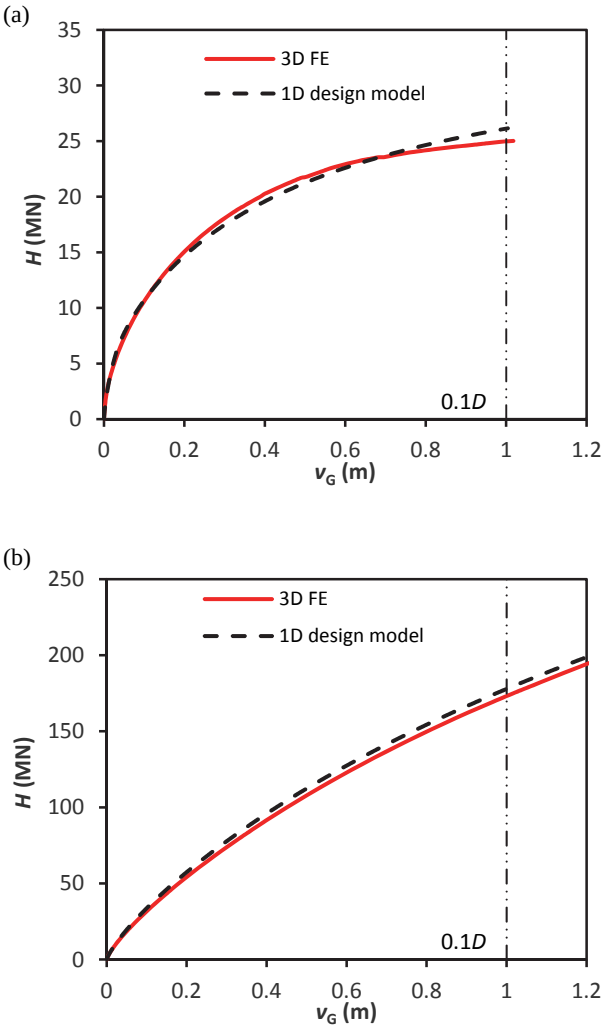

Figure 10. Comparisons between the 3D finite element calibration analyses and the 1D model computed response (a) for pile C1 (D = 10 m, L = 20 m) (b) for pile C4 (D = 10 m, L = 60 m).

Provided that significant systematic errors are absent from the 1D model, the averaging process employed in the modelling procedure appears to have the consequence that the model is remarkably tolerant of imperfect fitting of the data at a local level.

6 DESIGN EXAMPLE

Once the 1D model has been calibrated – or 'trained' – it can be used to determine the performance of a monopile foundation for arbitrary values of geometry and loading parameters that lie within the calibration space. To demonstrate the predictive capability of the model, two separate example design analyses have been considered. The geometric configurations adopted for these test cases, specified in Table 2 (where t is pile wall thickness), were selected to fall within the parameter space adopted for the calibration analyses, as indicated in Figure 11.

Table 2. Pile parameters selected for the two design examples.

Reference	D (m)	H (m)	L (m)	t (mm)
D1	7.5	37.5	22.5	68
D2	8.75	8.75	35	91

The load-displacement responses computed using the 1D model and subsequently the 3D finite element model for both of the design examples, D1 and D2, are shown in Figure 12. The results indicate a close match between the two sets of data over the full range of applied loading (up to a ground level pile displacement of $v_G = 0.1D$). Figure 13 shows the lateral displacements induced in the embedded portions of the piles for an applied horizontal load of $H = 0.75\,H_{max}$, where H_{max} is the value of horizontal load at $v_G = 0.1D$ determined from the 3D finite element analysis. The two sets of data are seen to agree well. The close agreement between the computed responses obtained using the 3D and 1D models for these two design cases is consistent with the assumption implicit in the PISA methodology, that the 1D model provides an efficient means of interpolating the overall pile response computed using the 3D calibration calculations to other pile geometries within the calibration space.

7 DISCUSSION

A method has been presented to calibrate a 1D model of monopile behaviour using a suite of 3D calibration analyses.

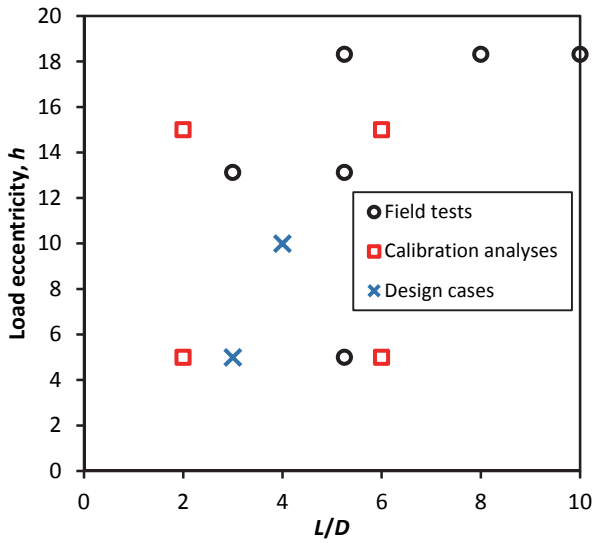

Figure 11. Parametric geometry space for the field tests, the calibration analyses and the design examples.

The calibration process has been demonstrated for an example offshore site where the soil is a uniform, dense sand. In this example, the 1D model is shown to provide a close representation of the overall pile behaviour for each of the calibration analyses. Comparing the 1D model with the data that were used to calibrate it does not, in itself, provide any evidence of its predictive capability. This comparison exercise does, however, indicate that the various approximations and assumptions inherent in the 1D model do not detract significantly from its reliability.

The predictive capability of the 1D model has been demonstrated by means of two independent design examples with pile parameters that differ from those employed in the calibration set (although within the bounds of the calibration space).

It is suggested that the PISA modelling approach could be employed for monopile design in one of two ways. For initial design calculations, it may be appropriate to employ pre-defined functions and parameters to represent the soil reaction curves based on the soil profiles established for any given site

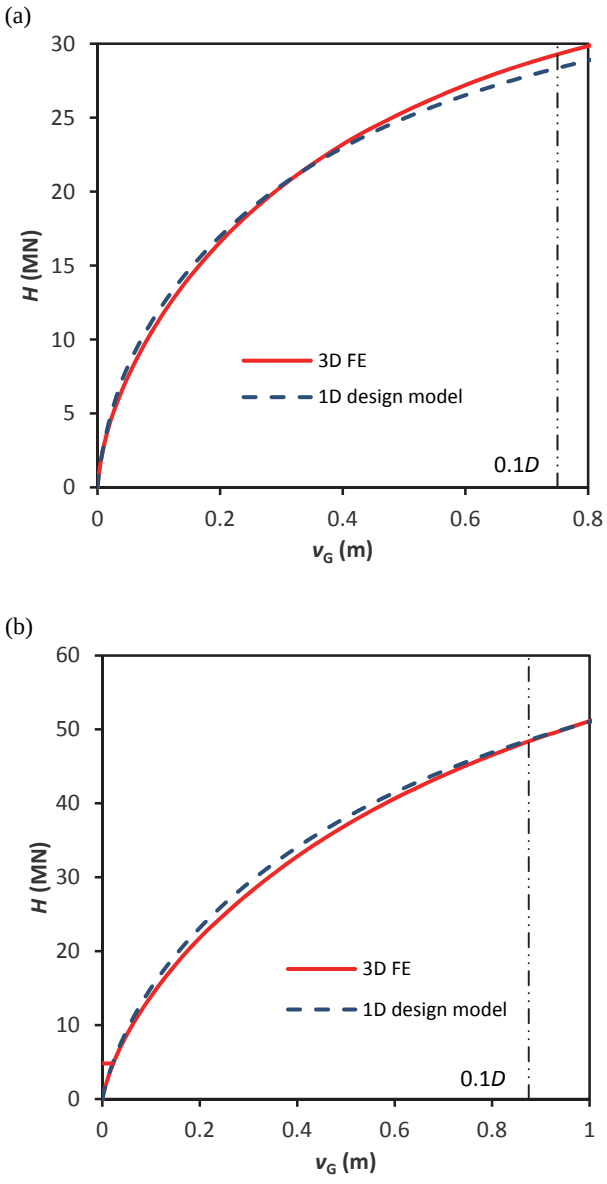

Figure 12. Comparisons between load-displacement responses computed using the 3D finite element model and the 1D model for the two design examples (a) D1 (b) D2.

as characterized by relatively simple index or other testing. (This process is broadly similar to current forms of the *p-y* method). In the PISA terminology, this approach is referred to as the 'rule-based' method.

For more detailed and robust design calculations, an alternative route is proposed in which the site conditions are investigated more intensively with advanced sampling, laboratory and field techniques being applied to establish the detailed behavior of the principal soil types present at any given wind farm location. Bespoke 3D finite element calculations may then be performed that span the likely ranges of soil profiles and the parameter space that will control the final design. Soil reaction curves may then be extracted from the finite element analyses predictions for the soil-pile interface tractions. Procedures for this latter approach – which is termed the 'numerical-based' method – are demonstrated in the current paper for a homogeneous dense sand site. The numerical-based approach is essentially a procedure to train a relatively simple calculation (the PISA 1D model) using data from more detailed 3D finite element analyses. The 1D calculation is rapid to compute, with accuracy that is linked to the fidelity of the 3D finite element models that are employed in the calibration process. This approach means that full use can be made of any site investigation data (via the constitutive model employed in the 3D calibration analyses) in the formulation of the soil reaction curves. Moreover, the method can evolve with future developments in site investigation, constitutive modelling and finite element analysis.

The PISA modelling process is suitable for assessments of the ULS performance as well as for predicting the small-displacement dynamic performance of an offshore wind turbine structure. The current paper is limited to the modelling of monopile behaviour in a dense sand (although a similar calibration study, not reported here, has been completed for an overconsolidated clay till). Further development work is needed to extend the method to other soil types, included layered soils, and to include the effects of cyclic loading.

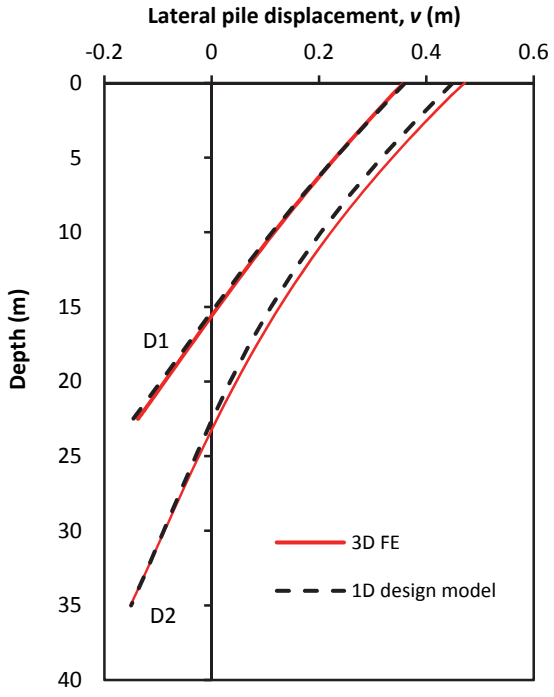

Figure 13. Below-ground lateral displacements for design examples D1 and D2 computed using the 3D finite element model and the calibrated 1D design model. The D1 and D2 results correspond to H = 22.1 MN and 36.15 MN respectively.

8 ACKNOWLEDGEMENTS

The PISA Project was funded by the UK Department for Energy and Climate Change (DECC) and the PISA Industry Partners under the umbrella of the Offshore Wind Accelerator (OWA) program which was designed and is led by the Carbon Trust. The Authors acknowledge the provision of financial and technical support by the following project partners: Alstom Wind, DONG Energy, E.ON, EDF, Iberdrola, innogy, SSE, Statkraft, Statoil, Van Oord and Vattenfall. The Authors also acknowledge the main test contractor for the field test campaign, ESG. Christelle Abadie contributed to the production of the data presented in the paper on the two design examples.

9 REFERENCES

Aghakouchak A. 2015. *Advanced laboratory studies to explore the axial cyclic behaviour of driven piles.* PhD thesis, Imperial College London.

Aghakouchak A., Sim W.W. and Jardine R.J. 2015. Stress-path laboratory tests to characterise the cyclic behaviour of piles driven in sands. *Soils & Foundations*. 44(5), 917-928.

Alderlieste E. A., Dijkstra, J. and Van Tol A. F. 2011. Experimental investigation into pile diameter effects of laterally loaded mono-piles. In *ASME 2011 30th International Conference on Ocean, Offshore and Arctic Engineering*. American Society of Mechanical Engineers, 985-990.

API 2010. *RP 2A-WSD – Recommended Practice for Planning, Designing and Constructing Fixed Offshore Platforms.* Washington: American Petroleum Institute.

Byrne B.W., McAdam R.A., Burd H.J., Houlsby G.T., Martin C.M., Beuckelaers W.J.A.P., Zdravković L., Taborda D.M.G., Potts D.M., Jardine R.J., Ushev E., Liu T., Abadias D., Gavin K., Igoe D., Doherty P., Skov Gretlund J., Pacheco Andrade M., Muir Wood A., Schroeder F.C., Turner S. & Plummer M.A.L. 2017. PISA: new design methods for offshore wind turbine monopiles. *Proceedings of the Society for Underwater Technology Offshore Site Investigation and Geotechnics 8th International Conference on "Smarter Solutions for Future Offshore Developments"*, London.

Byrne B. W., McAdam R., Burd H. J., Houlsby G. T., Martin C. M., Zdravković L., Taborda D. M. G., Potts D. M., Jardine R. J., Sideri M., Schroeder F. C., Gavin K., Doherty P., Igoe D., Muir Wood A., Kellahave D. and Skov Gretlund J. 2015a. New design methods for large diameter piles under lateral loading for offshore wind applications. *Proceedings of Third International Symposium on Frontiers in Offshore Geotechics* 1, 705-710.

Byrne B. W., McAdam R., Burd H. J., Houlsby G. T., Martin C. M., Gavin K., Doherty P., Igoe D., Zdravković L., Taborda D. M. G., Potts D. M., Jardine R. J., Sideri M., Schroeder F. C., Muir Wood A., Kellahave D. and Skov Gretlund J. 2015b. Field testing of large diameter piles under lateral loading for offshore wind applications. *Proceedings of XVI European Conference on Soil Mechanics and Geotechnical Engineering*, Edinburgh, 1255-1260.

Chow F.C. 1997. *Investigations into displacement pile behaviour for offshore foundations.* Ph.D Thesis, Imperial College London.

DNV, 2016. *DNVGL-ST-0126 – Support structures for wind turbines.*

Doherty P. and Gavin K. 2011. Laterally loaded monopile design for offshore wind farms. *Proceedings of the ICE – Energy* 165(EN1), 7-17.

Jardine R.J, Standing J.R and Chow F.C. 2006. Some observations of the effects of time on the capacity of piles driven in sand. *Géotechnique* 55(4), 227-244.

Kuwano, R. 1999. *The stiffness and yielding anisotropy of sand.* PhD Thesis, Imperial College London.

Lam, I.P.O. 2013. Diameter effects on p-y curves. *Deep Marine Foundations - A Perspective on the Design and Construction of Deep Marine Foundations.*

Liu T.F, Aghakouchak A., Taborda D.M.G. and Jardine R.J. 2017. Advanced laboratory characterization of a fine marine sand from Dunkirk, France. *Proc. 19th ICSMGE*, Seoul.

Potts D. M. and Zdravković L. 1999. *Finite element analysis in geotechnical engineering: theory*. London: Thomas Telford.

Taborda D.M.G., Zdravković L., Kontoe S. and Potts D.M. 2014. Computational study on the modification of a bounding surface plasticity model for sands. *Computers and Geotechnics* 59, 145-160.

Zdravković L., Taborda D. M. G., Potts D. M., Jardine R. J., Sideri M., Schroeder F. C., Byrne B. W., McAdam R., Burd H. J., Houlsby G. T., Martin C. M., Gavin K., Doherty P., Igoe D., Muir Wood A., Kellehave D. and Skov Gretlund J. 2015. Numerical modelling of large diameter piles under lateral loading for offshore wind applications *Proceedings of Third International Symposium on Frontiers in Offshore Geotechnics* 1, 759-764.

Design Aspects of Suction Caissons for Offshore Wind Turbine Foundations

Aspects de conception des caissons d'aspiration pour les fondations de turbines éoliennes en mer

Sturm, Hendrik
Computational Geomechanics, Norwegian Geotechnial Institute (NGI), Oslo, Norway, hst@ngi.no

ABSTRACT: This paper provides an introduction to the geotechnical design of suction caisson foundations for *Offshore Wind Turbine* (OWT) foundations. It summarizes the experience gained in a number of projects from across the world and proposes a guidance for the design of future projects. The paper is structured in a logical manner; the first section introduces the general design approach of suction caisson foundations, whereas the individual design aspects are discussed in detail in the subsequent sections. Therein, all relevant aspects are covered, including design basis, installation-, capacity- and serviceability-analysis, assessment of the foundation stiffness, and soil reactions. In the last section other aspects such a grouting, integrated analysis, and application of the presented approach to complete wind farms is briefly discussed.

RÉSUMÉ: Ce papier introduit la conception géotechnique de fondations de caissons de succion utilisés dans les fondations des turbines des éoliennes en mer. Cet article résume l'expérience acquise au cours de projets menés à travers le monde et propose quelques conseils pour l'élaboration de projets futurs. Ce papier est structuré en trois sections. Dans la première partie, différentes approches utilisées lors de la conception des caissons de succion des fondations sont présentées de manière générale. Les aspects individuels et particuliers de la construction sont expliqués en détails plus loin dans cette même section. Tous les aspects pertinents sont couverts allant de la conception à l'analyse de l'installation, de la capacité et de la maintenance à l'évaluation de la rigidité de la fondation et des réactions du sol. Dans la dernier section, d'autres aspects, tels que le ciment, la conception intégrée, et l'application de l'approche présentée à un parc éolien complet sont discutés.

KEYWORDS: suction caissons, offshore wind, design

MOTS-CLES: caissons de succion, éoliennes en mer, design

1 INTRODUCTION

All major offshore wind energy developers worldwide are currently investigating alternatives to the *Monopile* concept, which is widely used for the foundation of *Offshore Wind Turbines* (OWT). This effort is driven by technical considerations – mainly increasing turbine capacities and deeper waters at future wind parks – as well as environmental and economical considerations. A promising foundation concept is the so-called *Suction Caisson*; a hollow steel cylinder closed at the top and opened at the bottom. Suction caissons are installed by means of the self-weight of the structure and a suction pressure applied inside the caisson. Once installed, they resist environmental loads like an embedded shallow foundation, but can also temporarily mobilize considerable suction, which further increases the capacity and stiffness.

Though suction caissons are already used since several decades, practical experience with the short- and long-term behavior of these foundations used for OWTs is limited so far. Notwithstanding the lack of experience, a number of projects have been initiated where suction caissons have been or will be applied. The *Norwegian Geotechnical Institute* (NGI) has been involved in most of these projects, including *Borkum Riffgrund 1* (BKR01), *Borkum Riffgrund 2* (BKR02), *Hornsea 1* (HOW01), *Aberdeen Offshore Wind Farm* (EOWDC), *Hywind Scotland Pilot Park*, and *Southwest Offshore Demonstration Wind Farm* (SWK), providing various services such as laboratory testing, geotechnical design, suction installation support, and health monitoring systems. The experience gained in these and other projects forms the basis for the presented work.

The objective of this paper is to provide an overview of the particular design-requirements and -challenges of suction caissons for the foundation of OWTs, and should assist decision makers to consider this foundation concept in future wind farm projects. The presented design aspects and recommendations can be directly applied in ongoing and future projects, and provides a basis for currently developed standards and guidelines for certification and approval. Not included in this contribution are detailed descriptions of design methodologies as they are widely discussed in the many other publications. However, some references to relevant design methodologies are included. Main focus is to outline OWT-specific design aspects, for both caissons for jackets and mono-caissons.

1.1 General design approach

Suction caissons are used since the 1980s in the *Oil & Gas* (O&G) industry as the foundation of both bottom fixed and floating offshore structures. It is estimated that by the end of 2010 more than 1000 permanent offshore suction caissons and anchors were installed.

In the last decades a vast amount of articles and journal papers were published presenting results of research work and practical experience with suction caissons and anchors. Most of these are addressing particularly deep-water application cases. While in the early years mainly suction caissons in clayey soils were considered, also sandy and layered soils came into the focus in the more recent years. Most publications present theoretical and numerical studies as well as small-scale 1g or Ng model tests (e.g. Byrne 2000, Johansson et al. 2003, Kelly et al. 2006, Jostad et al. 2015a). Only limited measurement data is found from actually built structures. Some examples of installation data are report by Sparrevik (2002), Colliat et al. (2007), Aas et al. (2009), Langford et al. (2012), Solhjell et al. (2014), Saue et al. (2017), and in-place measurement data on prototypes by Schonberg et al. (2017), Svanø et al. (1997).

The experience gained in the last 30 years from the O&G industry provides a good basis for the design of suction caissons for OWTs. However, there are a number of important aspects, which are different, and which require particular consideration in the design of caissons for OWTs:

- Most offshore wind farms are located in relatively shallow

waters where the sub-surface has been exposed in the more recent geological history to significant environmental changes such as glacial periods, dry periods and floods, yielding pronounced soil layering comprising a large range of different soil types and properties (e.g. Cotterill et al. 2017, Dove et al. 2016). As a result, soil profiles may vary significantly both in depth and horizontally.

- The loading conditions are different for OWT foundations. With increasing turbine size operational and other load cases can govern the geotechnical design, being potentially more severe than a conventional 50-, or 100-years storm event, which is typically used in the design of offshore O&G structures. In addition, these design-critical load cases may have considerably recurrence rates during the lifetime of an OWT.

- The response of the sub-structure of an OWT is very sensitive to the foundation behavior, i.e. stiffness and (differential) settlements. Although this can be an important design aspects for O&G structures, it is in general more important for OWTs due to the high-cyclic loading conditions during operation and the sensitivity of the turbine on a tilt.

To complicate matter, the supposed conservative assumptions made in the geotechnical design in order to cope with these and further challenges are not necessarily conservative for the structural design – and vise versa, for apparently conservative assumptions made in the structural design. Thus, input and assumptions in both the geotechnical and the the structural design need to be aligned and consistent.

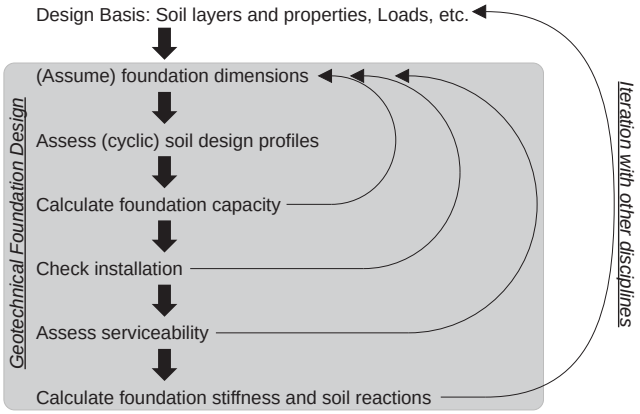

Figure 1: Schematic presentation of the iterative and interdependent workflow of suction caissons design

The consistency is achieved by an iterative design approach as illustrated in Figure 1. The geotechnical design of a suction caisson foundation comprises 5 main activities: 1) Assessment of the cyclic soil properties for the given boundary conditions, i.e. load conditions, foundation geometry, and soil layering and properties; 2) Foundation capacity assessment for short- and long-term loading; 3) Prediction of the installation resistance and corresponding required suction pressure; 4) Serviceability assessment, i.e. short- and long-term settlement, displacement and rotation; and 5) Calculation of the foundation stiffness including corresponding soil reactions. The activities are interdependent and typically need to be solved in an iterative manner in order to optimize the caisson geometry.

Furthermore the geotechnical design is embedded into a design loop interacting with other disciplines. The basis for the geotechnical design will be continuously updated based on the results of both the geotechnical analysis and other involved disciplines. The structural designer may update the properties of the caisson and the sub-structure, the turbine manufacturer may update the (cyclic) loads, and the soil layering and properties may be complemented by updated field and laboratory test data, to name a few.

The workflow of the (geotechnical) design approach illustrated in Figure 1 is not very much different to that of any other foundation. However, it is important to be aware of the interdependency, as this pose a natural limitation on the achievable optimization. A typical project comprises different phases; e.i. feasibility study, pre-FEED[1], FEED and Detailed Design. Each of these phases can comprise one or several iteration(s). Current research aims to solve some of the activities in an integrated manner (e.g. Krathe & Kaynia 2016, Page et al. 2016, Skau et al. 2017). That means it is tried to model the complete OWT in one analysis to capture the interdependency. However, all parts, and in particular the soil-foundation-system, is often represented in these analysis in a simplified way in order to limit the required calculation time. Thus an integrated analysis may not be suitable for an optimization, but can be very beneficial for other aspects, in particular for the assessment of loads.

1.2 Interface between disciplines

The iterative design approach illustrated in Figure 1 requires a physical interface between the different disciplines at which input, or output, respectively, is exchanged. There are in principal two types of information which need to be exchange between the geotechnical and structural designer:

- The geotechnical designer gets loads and delivers back the corresponding deformations, i.e. load-deformation curves. These curves are practically represented by lumped stiffness values describing the response of the soil-foundation-system in one point. The stiffness values are typically provided in matrix form and can comprise of linear secant stiffness values or non-linear tangential stiffness values.

- The structural designer requires for the caisson design distributed loads and/or deformations acting on the skirts and lid. These distributed loads/deformations are often denoted *Soil Reactions* as they describe the response of the soil. Soil reactions can be provided as unit loads, total loads or linear springs (i.e. Winkler-type springs).

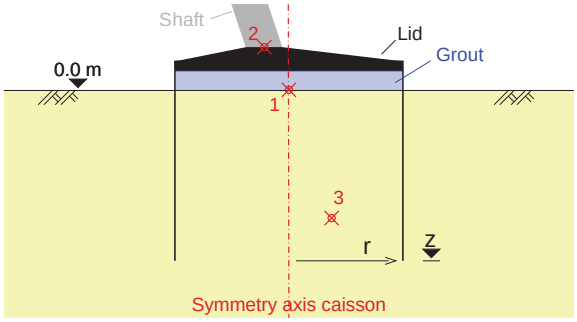

Figure 2: Possible interface points for the geotechnical and structural designer

Practically, three different points could be imagined for the load-stiffness exchange, as illustrated in Figure 2. Each point has advantages and disadvantages.

[1] Front End Engineering Design (FEED)

1. Traditionally, Point 1, located on the symmetry axis of the caisson at mudline, is very often used. However, the structural designer needs to establish loads at a point which is not connected to the structure. In order to do that, he needs to introduce a so-called *super-element*, connecting the structure with the ground in this point. Given that the structure – in this case the caisson lid and grout – is significantly stiffer than the soil for the considered load level, simplified, linear elastic properties can be assigned to the super element. If the flexibility of the structure is considerably larger and a interaction with the soil behavior may be expected, more complicated properties need to be assigned to the super element. However, these properties are very difficult to assess, which may not be possible. Experience from recent projects has shown, that both the lid and skirt flexibility is important and an optimization of the caisson geometry is difficult, for which reason, Point 1 is not recommended to be used in future projects.

2. Point 2, located at top of the caisson lid in the interface between the shaft of the sub-structure and the caisson, has been used in more recent projects. The advantage is, that Point 2 is also often an interface for the structural design, as the design of the caisson and sub-structure is often done separately. Loads are assessed by the load- or structural-designer using integrated analysis where only the sub-structure is modeled. The soil is therein often represented by set of springs in Point 2. That means no super-element is required, but the geotechnical designer needs to include the lid accurately in his analysis.

   The load-deformation response is complex, meaning that a reasonable stiffness matrix describing the load-deformation of the soil-caisson-system will have both diagonal and off-diagonal components. However, most programs used for integrated analysis cannot cope with a full stiffness matrix but can take only the positive diagonal terms. That means that the soil-foundation response can be only considered in a simplified manner when using Point 2.

3. In order to overcome the shortcoming of using a simplified stiffness matrix in the structural analysis, the stiffness matrix could be provided for the so-called *decoupling point*, which is illustrated in Figure 2 by Point 3. The decoupling point can be assessed in the stiffness analysis as described in Section 7, and is characterized by the fact that incremental horizontal, vertical or moment loads yield only displacements or rotations in the corresponding loading direction. That means that the stiffness matrix comprises only positive diagonal terms. If the geotechnical designer includes in the stiffness analysis the caisson with its correct properties, and applies the loads in Point 2, the structural designer can use a rigid super element connecting Point 2 with Point 3 and apply the stiffness matrix in the integrated analysis in Point 3. Though Point 3 seems to be the most appropriate point for the interface, the problem is, that the location of the decoupling point is not constant but depends on the load-level, combination of load components and load-deformation response.

Based on experience from recent projects, it is recommended that the structural designer provides the caisson model and the loads in Point 2, and the geotechnical designer delivers back a stiffness matrix in Point 2 and Point 3 as well as the coordinates of Point 3.

In Section 7 is introduced the concepts of a global model. Though this model is a considerable improvement as both the sub-structure, caisson and soil is modeled, it does not overcome the above described problem of finding an appropriate interface point. The structural designer will still need stiffness values at the bottom of the sub-structure.

In principal, stiffness values and soil reactions could be established from the same analysis as they are actually describing the same response. However, the extraction of soil reactions from FE analysis is difficult and very sensitive to the modeling technique, element-type and -size. As the soil reactions are only used for the caisson design, but neither for the load assessment nor the design of the sub-structure, it has been found most appropriate to establish reasonable ranges for the distributed loads acting on the skirts and lid based on empirical considerations.

2 DESIGN BASIS

The design basis is the input to the geotechnical design before any interpretation or processing is done. It comprises soil properties, loads, structural properties, guideline requirements, and other relevant boundary conditions such as weight- and size-limitations due to logistical considerations.

2.1 Site and soil parameters

The loading regime acting on a suction caisson requires special attention with respect to the soil parameters used in the design. The impact of cyclic loading on the soil strength and stress-strain-behavior needs to be quantified by a thoroughly planned laboratory testing program of all relevant soil layers. The following list outlines the recommended minimum site- and soil-investigation program to establish the required soil-profiles and -parameters:

- From a geotechnical perspective, a geophysical survey is recommended to identify the number and depth of the soil layers at the OWT location(s). The geophysical survey should provide an overview of the soil profile variability at a location, which is in particular relevant for multi-legged sub-structures having three or more caissons. In some recent projects, two surveys have been conducted. In a first survey the complete offshore wind farm was screened, whereas in a second survey high resolution 3d seismic scans of the shallow soil has been performed. The advantage of the latter survey is, that it allows to find also small boulders, which can be critical for the installation.

- Minimum one seabed *Cone Penetration Test* (CPT) per location with a minimum investigation depth z_a, measured from the skirt tip, where z_a is the maximum of

  - the depth below the caisson where the additional stresses $\Delta\sigma'_v$ due to the permanent weight of the structure does not exceed 15% - 25% of the in-situ stress prior to the installation of the caisson. Assuming a load spread angle of 1:3, a submerged foundation weight between 5 to 7MN, a caisson diameter between $D = 8$ and 10m, a submerged unit weight of the soil of $10\,\frac{\mathrm{kN}}{\mathrm{m}^3}$, and a skirt depth of $s = 0.6 \cdot D$, the required depth $s + z_a$ (measured from mudline) varies between 15 and 20m.
  - the depth of the governing failure mechanism in a bearing capacity analysis, which is a function of the caisson diameter D, the number of footings and distance of the legs, and the loading regime. A rotational failure is expected for mono-caissons, whereas a compression failure is expected for caissons supporting a jacket. In both cases, the depth measured from the skirt tip level is less

than the caisson diameter, given that there is no interaction between the footings of multi-legged structures. For the dimensions indicated above, the required depth $s + z_a$ (measured from mudline) varies between 10 and 14m.

Even though, neither combined deep failure mechanisms of multi-legged structures, nor exceptionally high weights, have been observed in past projects, it is recommended to check in the FEED study, whether the values given above are not exceeded. That means, it needs to be ensured that the additional stresses are not larger, nor the actual failure mode giving the lowest foundation capacity reaches deeper than assumed. If the required investigation depth cannot be achieved by the seabed CPT, complementary downhole CPT should be performed.

At sites and turbine locations where highly variable soil conditions are expected, several CPTs should be conducted.

In general, it is recommended to perform the CPTs outside the actual caisson location, to avoid open holes which will potentially affect the caisson installation and may even prevent the caisson to reach the target penetration depth.

- Sufficient boreholes at the site in order to extract samples of all relevant soil units. Number and locations of the boreholes should be selected based on the review and interpretation of the geophysical and CPT data, preferable on basis of a ground model (e.g. Forsberg et al. 2017)

- Laboratory tests of all relevant soil layers within the CPT depth. Andersen et al. (2013) provide a comprehensive list of required parameters for various foundation concepts. A summary of parameters for suction caissons is listed in Table 1. The crosses in brackets indicate parameters, which are, according to the author's experience, somewhat less relevant.

  In order to determine the required parameters, drained and undrained, monotonic and cyclic DSS, triaxial compression and triaxial extension tests need to be performed. Further, oedometer tests, bender element tests, and interface tests should be included in the testing program. For layers with few decimeter thickness, triaxial tests may be omitted. The number of tests depends on the loading conditions, available data from previous investigations at similar material, and the applied design methodologies. A representative set of laboratory tests per soil layer may comprise

  - 2 oedometer tests,
  - 1 monotonic undrained DSS test and 1 monotonic undrained triaxial compression test, as well as corresponding drained tests when testing sands,
  - 3-5 cyclic undrained DSS tests,
  - 4-6 cyclic undrained triaxial tests

  In addition, other tests such monotonic as drained triaxial extension, or resonant column tests may be conducted where necessary. Of particular importance is the soil-skirt interface strength. It may be best represented by a remolded DSS test consolidated to a stress equivalent to the lateral in-situ stress after installation. The stress level needs to be estimated. Reasonable stress ratios may be 0.5 and 1.0 times the vertical in-situ stress $\sigma'_v = \gamma'_{\mathrm{soil}} \cdot z$. Larger values may be less likely due to set-up effects and arching, but may need to be decided project specific.

Table 1: Recommended soil data for suction caisson design (after Andersen et al. 2013)

Soil parameter	Clay	Sand
Frictional characteristics		
Peak drained friction angle, φ'		x
Residual / critical drained friction angle, φ'_c		x
Undrained friction angle, φ'_u		x
Dilatancy angle, ψ		(x)
Slope of DSS drained failure line, α'		x
Slope of DSS undrained failure line, α_u		x
Interface friction angle, δ_{peak} and $\delta_{\mathrm{residual}}$		x
Monotonic data		
Undrained shear strength, s_u^{C}, s_u^{DSS}, s_u^{E}	x	x
Initial shear modulus, $G_{\max}$	x	x
Cyclic data (triaxial and DSS)		
Undr. shear strength, $\tau_{f,cy} = f(\tau_a, \tau_{cy}, N)$	x	x
Pore pressure, $u_p = f(\tau_a, \tau_{cy}, N)$	(x)	x
$u_p = f(\tau_{cy}, \log N)$ for $\tau_a = \tau_0$,	(x)	x
Stress strain data, γ_a, γ_p, $\gamma_{cy} = f(\tau_a, \tau_{cy}, N)$	x	x
$\gamma_{cy} = f(\tau_{cy}, \log N)$ for $\tau_a = \tau_0$	x	x
Damping	x	x
Consolidation characteristics, intact soil		
Preconsolidation stress (and OCR)	x	x
Un- and reloading constrained moduli	x	x
Permeability, k	(x)	x
Remoulded soil data		x
Sensitivity, S_t	x	
Undrained shear strength, s_u^{DSS}	x	
Cyclic undrained shear strength, $\tau_{f,cy}$	x	
Constrained modulus	(x)	
Permeability	(x)	
Thixotropy	(x)	

It is important to perform the tests at a stress and density or OCR, respectively, representative for the expected in-situ conditions before and after installation. Three zones need to be distinguished; inside the caisson, outside the caisson, and below the caisson. While the soil state outside the caisson will be less affected by the installation, the soil at the inside may undergo considerable shearing, which will affect the density and stresses. The soil below the caisson will be less affected by the installation, but the weight of the OWT will yield an increase of the vertical effective stresses (with time).

In addition, index parameters such as relative density D_r, plasticity coefficient I_p, water content w, and grain size distribution should be determined. These are in particular relevant in an early stage of the project for the feasibility study and preliminary sizing, where not all laboratory tests have been initiated yet, and where strength and stress-strain-behaviour has to be assessed based on correlations using index data and CPT soundings. Andersen (2015) proposes a comprehensive set of correlations, which can be used as a first estimate of the expected soil parameters.

In addition, information of scour development and/or scour protection is required. Type, thickness, submerged weight, and information on the stability of the planned scour protection need to be considered in the geotechnical analysis.

2.2 Loads

The geotechnical designer needs to consider two different load sets. One set is required for the actual geotechnical design, i.e. capacity and serviceability analysis. The other set is used in the load-stiffness iteration (outer loop in Figure 1). Some load cases may be included in both sets. But in general, the loads cases are different in both sets, since the governing design-loads and -criteria are typically different in the structural and the geotechnical design. That means each discipline has to identify the relevant load cases, and need to define them such that everyone involved in the design process has a common understanding. Since this is a very critical aspect of a successful project, a load document should be prepared, which is continuously updated. This has been proven beneficial in many projects.

Most design guidelines distinguish between loads for the *Ultimate Limit State* (ULS), *Serviceability Limit State* (SLS), and *Fatigue Limit State* (FLS)[2]. ULS loads are required by both the geotechnical and the structural designer. However, SLS loads are mainly relevant for the geotechnical analysis, whereas FLS loads are mainly relevant in the structural analysis. All load cases are assessed by the load or structural designer, and the geotechnical designer need to provide input to these.

Identifying or defining the required loads needs an experienced designer. A reasonable starting point for the capacity analysis is to look at the load cases comprising the maximum amplitudes; that means maximum compression, tension, moment, etc. The maximum load amplitudes often adhere a load event which is embedded into a cyclic load history, which can be a storm for example. The German *Bundesamt für Seeschifffahrt und Hydrographie* (BSH) introduced in the standard BSH (2015) a 35-hrs design storm based on a composition of the *Design Load Case* (DLC) 6.1 proposed in the IEC standard IEC (2009). This cyclic event shall be applied to assess the cyclically (degraded) soil strength, which is to be used in the (subsequent) geotechnical analysis. Practically, this event has also been also applied outside Germany, due to the lack of alternatives, since the DLC's defined in the IEC standard are 10 or 60 minute long load-time series, which cannot be directly used in a geotechnical design.

In more recent projects, where turbines with larger capacity were considered, it has been found that also other events can be critical, such as an (emergency) shut-down at relative high wind-speeds. In the event of an (emergency) shut-down, the OWT swings and the load spectrum corresponds to a damped vibration. Depending on the degree of damping, which affects the decay rate, subsequent load cycles with smaller amplitudes can be critical due to the cyclic degradation of the soil, induced by the previous larger load cycles. Another event found critical for the foundation capacity analysis of multi-legged structures is the prolonged tension load case, which typically occurs during operation of the turbine at high wind speeds.

In addition to the in-place loads, there may be further situations which needs to be considered in the design. These can be load cases during installation, maintenance, and decommissioning of the OWT.

[2]The author questions the appropriateness of the expression *limit state* in this context. However, since it is widely used, it is – due to convenience reasons – also adopted in this contribution.

More complicated is the identification of the load cases which should be used for the serviceability analysis. Two scenarios have to be distinguished; a maximum deflection and rotation during a severe load event, and accumulated average long-term deformation and rotation. The peak deflection may be assessed using the loads used in the capacity analysis. For assessment of the long term deformations and rotations, cyclic loads are required. Ideally, all loads during the lifetime of the OWT should be considered in chronological order. However, as this cannot be applied in a geotechnical analysis, simplified load histories are required.

It can be supposed that large cyclic load amplitudes will contribute most to the accumulated deformations and rotation. Thus focusing on a series of storm events may be a reasonable simplification. One option could be to use the 35-hrs design storm and assuming a Gumble distribution to extrapolate the peak amplitudes of other storms with different return periods. The accumulated average displacements and rotations can be calculated for each scaled 35-hrs design storm separately and then superimposed depending on the expected number of occurrences of each storm during the lifetime of the OWT.

The main challenge is to derive from the load-time-series the actual load amplitudes and corresponding mean values, and number of occurrences, both of the maximum- and the cyclic-load events. Most commonly the so-called *rainflow-counting-algorithm* is applied. Though this algorithm is widely used in structural fatigue analysis, it is important to be aware of its limitations:

- It is assumed that the loads are independent, meaning that the order of load cycles is not important.
- The information of the load frequency, that means the cyclic period, gets lost.
- Since only the peak values are counted (that means actually half-cycles are counted), no information can be directly derived of the actual corresponding mean load.

Depending on the soil type, drainage properties and boundary conditions, these information can be crucial. Thus, if these information would need to be considered, other counting methods may be applied where possible; for example the method proposed by Norén-Cosgriff et al. (2015). They apply high- and low-pass filters and determine the amplitude of each half-cycle from adjacent maxima and minima, which belong to the same load cycle. In addition, the proposed method keeps track of the corresponding average load and may also keep the information of the load period (frequency). The authors compared their method with the rainflow-counting-algorithm and showed that the calculated cyclically degraded soil strength using the example of a normally consolidated clay can be significantly different.

Cyclic load histories are often provided in from of a *Markov Matrix* comprising cyclic load amplitudes and corresponding mean load value as well as number of occurrences. Since these are often established using the rainflow-counting-algorithm, it is recommended that the geotechnical designer reviews also the original load-time-series from which the Markov Matrix has been established. This in particular applies to the load-time-series comprising the maximum load values used in the geotechnical capacity analysis. The load cycle yielding the maximum load values may sometimes appear to have a considerable offset from the rest of the cyclic loads history and it requires geotechnical judgment to decide on the load cycle which the soil actually experience. But also a critical review of the mean load value is important, as the soil behaves essentially different symmetric and asymmetric cyclic loads.

It is recommended that permanent and environmental loads are provided separately, and both as characteristic values, as occasionally, different partial safety factors need to be applied to the different load components in the geotechnical and structural analysis.

2.3 Structural properties

As outlined in Figure 2, it may be important to include structural components in the geotechnical analysis. With increasing complexity of the structural model, the stability and accuracy of numerical analysis may be quickly challenged. Thus, if structural models shall be included in a geotechnical analysis, they may be simplified as appropriate. Beam and plate elements should be preferred over continuum elements. Structural components such as stiffeners and stays may be omitted where possible.

For capacity analysis, a rigid structure may be assumed, as the the strength and stiffness of the soil at failure is several magnitudes smaller than the strength and stiffness of the structure, given that the yield stress of the caissons material is not exceeded at any time.

For installation purposes, the properties of the skirts are of fundamental importance and need to be considered in the penetration analysis as accurate as possible. In general, the skirt tip resistance increases with increasing wall thickness. If stepped skirts are considered, i.e. where the skirt wall thickness varies over the height, the skirt friction may be affected considerably, which also will affect the in-place behavior. It is also important to consider compartments[3] and stiffeners in the penetration analysis if present.

2.4 Guidelines and safety factors

A dedicated standard or guideline for the design of suction caissons for OWT applications does not exist. In the absence of such a document, other non-dedicated standards and guidelines need to be applied in the design. This requires to define a code hierarchy, where in general national standards rank highest, followed by offshore wind related standards as well general offshore standards, and finally other standards, guidelines and publications, which rank lowest. Some examples are presented in the following.

The IEC has proposed a series of documents addressing the particular design aspects of onshore and offshore wind turbines. For the load assessment and corresponding partially load factors, typically IEC standard 61400-3 is applied (IEC 2009). Other standards published by the IEC consider structural and geotechnical design aspects. However, these documents are so generally formulated, with respect to geotechnical requirements – and in particular suction caisson design – that other standards need to considered.

To the author's knowledge, all countries where OWTs are considered, have own national standards for geotechnical design. However, since these standards originate form onshore design requirements, the application of the recommended methods and procedures to offshore structures can be critical. Thus, some countries are in the process of establishing national standards particularly for OWTs. This has been done by the German BSH for example. The US *Bureau of Ocean Energy Management* (BOEM) and the German DIN are also working on corresponding documents.

As most OWTs need to be certified due to financial and insurance reasons, some certifiers have published their own guidelines, which are frequently used in the design. Most relevant is the DNV GL standard 0126 (DNV-GL 2016). This document provides valuable recommendations and includes also a section on suction caissons. However, it is very generally formulated and neither particular methods nor procedures are proposed.

Selecting appropriate safety factors for the design is difficult. Solely the DNV standard proposes a consistent safety concept for capacity analysis considering the particular offshore conditions. In general, the strength of the soil shall be reduced or carefully estimated for capacity and serviceability analysis. However, for the installation analysis, a higher strength is more critical, which is not considered in any standard. Sturm et al. (2015) proposes safety factors for installation analysis of suction caissons in sand, which were established based on probabilistic analysis. Similar type of analysis may be performed for other design aspects. No safety factors should be applied in the serviceability-, stiffness-, and soil reaction-analysis as detailed in the corresponding sections.

Due to the lack of long-term experience, it is recommended to consider a comprehensive monitoring system as part of the so-called *observational method*.

3 CYCLIC STRESS-STRAIN BEHAVIOR

The loading condition of an OWT is of inherent cyclic nature. Thus, all components including the soil, need to be designed accordingly. The general supposition is, that cyclic loading yields a decrease of strength and stiffness, often denoted as *cyclic degradation*. This applies to all soil types and foundation concepts.

A number of authors have proposed methods for assessing the effect of cyclic loading on the suction caisson foundation response. Therein two main approaches are followed; an *empirical approach* and an *analytical/numerical approach*.

- The ***empirical approach*** is typically based on model test where the soil-foundation system is considered as one entity. The caisson is subjected to cyclic loading and the response in the loading point is measured. The actual behavior of the structure and soil is not considered separately, hence it is a phenomenological approach. The results can be presented in interaction diagrams[4] or failure envelopes in the HVM space, where HVM is the horizontal, vertical, or moment load component, respectively. Failure envelopes allow a more detailed description of the foundation response compared to interaction diagrams. In addition, a failure envelope diagram can be extended to describe the actual load-displacement behavior by introducing a stack of HVM envelopes to which the corresponding displacement components are assigned. Since these diagrams are based on interpolation of some few data points, they are essentially *empirical*. Many, so-called *macro-elements*, are based the empirical approach. Some Macro elements are mathematical complex and can describe very detailed the load-deformation behavior of a caisson subjected to general cyclic loading. A number of authors have developed macro-elements for suction caissons, (e.g. Nguyen-Sy 2005, Nguyen-Sy & Houlsby 2005, Salciarini & Tamagnini 2009, Salciarini et al. 2011, Foglia et al. 2014, Skau et al. 2017). Macro-elements are well suited in integrated analysis for structural design and load assessment.

- In the ***analytical/numerical approach*** the response of the soil-foundation system is assessed by modeling the actual soil-structure interaction under consideration of the structural flexibility and stress-strain-behavior of the soil. This requires a detailed description of the skirt-soil- and lid-soil-interface behavior. In an analytical approach, the distribution of average and cyclic loads – or actually stresses – along the skirts need to be assumed, whereas the distribution is automatically calculated in a numerical approach. The assessment of the

[3] Compartment mean that the caisson lid area is divided into different cells

[4] Similar to diagrams used for cyclic axially loaded piles

cyclic stress-strain behavior and strength of the soil needs to be described by using appropriate soil models. The analytical/numerical approach is well suited for the geotechnical sizing of the caisson, but may also be used for assessment for the serviceability and calibrating of the input parameters to a macro-element.

NGI has developed a method for describing the behavior of cyclically loaded soil elements using so-called *cyclic contour diagrams*. The method, originally proposed in the early 70^{th}, which was continuously developed further, has been presented in a numerous publications; the most recent and comprehensive one is the article by Andersen (2015). Cyclic contour diagrams span a 3-dimensional space and provide a general relation between average and cyclic shear stresses and corresponding average and cyclic shear strains as function of number of applied cycles. Diagrams are established for one soil type and density or OCR, respectively. One complete set of 3d-diagrams for one soil unit comprises typically of 4 diagrams; 1 strain and 1 pore pressure diagrams for triaxial and DSS conditions, respectively. In many practical application cases, only some representative 2-dimensional cross-sections of the 3-dimensional space are required. This simplifies the approach and reduces the number of cyclically laboratory tests. The selection of appropriate cross-sections requires some experience and assumptions.

In combination with a cyclic load history, the cyclic contour diagrams can be used in the so-called *cyclic accumulation procedure*. The cyclic degradation due to the cyclic loading is calculated and the effect can be expressed by the so-called *Equivalent number of cycles* (N_{eq}).

As cyclic contour diagrams provide a relationship between stresses and strains, but the cyclic loads are given as forces, assumptions on the load transfer and stress distribution has to be made, which is best done using the *Finite Element Method* (FEM). This is in particular the case where complicated boundary conditions, soil layering and drainage conditions are analyzed, which is in general the case for suction caissons for OWTs. NGI has implemented the cyclic accumulation procedure using cyclic contour diagrams in an FE code. Jostad et al. (2014) present the procedure for fully undrained conditions during the considered cyclic load history (UDCAM)[5], whereas the procedure for partially drained conditions (PDCAM)[6] is presented by Jostad et al. (2015b). The cyclic accumulation is done for each integration point. The advantage of using the FEM is, that the stress redistribution is considered accurately and continuously updated if relevant, and that strain continuity is ensured. Furthermore, a output of such an analysis is not only the cyclic stress-strain behavior and degraded strength and stiffness, but also the accumulated displacements and rotations, which are required for the serviceability analysis.

Though the soil-structure interaction is modeled in detail (numerical approach), the description of the soil behavior using cyclic contour diagrams is an empirical approach.

An example of a PDCAM analysis of a suction caisson subjected to a combination of vertical and horizontal cyclic loading is shown in Figure 3. A suction caisson with 8m diameter and 6m skirt length in a homogeneous soil deposit with an average soil permeability of $k = 1 \cdot 10^{-5} \frac{\text{m}}{\text{s}}$ is modeled. At the peak phase of an 35-hrs design storm according to BSH (2015), the soil at skirt tip level accumulates considerable excess pore pressure. Due to the symmetric soil and load conditions the predicted pore pressure field is also almost completely symmetric.

[5]UnDrained Cyclic Accumulation Model
[6]Partially Drained Cyclic Accumulation Model

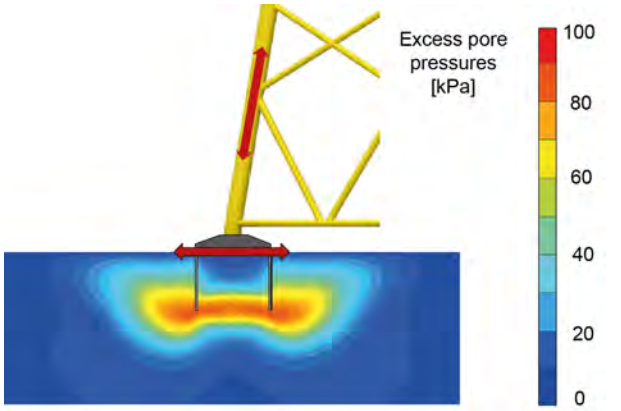

Figure 3: Finite element analysis of a suction caisson subjected to combined vertical and horizontal cyclic loading using the NGI soil model PDCAM. The contour plot shows the excess pore pressure at the end of the peak phase during a 35-hrs design storm.

4 FOUNDATION CAPACITY

The foundation capacity needs to be ensured for all possible load combinations. Two main load scenarios should be distinguished, which are detailed in the following.

4.1 Short-term loading

Short-term loading is characterized by a loading duration being so short that the soil behaves essentially undrained, meaning that the soil response depends on the undrained shear strength only. In sandy soils, the caisson may mobilize considerable suction below the lid and negative pore pressure in the soil, causing an increase in mean stresses and hence higher shear strength. Due to the shallow water depth at typically OWT sites, particular attention requires the cavitation limit. The cavitation limit cannot be exceeded by the suction or negative pore pressure, respectively. That is in particular important to consider when deriving the shear strength from laboratory tests where considerable back-pressures may have been applied, as these tests can potentially exceed the maximum achievable pore pressure and hence strength compared to the actual in-situ conditions. The theoretical cavitation limit $p_{\text{cav,max}}$ in a soil element is the sum of, the depth z of that element below mudline plus the water depth w_s, multiplied with the unit weight of water $\gamma_w = 10 \frac{\text{kN}}{\text{m}^3}$, and the atmospheric pressure $p_{\text{atm}} = 100\text{kPa}$, viz.

$$p_{\text{cav,max}} = (z + w_s) \cdot \gamma'_w + p_{\text{atm}} \tag{1}$$

At NGI, the short-term capacity analysis is often done using a total stress approach. Figure 4 shows a potential failure mechanism of a suction caisson under combined compression and moment loading. The undrained strength in the failure zone is described by the strength measured in undrained DSS tests, or in a trixial tests where different *Total Stress Paths* (TSP) are followed. Cyclic contour diagrams can be used for assessing corresponding cyclic shear strength values.

Figure 5 illustrates the four main different total – and corresponding effective – stress paths, using the example of a medium dense to dense sand specimen consolidated to a stress state of $k = \frac{\sigma'_h}{\sigma'_v} = 0.5$ at a vertical effective stress of $\sigma'_v = 200\text{kPa}$. The difference between the TSPs is the way the shear strength has been applied. For path 1 and 6 the cell pressure in a triaxial test has been decreased or increased, respectively, whereas for path 4 and 2 the vertical pressure has been increased or decreased, respectively.

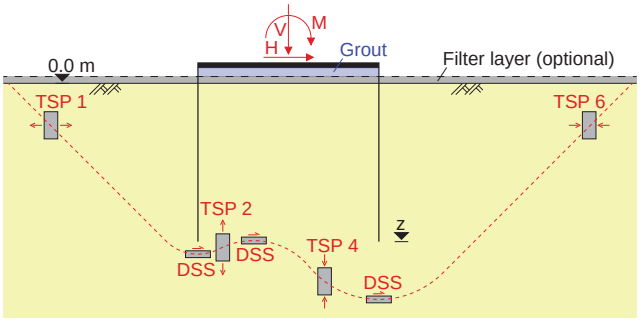

Figure 4: Possible failure mode of a caissons subjected to combined compression and moment loading

In addition, the total and effective stress path in direction 4 for a specimen consolidated to $\sigma'_v = 20\text{kPa}$ is shown.

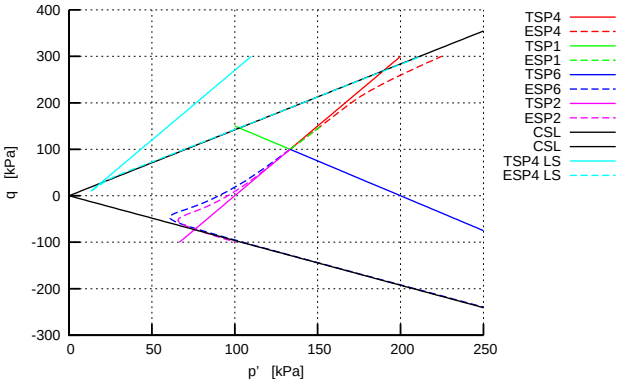

Figure 5: Total and Effective stress path in trixial tests where the shear stress is applied in different ways.

From Figure 5 becomes apparent that the soil strength of a sand specimen for a given initial density and stress state is depending on the loading path. The difference between the total and effective stress for the different paths equates the corresponding pore pressure. The maximum negative pore pressure cannot exceed the cavitation limit. Whether the NGI method or any other method is applied, it is important that the dependency of the stress path and the cavitation limit is considered accurately when assessing the soil strength profile.

The stress path dependency is equally relevant for clay specimens. In additon, due to the viscosity of clays, the dependency of the shear strength on the shear rate needs to be considered. The shear rate in laboratory tests may be different compared to in-situ loading rate for short-term loading, meaning the shear strength may need to be corrected accordingly.

The capacity of suction caissons to short-term loading is essentially governed by the load combination, that means horizontal, vertical and moment loading. As illustrated in Figure 1, the design basis, including the loads, is continuously updated. Figure 6 shows the dependency of the ULS loads on the rotational stiffness of a suction caisson at the example of a multi-legged substructure. The loads of a leg in compressions, are normalized with the reference loads provided in the 1$^{\text{st}}$ iteration. The predicted corresponding rotational stiffness – also normalized – is shown at the abscissa where all load components are crossing. Though the global loads acting on the OWT are constant, the local loads can vary considerably depending on the response of the caisson. The higher the rotational stiffness, the lower the vertical and torsional loads. Similar effects, but less pronounced is found for the other

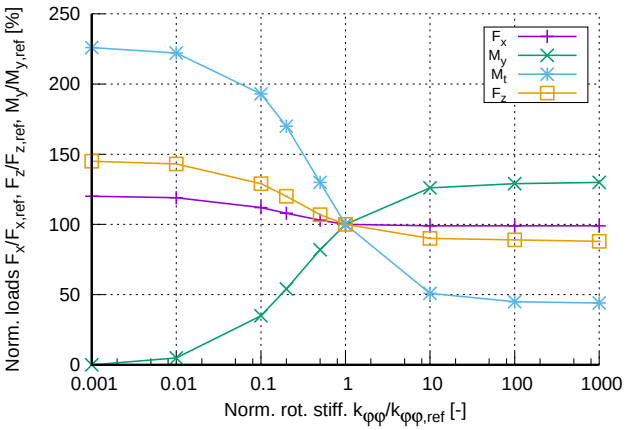

Figure 6: ULS loads as function of the rotational stiffness of caisson supporting a three-legged jacket.

stiffness components.

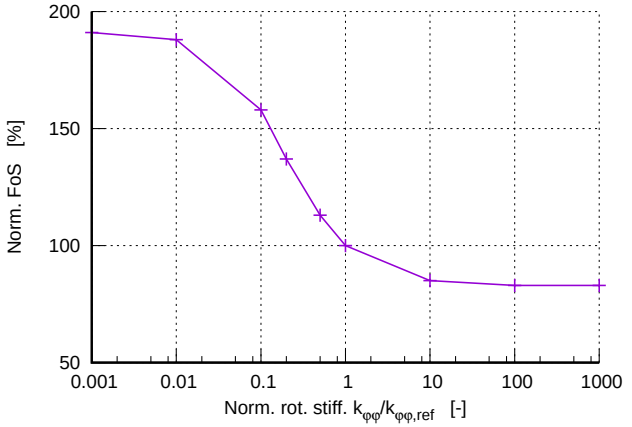

Figure 7: Normalised *Factor of Safety* (FoS) as function of the applied loads shown in Figure 6

The effect of the load combination shown in Figure 6 on the caisson capacity is shown in Figure 7, where the normalized *Factor of Safety* (FoS) is plotted on the abscissa. As it may be expected from conventional bearing capacity analysis, the normalized FoS is lower for larger moments, that means for a rotational failure mode. That applies also to a mono-caisson foundation, which is essentially subjected to environmental horizontal and moment loading only.

In offshore foundation design of multi-legged jacket structures, it is often assumed that the rotational stiffness of a foundation at ULS loading is considerably lower than the rotational stiffness of the corresponding leg of the sub-structure. Hence, the local moment loading at failure may be omitted in the capacity analysis. However, the relatively high jackets stiffness can be an issue for the fatigue design of an OWT, as the goal is, that the first eigenmode shall be in the range between 1P and 3P; e.g. typically between 0.25 and 0.35 Hz for turbines with 6 to 8MW. Thus, the structural designer tries to make the jacket more flexible, meaning, that omitting the local moment may be too optimistic.

To complicate matters, the local load components at a leg of a jacket do not scale proportionally with the global load amplitude, even though the global loads may be applied linearly increasing. Thus, the ULS load components provided in the design basis may

not be scaled proportionally with a load factor. However, as the soil will be always softer than the jacket leg in rotation when being at failure, overestimating the local moment may yield lower FoS as shown in Figure 7. Nevertheless, it is recommended to check the FoS for differently scaled local loads, that means lower load factor applied to the local moment and a larger load factors to the vertical, horizontal and torsional load components. For mono-caissons, a redistribution of the local loads is not expected and the same load factor should be applied to all load components.

For suction caissons subjected to tension loading, the same considerations discussed above apply. The TSP strength used in the analysis need to account for the different loading and hence stress conditions.

Gapping at the outside of the caisson may need to be considered in the capacity analysis, if previous load conditions or stepped skirts may have generated a gap. Due to the short-term loading, the drainage time may not be sufficient to generate a new gap during the considered load event. This depends of course on the load combination and soil type and may need to be checked.

Of particular importance is the scour development and scour protection. The stress and density state of the soil can be considerably affected, which can have an impact on the foundation capacity. Whether to include or omit the effect of a scour and scour protection should be discussed with the operator, as the presumption of a permanent scour protection may require more frequent on-site inspections, which can have an impact on the *Operational and Maintenance* (O&M) costs.

4.2 Long-term loading

Suction caissons have considerable capacity under short-term loading conditions. However, the resistance to long-term loading, can be very low, as the possibly mobilized suction may dissipate. This is in particular relevant for suction caissons supporting a jacket structure. During operational load cases the caisson(s) may experience considerable tension loading, which can last for hours or even days. The tension capacity of suction caissons is a function of the skirt wall friction and the soil permeability.

For caissons in clay the soil permeability will be low, meaning that the capacity can be calculated similar to the long-term capacity, but the shear strength needs to be reduced to account for the slow loading rate. In the absence of suitable tests, the decrease in shear strength may be estimated using

$$s_{u,\mathrm{slow}} = s_{u,\mathrm{ref}} \cdot \left(\frac{\dot{\gamma}_{\mathrm{slow}}}{\dot{\gamma}_{\mathrm{ref}}} \right)^{I_v} \tag{2}$$

where the $s_{u,\mathrm{ref}}$ is the shear strength measured in the laboratory at a shear rate of $\dot{\gamma}_{\mathrm{ref}}$. $\dot{\gamma}_{\mathrm{slow}}$ is the shear rate representative for the considered load case. I_v is a viscosity coefficient which typically varies between 0.03 and 0.07 for a silty or fat clay, respectively (Leinenkugel 1976). I_v can be determined with Equation 2 from an undrained static laboratory test, where the shear rate is varied.

If previous load cases, structural boundary condition or any other causes may have generated channels or gaps at the outside and inside of the caisson in the clay, only the skirt wall friction can be considered in the tension capacity analysis.

For caissons in sand, the soil permeability is considerably higher, meaning that a continuous flow of water from the outside to the inside can be expected, given that the tension load exceeds the resistance calculated by integrating the fully drained skirt wall friction over the skirt area at inside and outside of the caisson. In this case, the capacity is the sum of the drained skirt wall friction at the outside, a reduced drained friction at the inside – due to the upward flow reducing the effective vertical stresses – and a small suction pressure below the lid, which is required to maintain a constant flow. The friction capacity needs to be further reduced to account for the relative vertical movement of the caisson, which reduces the vertical stresses in the soil and hence the shear stresses in the soil-skirt-interface.

The difficulty is to decide upon the load and resistance factors which shall be applied. If a load case can potentially cause a failure of the structure, the full load and resistance factors according to the considered standard should be applied. However, if the loads for a considered load case can be controlled, for example by the turbine operation, the load factors may be reduced somewhat to acknowledge for the reduced uncertainty in the actual load amplitude. But also the failure mechanism may justify to apply somewhat lower safety factors. In case of a suction caisson in sand subjected to long-term tension loading, the structure may not experience a sudden failure, but may be pulled out gradually. If reduced load and resistance factors are applied, the serviceability needs to be ensured at any time, and an appropriate monitoring system should be installed, in order to apply the observational method. In addition, mitigation measures need to be prepared.

As the loading conditions of OWTs is of essentially cyclic nature, also the long-term tension loading is actually a cyclic load case. Thus, an appropriate cyclically degraded shear strength profile and corresponding stress-strain response need to be used. For that purpose assumptions need to be made on the distribution of the average long-term tension load and the cyclic amplitude. Depending on the considered load case, it may be assumed that the skirt-soil-interface at the outside of a caisson in clay may take the cyclic component and the soil below and inside the caisson may take the average component. Where this distinction should not be possible, an equally degraded strength profile may need to be assumed.

As the cyclic load components have relatively short period, the soil response of a caisson in sand will be essentially undrained to this component only. Thus, for a caisson in sand, the capacity needs to be checked for at least two cases; the resistance to the average tension load, and the resistance to combined cyclic and average load using an appropriate cyclic shear strength profile. When using the NGI framework based on cyclic contour diagrams, the strength and stress-strain response can be derived from diagrams where the average shear stress was applied drained in the corresponding laboratory test. Further information can be found in Andersen (2015).

The same considerations made for the short-term bearing capacity analysis on whether to include or to omit the effect of scour or scour protection, applies to the long-term bearing capacity analysis as well.

5 INSTALLATION

The installation is considered by many as one of the most challenging aspects of suction caisson application. However, experience from actual installations has demonstrated that installation in many different soil types and profiles is feasible. Moreover, the predicted penetration resistance and hence the required suction pressure agrees often reasonably well with the actual measured values (e.g. Sparrevik 2002, Colliat et al. 2007, Aas et al. 2009, Langford et al. 2012, Solhjell et al. 2014, Saue et al. 2017).

The governing mechanisms are well understood and several authors have developed calculation methods. Most methods can be applied in uniform and homogeneous soil conditions or soil profiles with perfectly horizontal layering. A general discussion of the

installation process and calculation methods is presented in Subsection 5.1.

All existing calculation procedures have limitation, and there are a number of aspects which need particular attention during the actual installation, since they cannot be considered by the existing calculation models. Some of the most relevant aspects are presented in Subsection 5.2. Possible mitigation measures are discussed in Subsection 5.3.

5.1 Calculation methods

The often reasonably accurate predictions of the penetration resistance and hence required suction pressures is a result of extensive research in this field. A number of authors have proposed methods for calculating the penetration resistance and required suction pressure in both clay, silt and sand layers; particularly noteworthy are the models proposed by Houlsby & Byrne (2005a,b), Andersen et al. (2008) and Senders & Randolph (2009). These are based on model tests, field tests and prototype installations.

The penetration resistance is a function of the skirt tip resistance Q_{tip} and the skirt wall friction Q_{wall}. Q_{tip} may be estimated using a bearing capacity based approach or correlations with measured CPT resistances. Q_{wall} is a function of the skirt-soil-interface strength τ_{fric} and the effective skirt wall area. τ_{fric} can be assessed by means of laboratory tests, such as DSS tests or ring shear tests. Alternatively, τ_{fric} can be estimated using correlations with measured CPT resistances.

If the total penetration resistance $Q = Q_{\mathrm{tip}} + Q_{\mathrm{wall}}$ exceeds the submerged weight of the caisson and sub-structure $W' = W'_{\mathrm{cais.}} + W'_{\mathrm{substr.}}$, an additional driving force needs to be applied in order to penetrate the caisson to the required *Target Penetration Depth* (TPD). This is done by applying a relative under- / suction-pressure p_{suc} at in the inside of the caisson. The additional driving force is calculated by integrating the applied suction pressure over the horizontally projected area A_{suc} to which the pressure is applied. The maximum achievable penetration depth is reached when the total resistance Q exceeds the driving forces $W' + p_{\mathrm{suc}} \cdot A_{\mathrm{suc}}$.

Two main scenarios need to be distinguished; an *undrained* penetration and a *drained* penetration. A penetration is *undrained* if the soil permeability k of the penetrated layer is so low, that no significant amounts of pore pressure will dissipated during the actual installation process. In contrast to an undrained penetration is the pore pressure dissipation considerably in a *drained* penetration, which will affect the the stress regime in the soil. Due to the applied suction pressure, a seepage flow through the soil from the outside to the inside will develop in a high permeable soil layer. The upward flow in the soil plug inside the caisson causes a decrease of the vertical effective stresses σ'_v and hence a decrease of the inside side friction τ_{fric}. Furthermore, also the tip resistance will decrease due to the potentially high gradient around the skirt tip. Both yield a considerable reduction of the penetration resistance, meaning that a suction pressure has a twofold effect in a drained penetration; it increases the driving force and reduces the resistance in high permeable soils. Figure 8 illustrates the driving forces (top), stresses in the soil (left bottom) and resulting reaction forces (right bottom) acting on a suction caisson during installation in a high permeable soil.

The maximum possible suction pressure $p_{\mathrm{suc,cav}}(z)$, which can be applied inside the caisson, is limited by the cavitation pressure. As detailed in Section 4, the cavitation pressure depends on the pump configuration, and is given by the sum of the atmospheric pressure $p_{\mathrm{atm}} = 100kPa$ and the unit weight of water $\gamma'_w = 10\frac{\mathrm{kN}}{\mathrm{m}^3}$ times the depth of either

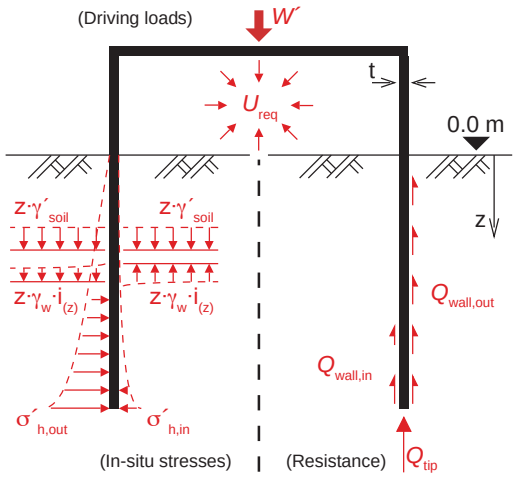

Figure 8: Forces and stresses acting on a caisson during suction installation in a high permeable soil; from Sturm et al. (2015)

- the submersion depth of the pump, given that the pump sits on top of the caisson lid, or
- the mudline depth, given that a closed system is established, where one hose is connecting the caisson with the pump and another hose returns the water from the outlet of the pump back to the mudline.

Though the pressure is theoretically higher for the latter case, it is technically more challenging. Furthermore, a considerable head loss can be expected due to the length of the hoses, which reduces the efficiency of the second solution.

The actual maximum achievable pressure $p'_{\mathrm{suc,cav}}(z)$ is practically somewhat less than the calculated value $p_{\mathrm{suc,cav}}(z)$, since the pump may not be able to go as low as to the theoretical pressure. Thus, a reduction of 20 to 50kPa of $p_{\mathrm{suc,cav}}(z)$ may be considered in the design, where the reduction should be adjusted based on the pump specifications.

The actual allowable suction pressure $p_{\mathrm{suc,all}}(z) \leq p'_{\mathrm{suc,cav}}(z)$ may be limited by geotechnical and structural stability considerations. The skirt needs to take the load without to buckle. In the initial phase when applying the first time a suction pressure right after the self-weight penetration phase, the caisson is exposed to buckling failure due to the lack of any soil support above mudline. This is in particular critical for penetration in stiff clays at shallow depths. But also in the course of further penetration when the required suction pressure $p'_{\mathrm{suc,req}}(z)$ increases with depth, the caisson may be exposed to buckling failure, if the inside soil support is low. This is typically the case for penetration in high permeable soils due to the upward flow of pore water in the soil plug reducing the stresses and hence strength.

Geotechnical limitations which can potentially affect $p_{\mathrm{suc,all}}(z)$ are reverse bearing failure, primarily when penetrating in low permeable soils, and hydraulic heave failure, primarily when penetrating in high permeable soils. Some authors have included in their calculation models criteria and functions to ensure that these failures are avoided.

Somewhat more complicated is the penetration in layered soil profiles. Two scenarios need to be distinguished; sand over clay and clay over sand, where sand is a high permeable layer and clay a low permeable layer. Sand over clay is a common profile in many areas of the North and Baltic Sea, and the penetration through these do not pose a particular challenge. However, clay over sand is subject of ongoing discussion. Some authors have found in centrifuge

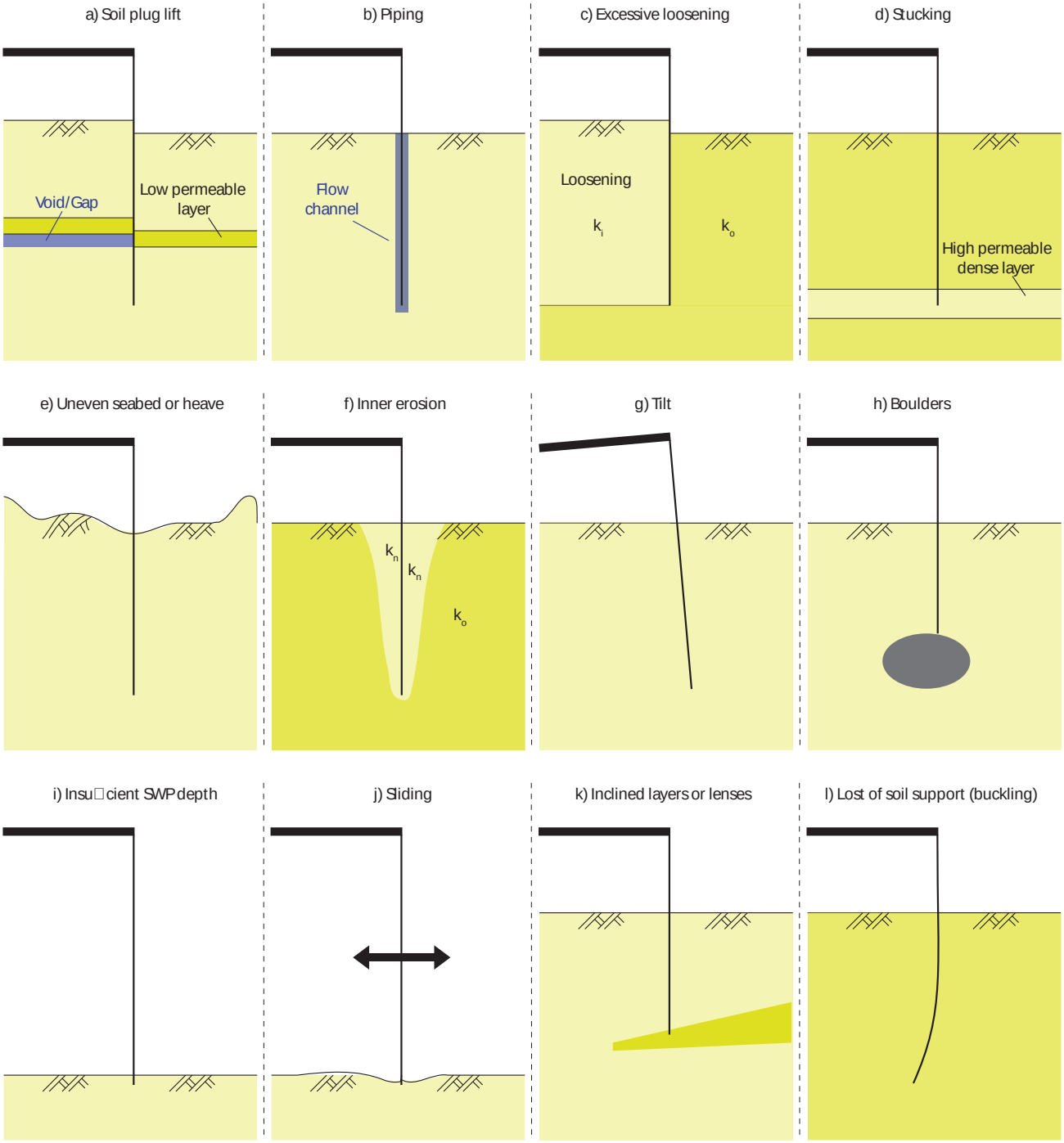

Figure 9: Some possible failure during installation, which cannot be predicted or insufficiently predicted with the available installation analysis models.

tests and/or small scale model tests, that penetration in the underlaying sand layer may not be possible without triggering a plug-lift failure (e.g. Cotter 2009). They recommend to stop the penetration above the sand layer, where the maximum allowable penetration depth into the clay is given by the shear strength of that layer below the skirt tip and the caisson geometry. However, installations of suction caissons in such layered soil profiles have demonstrated, that a penetration is in principal possible without a measurable soil plug-lift. In installations, where pore pressure sensors were placed at the in- and outside of the skirt walls above tip, it was found that the pressure gradient in the sand layer around the skirt tip, equates the gradient measured in installations in homogeneous clean sand deposits. That supports the assumption that a plug lift failure is not necessary. However, to generate a gradient in the sand layer covered by the clay, a seepage flow must have been developed. As the water cannot flow out through the soil plug in the caisson, the sand layer below the clay layer needs to take the water volume, meaning that the sand will reduce its density. Thus despite the fact, that the trial installations demonstrated that a penetration in layered soils is possible, it is recommended to penetrate relatively fast to avoid excessive loosening (soil plug heave) or eventually a soil plug lift.

5.2 Challenges

The methods mentioned in Subsection 5.1 are applicable for idealized conditions, i.e. uniform and homogeneous soil conditions

or perfectly horizontal layering, vertical and parallel skirts, and no structural imperfections, to name but a few. However, there are a number of situations which are not covered. Some of the most common ones are illustrated in Figure 9.

Soil plug lift is a failure often discussed in connection with penetration in layered soils. In contrast to soil plug heave, soil plug lift will generate a water filled void or gap in the ground. That needs to be avoided in order to not negatively affect the in-place behavior of the suction caisson. Furthermore soil plug lift may prevent the caisson from penetrating to the TPD as the caisson will be filled up with soil. Practical experience form installations in layered soil profiles suggest to apply a minimum penetration rate in order to reduce the amount of water flowing into the soil plug and potential void.

Piping is a critical failure, as the volume of water per time flowing from the outside to the inside will increase considerably. If the water volume exceeds a certain amount, the pump may not be able to apply the required suction pressure and the TPD may not be reached. Furthermore, piping channels generated during installation can negatively affect the in-place performance, as the temporary suction during short-term loading will dissipate much faster which can potentially decreases the capacity significantly. Piping can be triggered by obstacles below the skirt tip which are dragged down while penetrating the caisson. These obstacles can leave a highly disturbed zone along the skirt wall. But also locally varying soil properties in combination with penetration at high suction pressures and hence penetration rate can trigger the generation of piping.

Excessive loosening may occur in installation in permeable soils. Due to the reduced vertical stresses and additional shearing of the material inside the caisson, the soil will dilate. That will affect the soil permeability and hence the seepage flow pattern, which can prevent the caisson to reach the TPD, since the required flow gradient in the soil cannot be achieved. Experience from installations in homogeneous sand deposits indicate that the degree of loosening correlates positively with the installation time, meaning that penetration at higher rate may potentially avoid excessive loosening. Sturm et al. (2015) proposes safety factors for the penetration analysis capturing the uncertainty of an excessive loosening.

Embedded and thin granular but relatively low permeable soil layers and lenses may cause the caisson to ***stuck***, if the required suction pressure exceeds an allowable value and if no seepage flow can be mobilized in that layer, which would reduce the tip resistance considerably.

An ***uneven mudline*** may prevent the caisson to reach the TPD, if not considered in the design of the so-called *free height*, which is the skirt length in addition to the calculated required penetration depth. The free height is typically measured from the original mudline and need to accommodate the soil plug heave, grout, and pre-installed filter material if applied, and seabed elevation. An uneven mudline can be also critical for the self-weight penetration phase, if the penetration resistance is locally too high preventing the whole caisson circumferences to penetrate and to establish a sealing, which is required to apply a suction pressure.

Soil layers with a gap graded grain size distribution curve, where the large diameter grains can form a stable matrix, are sensitive to ***inner erosion***. Fine grained particles are washed out of the soil due to the applied suction, and a very high permeable grain skeleton remains in the ground. Since the amount of water volume flowing into the caisson per time increases, the pump may not be able to apply the required suction pressure, meaning that the TPD cannot be reached.

Tilt of the caisson can be critical, as the penetration resistance increases. Installations with single caissons and anchors showed that a caisson is a self-stabilizing system, meaning that it rectifies due to the lateral soil resistance. However, if the caisson is constrained – for example when attached to a jacket – the loads can become critical for the sub-structure. Thus it is important to ensure a minimum degree of verticality of all caisson of a multi-legged sub-structure during the fabrication.

Boulders and other large obstacles can prevent the caisson to reach the TPD as the penetration resistance will increase considerably. If not identified in due time by the pump operator, the caisson skirts may be damaged or buckled. Small boulders may flip or pushed to the inside due to the suction pressure. Boulders can be detected by means of suitable geophysical site investigations. If boulders are met, the caisson may be retrieved and relocated, given that the structure has not been damaged.

If the submerged weight of the caisson and substructure is too low, the ***self-weight penetration*** may not be sufficient to ensure a seal at skirt tip level, which is necessary to apply a suction pressure.

Sliding during the lowering and touch-down phase of the caisson may remove soil in the vicinity of the skirt tip, preventing sufficient seal, which is necessary to apply a suction pressure. Hence, allowable sea states for the installation should be assessed in the design.

Particularly challenging is the penetration of profiles comprising ***inclined layers and lenses***. In case of an inclined clay layer or lens below or in a sand layer, respectively, the pore pressure gradient at skirt tip level may become critically high, since the changed drainage conditions will affect the seepage flow pattern. That can potentially trigger a local failure or piping along the skirt at the side of the caissons which is still in the sand. In case of an inclined sand layer or lens below or in a clay layer, respectively, the penetration resistance may considerably increase since a seepage flow, as described for perfectly horizontally layered profiles, may not be established. Furthermore, the soil resistance will be asymmetric and potentially causing a tilt of the caisson or local moment in the leg of the sub-structure, respectively. However, the deeper the caisson has penetrated the more soil support at the outside of the caisson is available, which can compensate for the asymmetric penetration resistance.

Imperfections or ***buckling*** at skirt tip level can increase the penetration resistance considerably and also affect negatively the in-place behavior of the suction caisson. Thus the allowable suction pressure should not be exceeded and a maximum tolerance for imperfections and misalignments shall be considered in the fabrication.

5.3 Mitigation measures

In case that the penetration resistance is higher than predicted, the required suction pressure to penetrate the caisson will be higher as well. Where it is not possible to apply the required suction pressure due to geotechnical, structural or technical limitations, one may consider to abort the penetration or apply mitigation measure in order to try to penetrate further until reaching the TPD. The decision should depend on the achieved penetration depth as well as on the course of the penetration process. If for example, the caisson has penetrated 80 or 90% of the TPD and the penetration resistance had been continuously higher than predicted in the design, it may indicate that the foundation has already sufficient capacity for the actual reached penetration depth. More challenging is the impact of the stiffness for a lower penetration depth.Sturm & Mirdamadi (2017) propose a reliability based method for assessing foundation stiffness, which can be used during installation, on which basis a decision can be made if the caisson(s) need to be penetrated further

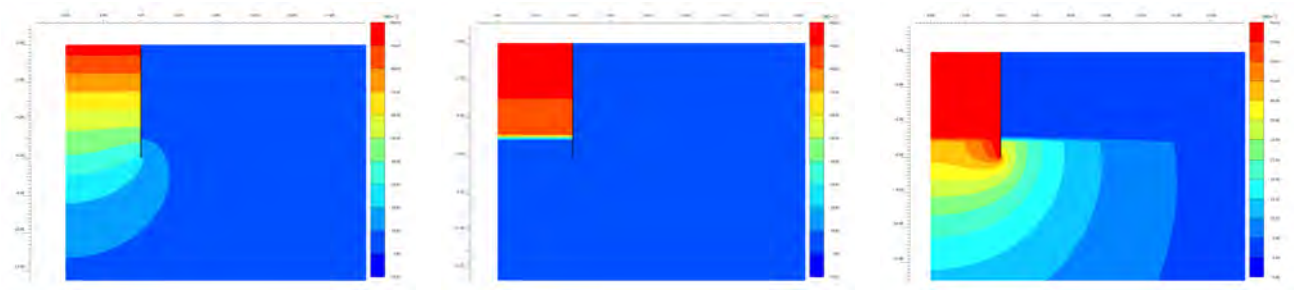

Figure 10: Pressure gradient in the soil for a clean sand profile (left), a sand profile with a clay layer a skirt tip (center), and sand profile with a clay layer a skirt tip with a stepped skirt (right)

by means of applying mitigation measure.

Two categories of mitigation measures need to be distinguished; preemptive and reactive mitigation measures. Preemptive methods are those which have been considered before the actual installation. Reactive methods are applied during the actual installation and do not require any particular structural considerations.

A simple but often effective reactive mitigation is to ***ballast the structure*** to increase its weight. This can help in many situations discussed in Subsection 5.2, for example in case of piping, inner erosion, stucking, and insufficient self-weight penetration.

Another reactive mitigation measure is to ***cycle the suction pressure***, which is illustrated in Figure 11. Cycling has been applied in many installations to successfully penetrate to the TPD.

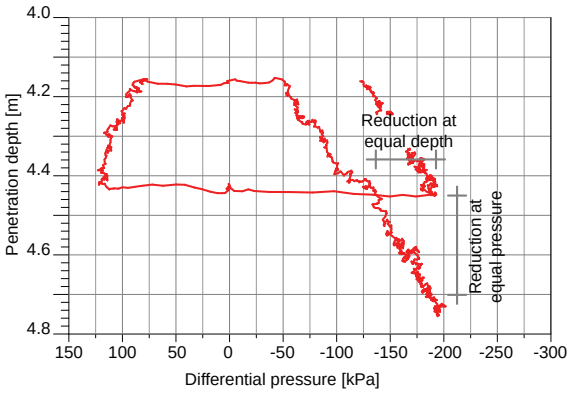

Figure 11: Suction pressure versus vertical displacement during cycling as a reactive mitigation measure

Due to the cycling of suction pressure, the caisson will move somewhat up and down, which will affect the soil in the vicinity of the skirts. Over-consolidated clays will be remolded due to the cycling and the shear strength will decrease. This will mainly affect the skirt wall friction Q_{wall}. Cycling when penetrating in sand layers can be beneficial as well, as the soil below the skirt tip will dilate due to the unloading, which will decrease the tip resistance (see Cudmani & Sturm 2006). The effectiveness of cycling can be described by considering the reduced suction pressure at equal penetration depth or the achieved additional penetration depth at equal suction pressure; both illustrated in Figure 11.

A systematic evaluation of NGI in-house installation data, where the suction pressure was cycled, showed that both measures are equivalent, though more practical relevance has the increase in depth at equal pressure. Further, a general tendency can be observed that the effectiveness of cycling increases with increasing penetration resistance. This may be expected as the decrease in strength due to remolding is higher for over-consolidated material than for normal consolidated material. In fact cycling may have a negative affect on the resistance in normal and low consolidated clays, as the soil may partially drain and by that increases its strength. The soil sensitivity may provide an indication of the expected efficiency of cycling.

The effectiveness of cycling depends further on the cyclic displacement amplitude which is also indicated by the results presented by (Cudmani & Sturm 2006). The larger the displacement amplitude the more effective the cycling, which can be explained by an increased shearing of the soil. In addition, the cycling rate may have an effect on the effectiveness as it allows the soil to drain somewhat.

A preemptive mitigation measure is a ***stepped skirt***. A stepped skirt has different wall thicknesses over the height. Similar to driving shoes used for piles, a stepped skirt, as considered herein, will be thicker at the tip compared to the rest of the skirt wall. This will generate a thin gap or disturbed zone along the skirt, which needs to be at the inside of the caisson, in order to be effective for the penetration. The stepped skirt functions as a *friction breaker*.

Figure 10 shows the required pore pressure field to penetrate a caisson in a clean sand deposit (left figure). When penetrating through a thin clay layer embedded in the sand, the seepage flow is prevented and the required gradient around the skirt tip cannot be achieved (center figure). The caisson cannot be penetrated further. However, when using a friction breaker, a gap or disturbed zone along the skirts, and in particular in the thin clay layer, may be generated, which allows to establish a seepage flow from the outside to the inside. Due to the different seepage flow pattern, the actual required suction pressure to achieve the same pressure gradient at skirt tip is less than the required suction pressure in a clean sand profile (right figure). This indicates that a friction breaker can be a very effective mitigation. However, due to the disturbed zone, the in-place performance of the caisson may be negatively affected, since the suction generated during short-term loading will dissipate faster. And also the resistance to long term loading may be reduced compared to a caisson with constant wall thickness.

Another preemptive mitigation measure is the ***water injection*** system, where at a pipe with nozzles through which water can be injected into the soil is arranged at the skirt tip. Purpose of the water injection system is to reduce the penetration resistance. This is achieved in sand by a loosening the soil at skirt tip, and in clay by remolding the soil along the skirts. Injection of water appears to be most effective in combination with cycling, where the amount of injected water is adjusted to the void generated by the skirt when moving upwards. This will have a minimal effect on the soil state after installation. Water should be injected in any case at low pressure to avoid excessive soil disturbance, which can potentially negatively affect the in-place behavior of the caisson. Aas et al. (2009) reports results of a water injection system used in layered profiles.

6 FOUNDATION SERVICEABILITY

The foundation serviceability is probably one of the most imprecisely predictable aspects in geotechnical engineering. Serviceability in this context means settlements, lateral displacements, and rotation or tilt, respectively. Most critical is the tilt of an OWT as it affects the operation of the turbine. Pure settlements are typically less critical, though some secondary steel components such as the J-tube or the boat lander may be affected. The lateral displacements are typically small, and have practically no relevance in the projects considered so far. Thus main focus is given in the following on differential settlements or tilt of multi-legged substructures or mono-caissons, respectively.

In order to assess the *Serviceability Limit State* (SLS), corresponding limit values need to be defined. These are typically given by the turbine supplier. In addition, the maximum tilt may be limited in order to reduce operational loads, which is in particular relevant for multi-legged OWTs; increased average tilt yield typically an increased average tension load.

Three different types of settlement/tilt components need to be distinguished:

- ***Static*** settlement/tilt due to the submerged weight of the OWT.
- ***Peak*** settlement/tilt due to a ULS loads.
- ***Accumulated (average)*** settlement/tilt due to cyclic loading from wind, wave and operation loads.

Following traditional geomechanics, the *static* settlement/tilt can be further distinguished into immediate-, consolidation- and creep-settlements/tilt. The corresponding values can be computed using well established geotechnical calculations procedures.

The *peak* settlement/tilt can be assessed by means of a monotonic pushover FE analysis. The soil model needs to be calibrated in order to reproduce the correct stress-strain-behavior of the soil. Where necessary, the decrease of strength and stiffness due to cyclic loading needs to be included. This may be done for example by using a total-stress-based model with adjusted stress-strain curves based on cyclic contour diagrams, or an effective-stress-based model to which a pore pressure field is superimposed; see also Section 3. The peak settlement/tilt represents actually the maximum expected value, meaning that the load case considered is in general the same used in the ULS capacity analysis, but without applying load and resistance factors. Practically, this value is less relevant, as the settlement – and more important the tilt – will immediately decrease again in the subsequent unloading. Further, the OWT may not be in operation during the ULS event, for which reason the allowable serviceability limit criteria may not apply.

Most relevant is the assessment of the *accumulated average* settlement/tilt, which, however, is also one of the most challenging components. Thereto, different strategies can be applied. One of the most conservative assumptions is to take all load cycles which occur during the lifetime of an OWT and sort them in ascending order. This sorted cyclic load history can be applied in a calculation procedure, for example in the NGI method (Jostad et al. 2014, 2015b), or in an FE analysis using the high-cyclic accumulation model (Niemunis et al. 2005, Wichtmann et al. 2010).

Since small load cycles will typically not contribute significantly to the accumulated total displacements, a different approach has been followed in more recent projects. The design storm used in the ULS analysis, which is based on a 50 years wind wave event, has been extrapolated to other storm events with different recurrences using a Gumble distribution. That enables to calculate the displacements for a given cyclic history, but at different scaling factors. The accumulated total displacements can be than determined by summing up the the calculated displacements for the different storm events multiplied with the number of occurrences of the corresponding event.

However, both approaches miss out important aspects. Different to engineering materials such as steel or concrete, soils are sensitive to the order of cyclic loading. While large cyclic load amplitudes can cause a degradation of the soil strength and stiffness, can the soil regain strength and stiffness when subjected to lower cyclic load amplitudes, which can be described as *self-healing*. The influence of varying strength and stiffness of the soil on the settlement and tilt depending on the cyclic loading conditions is described in Sturm (2009) and Sturm (2011) at the example of skirted shallow foundations. It is introduced the concept of the so-called *cyclic attractor*, which is a value being asymptotically approached by a given cyclic load history with constant amplitude. Given that the foundation is stable for all relevant cyclic load histories, the value of the cyclic attractor is proportionally to the composition and intensity of the cyclic load history. Thus, for the assessment of the cyclic accumulated average tilt of a stable OWT, only the cyclic attractor for the largest cyclic load event needs to be determined, meaning that only one cyclic load history needs to be considered in the design. Cyclic attractors can be found for the accumulated average tilt of shallow foundations. However, no attractors exist for vertical settlements of shallow foundations.

7 FOUNDATION STIFFNESS

The local foundation stiffness is the link between the geotechnical and structural designer. Foundation stiffness is an output of the geotechnical analysis, but is not part of the actual sizing, i.e. capacity serviceability and installation analysis. However, the results of the stiffness analysis will affect the design basis as illustrated in Figure 2. As detailed in Subsection 1.2, foundation stiffness can be provided as single secant stiffness values, nonlinear tangential stiffness values, or full linear or non-linear stiffness matrices including coupling terms if necessary. This needs to be agreed in upfront with the involved disciplines and may be included in the load document. Further, it need to be agreed on the load cases for which the foundation stiffness shall be assessed.

Foundation stiffness can be established using simplified analytical methods or advanced FEM based methods. Gazetas (1991) has proposed a large number of closed form equations for assessing the stiffness of different foundation types and ground conditions. In contrast to the simplified methods, which consider linear soil properties, the FEM allows to capture the non-linearity of the soil and the flexibility of the structure, i.e. the soil-structure-interaction. The methods used for assessing the foundation stiffness should be adjusted based on the stage of a project and anticipated degree of optimization. In an early stage of a project, i.e. feasibility and concept study, simplified analytical methods may be used, whereas in a FEED and Detailed Design the FEM may be more appropriate.

Typically the foundation stiffness is provided as a range with high-, best- and low-estimate. The width of the range should be narrowed down during the project and every design iteration. No attempts should be made by the geotechnical designer to assume any particular soil profile which may be conservative for the structural design. The selected soil profiles should rather reflect the inherent uncertainties of the soil state after installation and load conditions.

Two different type of stiffness values need to be distinguished; stiffness values for the structural utilization (denoted in the following ULS load case) and stiffness values for the load assessment,

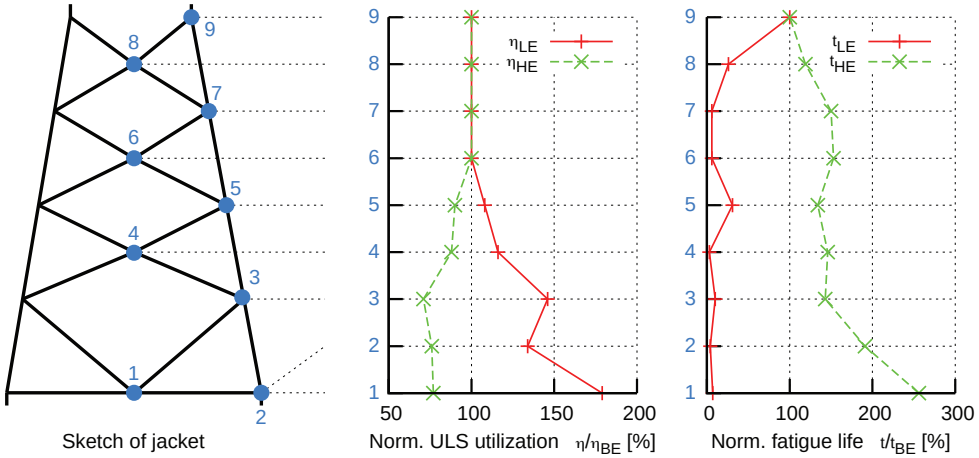

Figure 12: Impact of the HE and LE ULS and FLS stiffness on the jacket response

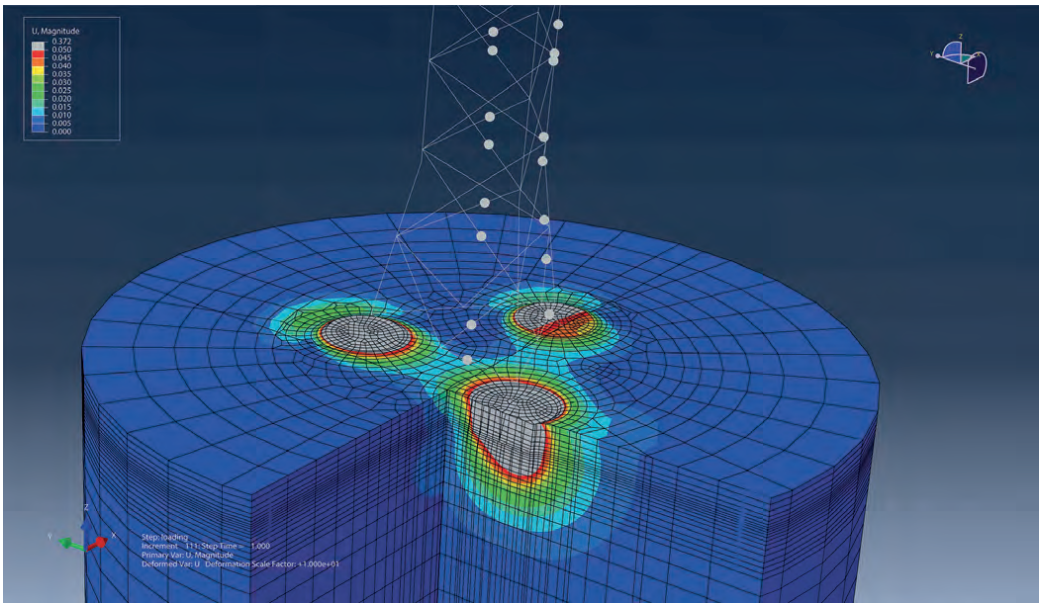

Figure 13: Example of a global model used for assessing local foundation stiffness

structural fatigue analysis and eigenmode analysis (denoted in the following FLS load case). In general the ULS stiffness is non-linear due to the high mobilization of the foundation, wheres the FLS stiffness appears often to be linear due to the significant lower load amplitudes. The soil profiles used in both the simplified and the advanced analysis need to reflect the different loading conditions. The FLS load case is governed by the cyclic amplitude, where the average or mean load is of less important.

Table 2: Variation of the HE and LE ULS and FLS stiffness normalized by the corresponding Best Estimate (BE) stiffness

	ULS	FLS
High Estimate (HE)	288%	189%
Low Estimate (LE)	37 %	69%

Figure 12 shows the impact of the high-, best- and low-estimate foundation stiffness on both the fatigue life and the structural utilization of a jacket supported by three suction caissons. Basis for this analysis are the structural and geotechnical properties at the end of the first iteration of a generic FEED study. The corresponding values are normalised by the best-estimate values. The corresponding normalized stiffness values are listed in Table 2.

It becomes apparent that the structural utilization scales approximately proportional with the ULS foundation stiffness. The variation in utilization, however, is not reflecting the relatively large range in ULS foundation stiffness values, meaning that the jacket is less sensitive to variations in foundation stiffness. In contrast to that, is the impact of the high- and low-estimate FLS stiffness on the fatigue life very pronounced. Even though, the low estimate FLS stiffness is 69% of the best-estimate FLS stiffness, the fatigue life decreases to less than 10%.

This example illustrates, that an optimization of an OWT can be challenging, if the range of foundation stiffness values is too large. Furthermore the implications of assumptions in the geotechnical design on the structural design can be hardly estimated without performing corresponding structural analysis.

When assessing the foundation stiffness for a mono-caisson using the FEM, the loads provided in the design basis can be directly applied to the caisson. When using the calculated foundation stiffness values in the subsequent structural analysis the updated

loads are typically of similar order and ratio. That means the load-stiffness iteration – outer loop in Figure 1 – converge relatively fast.

This is somewhat more complicated for multi-legged sub-structures. Depending on the footprint width, caisson dimensions, load conditions, and ground conditions, the loads can be redistributed between the different legs due to both the flexibility of the sub-structure – i.e. the jacket – and the interaction of the caissons in the ground. Using FE models of single caissons only will not capture the redistribution correctly. More accurate would be to model both the caissons, the sub-structure and the soil. This is denoted *global FE model* and is shown in Figure 13. The difference between a global model and an integrated model is the type of analysis. A global model is typically used in monotonic push-over analysis, whereas an integrated model is used in a time domain analysis.

Advantage of a global model is, that the loads and foundation stiffness values can converge relatively fast in just some few load-stiffness iterations. However, such analysis are time consuming, and – depending on the stage of a project – single caisson models may be used instead, though the accuracy is less good. Based on recent experience, it is recommended to use global FE model in FEED and detailed design at some representative locations of an offshore wind farm. The identification of relevant locations can be reasonably well done using the simplified methods or single FE models, as the *error* is in general proportional.

It may be noted that global FE models are particular relevant for assessing ULS foundation stiffness due to the large mobilization. For FLS load cases, single caissons models are sufficient. An exception is the assessment of foundation damping, both for ULS and FLS. If FE analysis is used for determine foundation damping, the complete soil may be modeled to capture the interaction and larger soil mass.

In addition should be mentioned that attempts are undertaken to use macro elements in structural analysis. However, the macro elements require a calibration of the particular site and caisson geometry, which can be done for some models using the above described methods.

8 SOIL REACTIONS

Soil reactions are, like foundation stiffness, an output of the geotechnical design, but are not considered in the geotechnical sizing of the caisson. However, the results of the stiffness analysis can affect the design basis as illustrated in Figure 2. Soil reactions are typically provided as loads distributed over the skirt(s) and lid which is in contact with the soil. The assessment of load reactions is difficult and depends on many factors, such as the flexibility of the caisson, the soil layering, the recent cyclic load history, and the actual applied load for which the soil reactions shall be provided.

Soil reactions are used for the structural design of the caisson, and need to be provided for two different cases; for installation and for in-place conditions. The soil reactions during installation will typically govern the required thickness and shape of the skirt wall – assessed in buckling analysis – whereas the in-place soil reactions will primarily govern the design of the caisson lid. Of particular importance is the distribution of the loads carried by the lid and the skirts.

Figures 14 and 15 show the result of FE analysis of five suction caissons with different geometries and soil conditions, subjected to short-term compression or tension loading, respectively. The load conditions are representative for a compression or tension leg of a multi-legged sub-structure. From Figure 14 becomes apparent, that the load taken by the lid scales proportionally with the

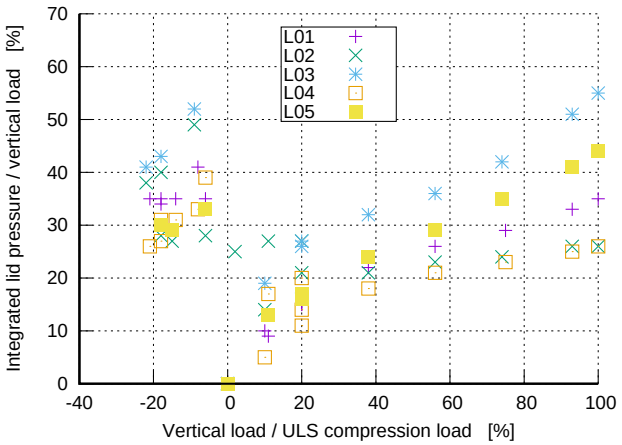

Figure 14: Ration between the loads carried by the lid and the skirts as function of the load amplitude

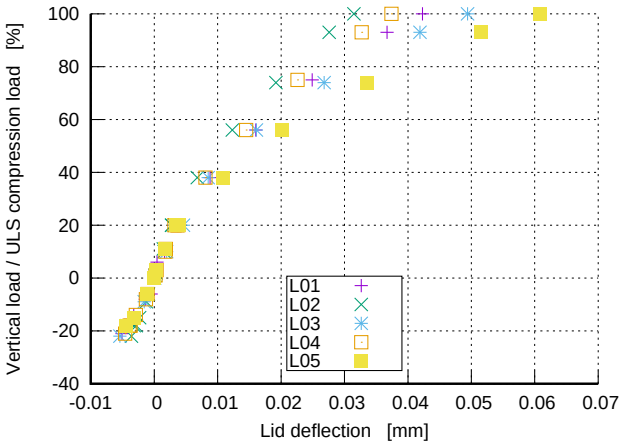

Figure 15: Deflection of the lid as function of the load amplitude

applied load. Small load amplitudes are taken solely by the skirts. The increase in lid pressure is linear and larger for tension loading, though a considerable scatter can be observed on the tension side.

Figure 15 shows the displacements of the caisson at the loading point, which is in this case the top of the lid. It appears to be very linear for low and medium sized load amplitudes, whereas it becomes pronounced non-linear for larger loads. Variations of the lid and caisson stiffness showed, that the linear response at low and medium sized loads is directly proportionally to the caisson stiffness. The soil non-linearity becomes first visible at larger loads. This demonstrates the importance to select the correct geotechnical-structural interface point discussed in Section 1.2.

Thought the results are encouraging, the calculation of the actual values using the FEM is very time consuming and sensitive to the modeling. The stresses depend on the size, number, shape, and type of continuum element used in the analysis. Further, the tip resistance is difficult to assess due to the ratio of wall thickness to caisson diameter, which requires exceptionally small elements along the skirt and below the tip. Thus, the FEM may be used as a complementary method for assessing the soil reactions.

In conventional offshore geotechnical engineering, soil reactions are established based on engineering judgement and are provided as so-called *unit loads*. Unit loads scale proportionally with the applied total load. Assumptions are made on the distribution; similar to the one shown in Figure 14. Upper and lower estimates of the distribution need to be provided.

Soil reactions for the installation can be derived from the ac-

tual penetration analysis, where both skirt wall friction, skirt tip resistance, and required suction pressure are calculated. More complicated is to assess the soil support during installation. It may be assumed that almost no support is provided for penetration in sand where significant flow gradients in the soil plug is expected (drained penetration). Some support may be assumed for undrained penetration, which may be estimated based on suitable laboratory tests.

9 OTHER ASPECTS

9.1 Grouting

An issue often discussed is the necessity of grouting. Grout is used to fill the void between the lid and the soil at the inside of the caisson. Most suction caissons and anchors installed so far were grouted with only some few exception. Main reason of using grout for suction caissons of bottom fixed OWTs is to reduce or avoid potential (differential) settlements, and *pumping*-effects. Due to cyclic vertical loading, the water cushion below the lid is exposed to continuous pressure pulses, which can trigger a local piping failure along the skirts. In addition, a lack of soil/grout support below the lid will cause large local stresses and moments in the lid. All loads need to be transferred trough the lid into the skirts. This requires a thick, massive lid, to avoid large deflections and fatigue issues.

In order to improve the bearing behavior of the lid and and to avoid the afore mentioned negative effects when omitting grout, structural components may be applied to replace the grout. Stopper-pods, which are elements made of steel, hard rubber, or composite materials, can be attached under the lid. The caisson need to penetrate until the pods are in contact with the mudline enabling to transfer loads from the lid into the soil. Alternatively, small ribs or T-beams may be welded under the lid dividing the base into compartments. The structural elements may be slightly cone-shaped to allow partially penetration into the ground in order to compensate for inclined mudline or uneven soil heave. If, an uneven soil surface is expected, a jetting system may be used to flush the upper soil and by that generating a slurry mixture which slowly consolidated during the final phase of the installation.

Disadvantage with using structural and jetting systems is, that the soil which is in contact with the structural components is soft, and the stresses in the lid may be concentrated to some few points only. Based on current experience, the use of grout seems to be appropriate to optimize the lid geometry. However, the cost savings due to an optimized lid geometry, needs to be compared to the costs of the additional offshore work for the grouting.

9.2 Integrated design approach

As mentioned in the several sections, so-called *integrated analysis* are performed in OWT design (e.g. Krathe & Kaynia 2016, Page et al. 2016, Skau et al. 2017). Such analysis are particularity suited for structural analysis, such as in the load or eigenmode assessment. Integrated analysis are not appropriate for the foundation sizing, though some macro-elements may indicate this possibility. The foundation response can be very sensitive to soil layering and size of the caisson and skirt, which cannot be considered by the macro-elements. Furthermore, also other aspects than capacity and serviceability may be design driving as detailed in the corresponding sections in this contribution.

Until today, the geotechnical sizing is uncoupled from the structural analysis and it is not expected that this may change in the near future without compromising an optimization of the caisson geometry.

9.3 Earthquake loading

In some parts of the world, earthquake loading and earthquake induced liquefaction needs to be considered in the design. Both can be considered in the design using existing methods. The loads from the earthquake represent just another load case to which particular soil conditions need to be assigned in the corresponding analysis. Kaynia (2017) provides a comprehensive introduction to the design of OWTs subjected to earthquake loading.

9.4 Observational method

OWTs supported by caissons are a relatively new concept and long-term experience does not exist yet. Thus, the observational method may be considered in current projects. It can be applied during both installation and operation. In order to use the observational method, it is important that the failure is ductile, which allows to initiate mitigation measures(s) in time.

The observational method is a combination of predictions and measurements. The behavior of the OWT is calculated using existing methods. Further, ranges of allowable values need to be defined. If exceeded, mitigation measures need to be initiated, which need to be planned in the forehand.

Examples of mitigation measures during installation are presented in Subsection 5.3. The decision value is typically the required suction pressure, which shall be provided as a range with high and low estimate. If the high estimate value is exceeded, the mitigation measures may need to be applied. The same concept can be applied for the serviceability. When a maximum tilt is exceeded the OWT may need to be rectified.

For a successful application, it is important to plan both an appropriate health monitoring system and mitigation measures. Aspects of monitoring systems are presented by Sparrevik & Strout (2015). The usefulness of such systems is presented by Schonberg et al. (2017) at the example of the Borkum Riffgrund 1 Suction Bucket Jacket.

9.5 Wind farm design

So far, only single OWT foundations were considered herein. An iterative approach as outlined in Section 1.1 at each turbine location of an *Offshore Wind Farm* (OWF) would require considerable time, which may not be possible in the given project time frame. Thus, a clustering may be introduced. Typically, the clustering is a based on the water depth, since the loads are expected to be very similar for a given depth. Foundation capacity and installation analysis can be relatively quickly performed. The results of these can be used for the sizing. If FEM is used for the capacity analysis, as described by Jostad & Andersen (2015), the foundation stiffness can be qualitatively estimated. Based on that, the softest and stiffest location within a cluster can be identified. These two can then used in the stiffness and soil reaction analysis, representing the parameters used in the iteration process, given that the same sub-structure will be applied in the cluster.

10 OUTLOOK

In this article a general overview of the geotechnical design of suction caissons for OWTs has been provided. The different phases of the design were detailed, and the relevant aspects were outlined. The general design of suction caissons is reasonably well understood and many authors have proposed numerous methodologies for specific geotechnical calculations, such as capacity, installation and stiffness analysis. Only some few were mentioned in this article; mainly those which are familiar to the author from personal

experience. The reader is encouraged to get himself an overview of the numerous methods proposed in the literature. The article at hand may serve as a guideline to evaluate the suitability of a method for the particular design aspect.

Due to the increased interest in suction caissons for OWTs, a number of researchers and practitioners are currently working to continuously advance the knowledge. Several of the currently designed and installed OWTs are equipped with comprehensive health monitoring systems, which will provide further inside into the short- and long-term behavior of suction caissons.

ACKNOWLEDGMENT

The authors gratefully acknowledge the support by his colleagues at NGI in the numerous projects which provided the basis for this article. Thanks goes to Knut H. Andersen and Youhu Zhang for the review of the manuscript.

11 REFERENCES

Aas, P., Saue, M. & Aarsnes, J. (2009), Design predictions and measurements during installation of suction anchors with and without water-flow system to help installation through layered soil profiles, *in* 'Offshore Technology Conference, 40. Houston', number OTC-20294-MS.

Andersen, K. (2015), Cyclic soil parameters for offshore foundation design : The third issmge mcclelland lecture, *in* V. Meyer, ed., 'Frontiers in Offshore Geotechnics III, Oslo, Norway', pp. 5–82. Revised version in: http://www.issmge.org/committees/technical-committees/applications/offshore and click on *Additional Information*.

Andersen, K., Jostad, H. & Dyvik, R. (2008), 'Penetration resistance of offshore skirted foundations and anchors in dense sand', *Journal of geotechnological and geoenvironmental engineering* **134**(1), 106–116.

Andersen, K., Puech, A. & Jardine, R. (2013), Cyclic resistant geotechnical design and parameter selection for offshore engineering and other applications, *in* 'ISSMGE - TC 209 Workshop - Design for cyclic loading: Piles and other foundations - Proceedings of TC 209 Workshop, 18th ICMGE, Paris'.

BSH (2015), *Minimum requirements concerning the constructive design of offshore structures within the Exclusive Economic Zone (EEZ)*, number 7005, 2 edn, BSH.

Byrne, B. (2000), Investigations of suction caissons in dense sand, PhD thesis, Department of Engineering Science, The University of Oxford.

Colliat, J., Dendani, H. & Schroeder, K. (2007), Installation of suction piles at deepwater sites in angola, *in* 'Offshore Site Investigation and Geotechnics: Confronting New Challenges and Sharing Knowledge (SUT-OSIG)'.

Cotter, O. (2009), The installation of suction caisson foundations for offshore renewable energy systems, PhD thesis, University of Oxford, Magdalen College.

Cotterill, C., Phillips, E., James, L., Forsberg, C., Tjelta, T., Carter, G. & Dove, D. (2017), 'The evolution of the dogger bank, north sea: A complex history of terrestrial, glacial and marine environmental change', *Quaternary Science Reviews* (171), 136–153.

Cudmani, R. & Sturm, H. (2006), An investigation of the tip resistance in granular and soft soils during static, alternating and dynamic penetration, *in* 'Int. Sym. on vibratory pile driving and deep soil compaction, TRANSVIB'.

DNV-GL (2016), Support structures for wind turbines, Standard DNVGL-ST-0126.

Dove, D., Roberts, D., Evans, D., Tappin, D., Lee, J., Long, D., Mellett, C. & Callard, S. (2016), Refining glacial statigraphy in the southern north sea - new bathymetric model brings renewed value to legacy seismic, *in* 'Near Surface Geoscience 2016 - Second Applied Shallow Marine Geophysics Conference', EAGE.

Foglia, A., Govoni, L., Gottardi, G. & Ibsen, L. (2014), Investigations on macro-element modelling of bucket foundations for offshore wind turbines, DCE Technical Memorandum 48, Aalborg: Department of Civil Engineering, Aalborg University.

Forsberg, C., Lunne, T., Vanneste, M., James, L., Tjelta, T., Barwise, A. & Duffy, C. (2017), Synthetic cpts from intelligent ground models based on the integration of geology, geotechnics and geophysics as a tool for conceptual foundation design and soil investigation planning, *in* 'Offshore Site Investigation and Geotechnics: Smarter Solutions for Future Offshore Developments (SUT-OSIG)'.

Gazetas, G. (1991), Foundation vibrations, *in* H.-Y. Fang, ed., 'Foundation Engineering Handbook', Springer Science+Business Media.

Houlsby, G. & Byrne, B. (2005a), 'Design procedures for installation of suction caissons in clay and other materials', *Proceedings of the Institution of Civil Engineers - Geotechnical Engineering* **158**(GE2), 75–82.

Houlsby, G. & Byrne, B. (2005b), 'Design procedures for installation of suction caissons in sand', *Proceedings of the Institution of Civil Engineers - Geotechnical Engineering* **158**(GE3), 135–144.

IEC (2009), Wind turbines - part 3: Design requirements for offshore wind turbines, Standard IEC 61400-3:2009, International Electrotechnical Commission.

Johansson, P., Aas, P. & Hansen, S. (2003), Field model tests for a novel suction anchor application, *in* '6. International Symposium on Field Measurements in Geomechanics, Oslo, Norway', pp. 145–153.

Jostad, H. & Andersen, K. (2015), Calculation of undrained holding capacity of suction anchors in clays, *in* V. Meyer, ed., 'Frontiers in Offshore Geotechnics III, Oslo, Norway', pp. 263–268.

Jostad, H., Andersen, K., Khoa, H. & Colliat, J. (2015a), Interpretation of centrifuge tests of suction anchors in reconstituted soft clay, *in* V. Meyer, ed., 'Frontiers in Offshore Geotechnics III, Oslo, Norway', pp. 269–276.

Jostad, H., Grimstad, G., Andersen, K., Saue, M., Shin, Y. & You, D. (2014), 'A fe procedure for foundation design of offshore structures – applied to study a potential owt monopile foundation in the korean western sea', *Geotechnical Engineering* **45**(4), 63–72.

Jostad, H., Grimstad, G., Andersen, K. & Sivasithamparam, N. (2015b), A fe procedure for calculation of cyclic behaviour of offshore foundations under partly drained conditions, *in* V. Meyer, ed., 'Frontiers in Offshore Geotechnics III, Oslo, Norway', pp. 153–172.

Kaynia, A. (2017), Earthquake response of offshore wind turbines, *in* 'International Conference on Performance-based Design in Earthquake Geotechnical Engineering (PBD-III)'.

Kelly, R., Houlsby, G. & Byrne, B. (2006), 'A comparison of field and laboratory tests of caisson foundations in sand and clay', *Géotechnique* **56**(9), 617–626.

Krathe, V. & Kaynia, A. (2016), 'Implementation of a non-linear foundation model for soil-structure interaction analysis of offshore wind turbines in fast', *Wind Energy* **20**(4), 695–712.

Langford, T., Solhjell, E., Hampson, K. & Hondebrink, L. (2012), Geotechnical design and installation of suction anchors for the skarv fpso, offshore norway, *in* 'Offshore Site Investigation and

Geotechnics: Integrated Geotechnologies - Present and Future (SUT-OSIG)', pp. 613–620.

Leinenkugel, H. (1976), Deformations- und Festigkeitsverhalten bindiger Erdstoffe. Experimentelle Ergebnisse und ihre physikalische Deutung, PhD thesis, University of Karlsruhe.

Nguyen-Sy, L. (2005), The theoretical modelling of circular shallow foundations for offshore wind turbines, PhD thesis, University of Oxford, Magdalen College.

Nguyen-Sy, L. & Houlsby, G. (2005), The theoretical modelling of a suction caisson foundation using hyperplasticity theory, *in* 'Frontiers in Offshore Geotechnics I, Perth, Austrlia', pp. 417–423.

Niemunis, A., Wichtmann, T. & Triantafyllidis, T. (2005), 'A high-cycle accumulation model for sand', *Computers and Geotechnics* **32**(4), 245–263.

Norén-Cosgriff, K., Jostad, H. & Madshus, C. (2015), Idealized load composition for determination of cyclic undrained degradation of soils, *in* V. Meyer, ed., 'Frontiers in Offshore Geotechnics III, Oslo, Norway', pp. 1097–1102.

Page, A. M., Schafhirt, S., Eiksund, G., Skau, K., Jostad, H. & Sturm, H. (2016), Alternative numerical pile foundation models for integrated analyses of monopile-based offshore wind turbines, *in* '26. International Offshore and Polar Engineering Conference (ISOPE)', pp. 111–119.

Salciarini, D., Bienen, B. & Tamagnini, C. (2011), A hypoplastic macroelement for shallow foundations subject to six-dimensional loading paths, *in* 'International Symposium on Computational Geomechanics (ComGeo II), Cavtat-Dubrovnik, Croatia', pp. 721–733.

Salciarini, D. & Tamagnini, C. (2009), 'A hypoplastic macroelement model for shallow foundations under monotonic and cyclic loads', *Acta Geotechnica* **4**(3), 163–176.

Saue, M., Aas, P., Andersen, K. & E., S. (2017), Installation of suction anchors in layered soils, *in* 'Offshore Site Investigation and Geotechnics: Smarter Solutions for Future Offshore Developments (SUT-OSIG)'.

Schonberg, A., Harte, M., Aghakouchak, A., Brown, C., Andrade, M. & Liingaard, M. (2017), Suction bucket jackets for offshore wind turbines: applications from in situ observations, *in* 'In Proceedings of TC209 Workshop (Foundation design of offshore wind structures): 19th International Conference on Soil Mechanics and Geotechnical Engineering, Seoul, South Korea'.

Senders, M. & Randolph, M. (2009), 'Cpt-based method for the installation of suction caissons in sand', *Journal of geotechnological and geoenvironmental engineering* **135**(1), 14–25.

Skau, K., Chen, Y. & Jostad, H. (2017), 'A numerical study of capacity and stiffness of circular skirted foundations in clay subjected to combined static and cyclic general loading', *Géotechnique* .

Solhjell, E., Blaker, Ø., Knudsen, S. & Rahim, A. (2014), Geotechnical design and installation of suction anchors for the goliat fpso, offshore norway, *in* 'Offshore Technology Conference Asia, Kuala Lumpur, Malaysia', number OTC-24989-MS.

Sparrevik, P. (2002), Suction pile technology and installation in deep waters, *in* '34. Offshore Technology Conference (OTC), Houston, US', number OTC 14241.

Sparrevik, P. & Strout, J. (2015), Novel monitoring solutions solving geotechnical problems and offshore installation challenges, *in* V. Meyer, ed., 'Frontiers in Offshore Geotechnics III, Oslo, Norway'.

Sturm, H. (2009), 'Numerical investigation of the stabilisation behaviour of shallow foundations under alternate loading', *Acta Geotechnica* **4**(4), 283–292.

Sturm, H. (2011), 'Geotechnical performance of a novel gravity base type shallow foundation for offshore wind turbines', *Geotechnik* **34**(2), 85–96.

Sturm, H. & Mirdamadi, A. (2017), Reliability based stiffness analysis for application during installation of suction caissons, *in* 'Proceedings of the 36$^{\text{th}}$ International Conference on Ocean, Offshore and Arctic Engineering, OMAE', number OMAE2017-62043.

Sturm, H., Nadim, F. & Page, A. (2015), A safety concept for penetration analyses of suction caissons in sand, *in* V. Meyer, ed., 'Frontiers in Offshore Geotechnics III, Oslo, Norway', pp. 1393–1398.

Svanø, G., Eiksund, G., Kavli, A., Langø, H., Karunakaran, D. & Tjelta, T. (1997), Soil-structure interaction of the draupner e bucket foundation during storm conditions, *in* '8. International Conference on the Behaviour of Offshore Structures, Delft', Vol. 1, pp. 163–176.

Wichtmann, T., Niemunis, A. & Triantafyllidis, T. (2010), Application of a high-cycle accumulation model for the prediction of permanent deformations of the foundations of offshore wind power plants, *in* 'Frontiers in Offshore Geotechnics II, Perth, Austrlia'.

Suction bucket jackets for offshore wind turbines: applications from in situ observations

Suction caisson jackets pour des éoliennes en mer: applications des observations in situ

Avi Shonberg, Michael Harte, Amin Aghakouchak, Cameron S. D. Brown, Miguel Pacheco Andrade and Morten A. Liingaard
DONG Energy, avish@dongenergy.co.uk

ABSTRACT: Offshore wind foundations of the future face many challenges. Due to the growing demand for renewable energy, future projects will be built further offshore in deeper water with larger wind turbine generators (WTGs) leading to increased foundation loads. Furthermore, in some regions, foundations must be installed without exceeding strict regulatory requirements on underwater noise. Thus, traditional foundation solutions are being pushed to their limits and there is a need for innovative foundation concepts. The suction bucket jacket (SBJ) is one such foundation solution which addresses these future challenges. In 2014, DONG Energy installed a highly instrumented SBJ at the Borkum Riffgrund 1 wind farm to support a Siemens 4 MW WTG. This is the first wind turbine to be founded on a SBJ. Using monitoring data obtained between September 2014 and January 2016, this paper outlines some key findings. The paper focuses on the in-place response of the SBJ to loading including long term behaviour of the structure, vertical stiffness response, load transfer along the bucket skirt and the variation of pore water pressures.

RÉSUMÉ: Les fondations des futures éoliennes en mer font face aux nombreux défis. Par suite de la croissance des énergies renouvelables, les futurs parcs éoliens en mer seront construits plus loin de la côte dans des plus grandes profondeurs d'eau et les éoliennes seront plus grandes avec des charges augmentées sur les fondations. En plus, dans certains régions du monde il y a des limitations sur les nuisances sonores sous-marin qui sont générés pendant l'installation des fondations. Les solutions des fondations traditionnelles sont à leurs limites ce qui augmente la demande des idées innovantes. La technologie "suction caissons" réponds à ces futurs défis. DONG Energy a déjà installé une fondation type "suction caissons" au parc éolien Borkum Riffgrund 1 avec une éolienne de 4MW de capacité fabriqué par Siemens. C'est la première éolienne en mer qui est construit sur une fondation du type "suction caissons". Des mesures ont été fait depuis l'installation de la fondation en 2014 jusqu'à janvier 2016. Les résultats de l'analyse de ces données sont présentés dans cet article. Cet article mettra l'accent sur la réaction in-situ de la fondation type "suction caissons" au chargement y compris le comportement à long terme de la structure, ainsi que la réaction au rigidité verticale, le transfert de charge le long de la caisson et la variation de la pression interstitielle.

KEYWORDS: suction bucket jacket, shallow foundation, in place performance, case study

1 INTRODUCTION

A suction bucket jacket (SBJ) foundation has been installed at the Borkum Riffgrund 1 (BKR01) offshore wind farm to support a Siemens 4 MW wind turbine generator (WTG). The innovative foundation concept (shown in Figure 1) was installed by DONG Energy in 2014 in collaboration with the Carbon Trust Offshore Wind Accelerator (OWA) program in order to addresses future challenges associated with offshore wind farm developments. Whilst the SBJ is not a new concept, the BKR01 SBJ is the first wind turbine to be founded on a SBJ structure.

The BKR01 SBJ has been instrumented with a comprehensive measurement system to monitor the structural and geotechnical behaviour during the lifetime of the structure. This paper outlines some key findings from analysis of the monitoring data collected from 2014 to 2016. The paper analyses the in-place response of the SBJ subjected to environmental wind and wave loading acting on the WTG. This includes analyses over a full year of monitoring data and much smaller subsets of data where appropriate.

This paper investigates the long term behaviour of the structure and the average vertical stiffness response of the different suction bucket components. Importantly, the stiffness response is also investigated as a function of loading direction and loading level. Furthermore, the load transfer along the bucket skirt using strain gauge measurements is compared with hand calculations using conventional methods. Finally, the pore water pressure response to different loading frequencies are analysed to estimate the boundaries between drained and undrained suction bucket behaviour.

Overall, this paper uses the in situ observations from a world-first full scale monitoring system to better understand the behaviour of the SBJ under environmental loading conditions.

2 BACKGROUND

The 312 MW BKR01 offshore windfarm is located in the German sector of the North Sea, approximately 38 km north of the island of Borkum (Figure 2). The wind farm contains 78 WTGs and covers an area of approximately 36 km^2.

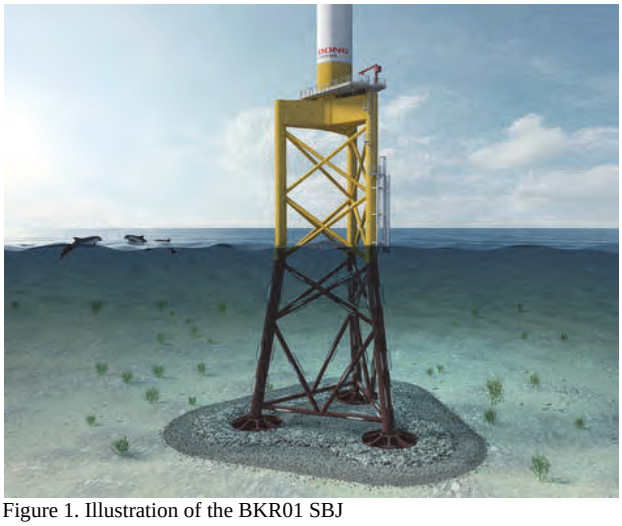

Figure 1. Illustration of the BKR01 SBJ

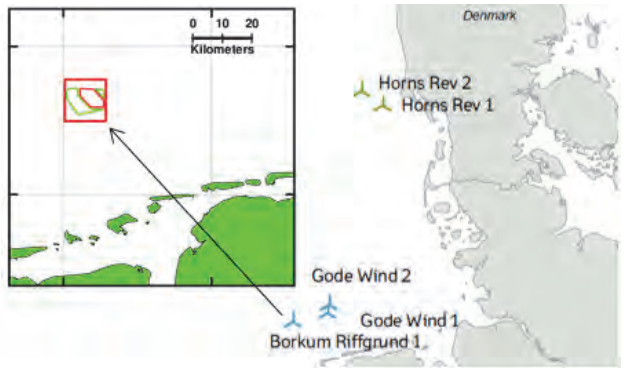

Figure 2. Location of the BKR01 wind farm

One of the foundations installed at BKR01 is a three-legged SBJ foundation as illustrated in Figure 1. The layout and bucket naming convention is shown in Figure 3. At BKR01, the remaining WTGs are supported by monopile foundations. The SBJ foundation has a soft-stiff design and supports a Siemens 4MW WTG. The BKR01 SBJ was successfully installed using a suction assisted operation in the summer of 2014.

Prior to the BKR01 project, the SBJ foundation concept had been used for other North Sea foundation structures, such as the Sleipner T (Tjelta, 1994; Bye *et al*., 1995; Tjelta, 1995) and Draupner E structures (Erbrich & Tjelta, 1999) but never as a foundation for a WTG. The BKR01 SBJ was commissioned to assess the economic and environmental benefits associated with jacket structures and suction assisted installation for WTG foundations.

The soil conditions at the site are typical of German North Sea conditions with the near surface consisting of medium dense to dense sands. A layer of more silty sand is present at between approximately 3 m and 6 m below seafloor (bsf).

The suction buckets installed at BKR01 have a diameter (D) of 8 m and a skirt length (L) of 8 m, giving a length to diameter (L/D) ratio of 1. The skirt length adopted included an allowance for the expected soil heave during installation and a minimum volume for grout post installation. The grout injection, undertaken after installation of the SBJ, ensured full contact between the underside of the bucket lids and the soil.

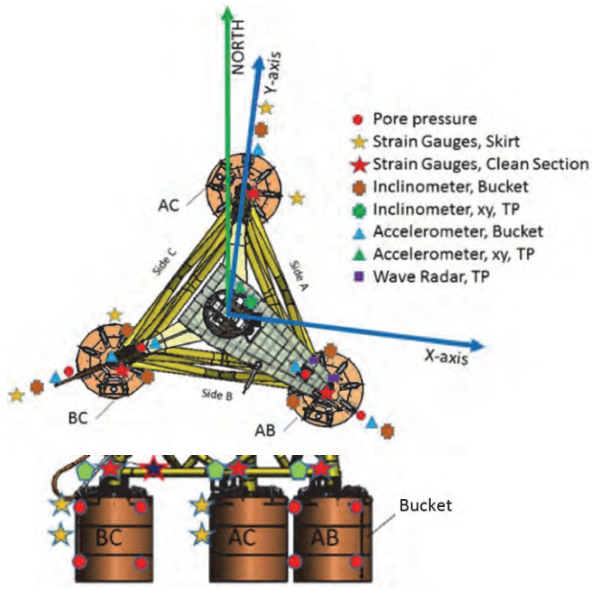

Figure 3. SBJ layout and monitoring system setup

3 MONITORING SYSTEM

The BKR01 SBJ is extensively instrumented with strain gauges, accelerometers, inclinometers, pressure sensors and temperature sensors. The monitoring system, designed by the Norwegian Geotechnical Institute (NGI), was installed to record the structural and geotechnical response of the SBJ during the offshore environmental loading experienced during the lifetime of the structure. As described by Sturm (2017), very few examples of full-scale monitoring systems for offshore structures similar to the BKR01 SBJ are found in the literature, thus the monitoring system installed at BKR01 provides a significant new dataset for observations of this nature. The monitoring system, as also described by Sparrevik & Strout (2015) and Ehrmann *et al*. (2016), included measurement points on the jacket, at the connection between the jacket and the buckets and on each of the three suction buckets.

Table 1, Figure 3, Figure 4 and Figure 5 provide an overview of the sensors installed on each bucket relevant to the geotechnical analyses. Bucket forces were measured in 6 degrees of freedom (DOF) at each bucket via a bespoke 'clean section' connection (further discussed in Section 3.1) between the bucket and jacket leg. For redundancy and efficiency, the monitoring system was different for each bucket. Bucket BC is the most heavily instrumented bucket.

Table 1. Bucket monitoring system measurements and number of sensors

Measurement or sensor	Bucket BC	Bucket AB	Bucket AC
Bucket forces in 6 DOF	Yes	Yes	Yes
Bucket lid accelerations [1]	3	2	1
Bucket lid inclinations [2]	3x1D	3x1D	1x2D
Skirt strains [1]	Yes	No	Yes
Excess pore pressures [3]	Yes	Yes	No

[1] See Figure 4 and Figure 5
[2] Where a 1D inclinometer measures inclinations about one axis only and a 2D inclinometer measures inclination about two axes.
[3] Pore pressure sensors are located under the bucket lid and at 0.5 m from the skirt tip (inside and outside). The sensors measure the differential pore pressures between their level and the top (outside) of the bucket where a reference sensor was located.

3.1 Clean section

A unique feature of the BKR01 SBJ monitoring system was the inclusion of a 'clean section' at the connection between the bucket and jacket leg to measure the force vector in 6DOF at this critical location. The bespoke 'clean section', designed by Ramboll, consisted of a ring stiffener to homogenise the forces in the section and an array of 12 strain gauges distributed around the inner circumference of the section which allowed for correlation between measured strains and the 6DOF section force vector. The 'clean section' was calibrated using known forces during the installation process.

3.2 Monitoring system operation

The monitoring system was operational during the installation of the SBJ, during placement of the tower and rotor/nacelle assembly (RNA) onto the SBJ and during regular periods between September 2014 and January 2016. The time periods for which data is available from 2016 are shown in
Figure 6 (red zones indicate periods of some sensor functionality loss, and the relevant sensor data has been excluded from the analyses). Monitoring continues to date, although the results from the aforementioned period are the only measurements considered in this study.

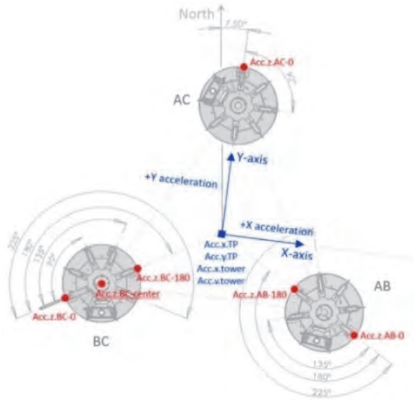

Figure 4. Position of accelerometers on the bucket lids

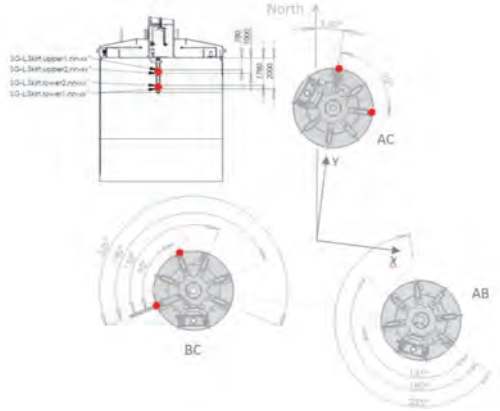

Figure 5. Position of strain gauges on the bucket skirts

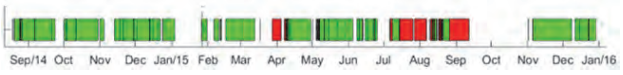

Figure 6. Monitoring system operations

4 SITE CHARACTERISTICS

4.1 Soil conditions

An extensive site investigation and laboratory testing program was carried out specifically for the BKR01 SBJ, which included a CPT at each suction bucket location (outside the footprint of each individual bucket) and a central borehole from which samples were retrieved.

The soil conditions at the site are typical of German North Sea conditions with the near surface generally consisting of medium dense to dense sands. A layer of more silty sand was identified by the CPTs between approximately 3 m and 6 m below the surface. Table 2 outlines the identified layers and interpreted soil parameters. The water depth at the SBJ location is 24.4m (relative to LAT). Scour protection was installed at the SBJ location which included a pre-installed 'filter layer' and post-installed rock armour layer.

4.2 Loading

Operational wind loads at BKR01 are generally omnidirectional but have a tendency towards emanating from headings between 200° and 300°. Storm wind loads and wave loads also tend to emanate from headings between 200° and 300°. During these conditions, higher compressive loads (referred to as 'compressive live loads') are observed in Bucket AB and Bucket AC and lower compressive loads (referred to as 'tensile live loads') are observed in Bucket BC. Under normal operational conditions, the horizontal to vertical load ratio at the mudline is approximately 0.1.

The dead load from the entire structure (including the SBJ, tower and RNA) have been deducted from all forces presented in this paper. Therefore, the forces presented are relative to the dead load of the entire structure. As shown in Figure 16, negative values represent compressive live loads and positive values represent tensile live loads. Absolute tensile forces have not been observed during the monitoring program.

Table 2. BKR01 SBJ soil profile

Top of layer (m bsf)	Description	Relative density (%)	Fines content (%)	Peak friction angle (°)
0	SAND, very dense, medium to coarse grained.	100	5 - 10	47
2.9	SAND, medium dense, fine to medium grained, some layers of silty sand.	70	5 - 20	40
5.6	SAND, very dense, medium to fine grained.	90	5 - 15	45
15.1	SAND, dense to very dense, fine to medium grained, some layers of silty sand to sandy silt.	70	5 - 10	40

5 IN PLACE BEHAVIOUR

5.1 Inclination

The inclination of the BKR01 SBJ structure is measured by a bi-directional inclinometer located on the transition piece (TP) above the water surface. The resultant inclination of the structure from Q4 2014 to Q1 2016 for standstill periods only (i.e. when the wind turbine is not operational) is shown in Figure 7. The 10 minute averages of inclination are shown in the light colour and the weekly average tilts are shown with the darker line. After first power, the 10 minute average inclination is effectively removed by the filtering as fewer standstill periods occur.

As expected, a minor change in inclination was observed immediately after the WTG installation, with the inclination from vertical reducing. Since installation of the WTG, the inclination from vertical of the BKR01 SBJ has generally stayed below 0.01°. Figure 7 shows that the resultant SBJ inclination has not varied significantly with time. This indicates that environmental loads have little impact on the overall tilt of the structure in the long term and that the structure is stable.

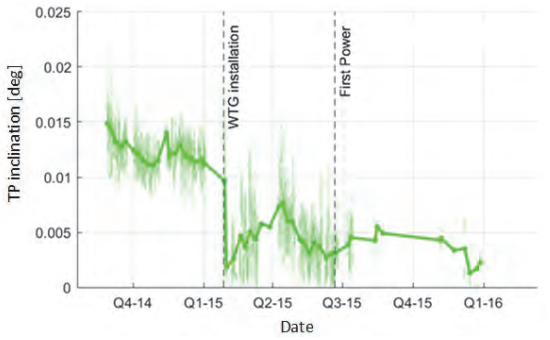

Figure 7. Inclination measurements through time, for standstill conditions only

When the 10 minute average inclination at the TP is plotted against wind speed (Figure 8), it can clearly be observed that the inclination varies with wind speed but returns to a small value at low wind speeds where the thrust-induced inclination is small. The maximum inclination correlates with the maximum bucket force associated with the rated wind speed of the WTG (approximately 12 m/s). The large scatter in inclinations at the

maximum wind speed is due to wind direction variation. The cluster of data points at low inclinations do not follow the general trend and these relate to standstill or no power conditions.

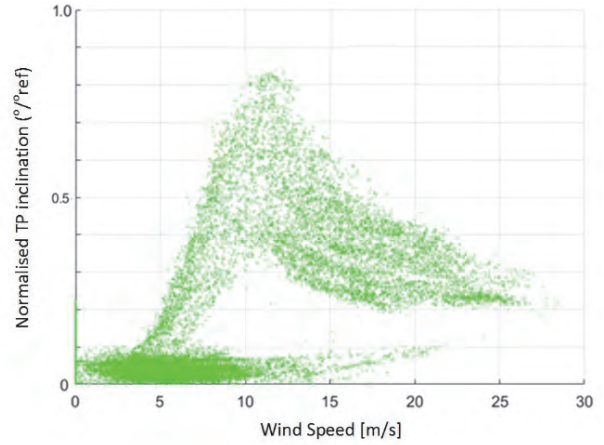

Figure 8. Normalised resultant TP inclination as function of wind speed

5.2 Excess pore pressures

Figure 9 shows the 10 minute average of the excess pore pressures measured for Bucket BC during the monitoring period. Up until the time of first power, the excess pore pressures do not vary from the long-term average indicating that the response is essentially drained. After first power, the excess pore pressures measured under the suction bucket lid show increased variability, indicating some generation of excess pore pressure associated with an undrained response. This trend is not observed at the skirt tip, indicating that excess pore pressure is not generated, or is at least not maintained, in the region of the skirt tip.

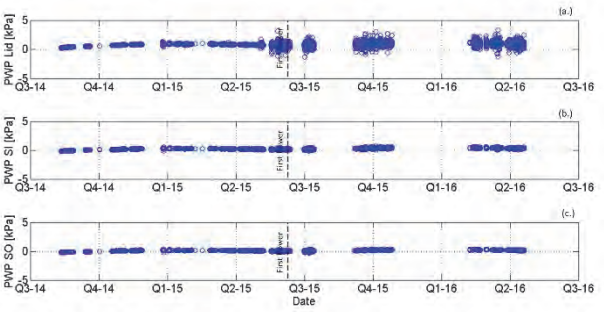

Figure 9. Excess pore water pressure with time for Bucket BC a) under the lid, b) inside skirt tip and c) outside skirt tip

6 SUCTION BUCKET RESPONSE TO LOADING

A key geotechnical input to the design of a multi-footed jacket structure is the response of the foundations. Similar to the assumptions commonly adopted for spudcan analyses (Houlsby, 2014) and as described by Dekker (2014) with specific reference to suction bucket foundations, a structural analysis of the jacket structure often requires the geotechnical engineer to provide a 6X6 stiffness matrix for use as the boundary condition in the jacket model. Numerous authors have proposed methods for estimating the 6DOF suction bucket response to loading (Doherty *et al.*, 2005; Suryasentana *et al.*, 2017) using a limited number of site specific inputs such as soil stiffness and suction bucket dimensions. Due to the 'push-pull' nature of the loading on the SBJ, the vertical stiffness will typically dominate the response in terms of soil structure interaction.

Both the Doherty *et al.* (2005) and Suryasentana *et al.* (2017) methods are calibrated from extensive numerical modelling. A key assumption of both methods is that the lid is a rigid element, although variations in skirt stiffness are taken into account by the former. However, the response of the BKR01 SBJ bucket shows that understanding the effect of the lid stiffness is vital to correctly predicting the overall bucket response.

6.1 BKR01 SBJ overall suction bucket response

The suction bucket's response to vertical loading is calculated using the bucket specific vertical force vector and the bucket specific vertical displacement, calculated by double integration of the accelerations measured on the top of the buckets (a_z in Figure 11). The bucket stiffness can only be estimated for the dynamic part of the load as the accelerometers cannot measure long term displacement relative to a reference point. Therefore, the measured vertical stiffness of the suction bucket is a measure of the suction bucket's response to dynamic vertical loading, often referred to as the FLS stiffness (Figure 10).

The suction bucket response to the dynamic portion of the load is predominantly undrained, as described in Section 9. Therefore, the estimated vertical stiffness of the suction buckets implicitly includes a contribution from the resistant force generated by the excess pore water pressure beneath the bucket lid.

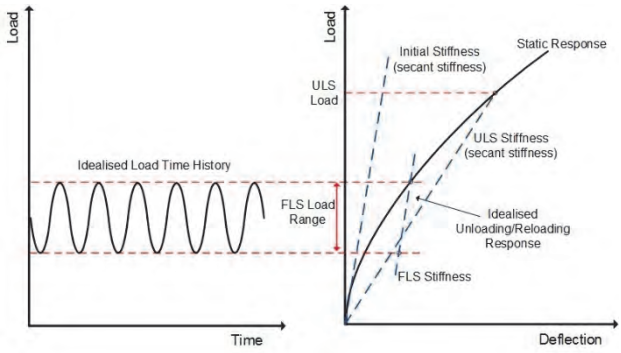

Figure 10. Idealised load-time history and load-deflection response

6.2 Stiffness components and calculation methodology

The measured bucket displacement is a combination of three motions: bucket plunge, bucket rotation and lid deflection (Figure 11). These motions are independently calculated and are then used to determine the deflection of the bucket lid and the deflection of the entire bucket for the vertical stiffness calculations. The rotational stiffness is not considered in this study.

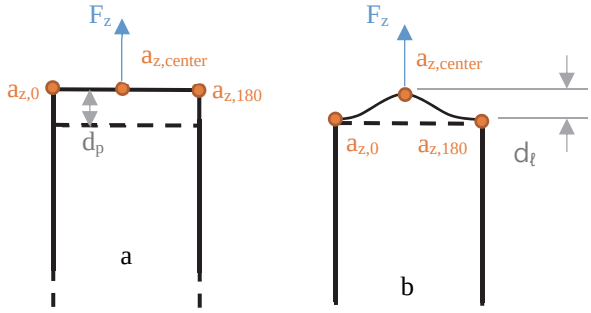

Figure 11. a) Bucket plunge (d_p) and b) bucket lid deflection (d_l)

The following vertical stiffness components can be estimated using the resolved force and the bucket displacement:

- The soil-skirt stiffness (using the bucket plunge)

- The lid stiffness (using the lid deflection)
- The total bucket stiffness (using the total deflection)

6.3 Stiffness observations and results

Figure 12 shows the 10 minute average normalised vertical stiffness for each stiffness component of Bucket BC after first power of the WTG. Results are presented from Bucket BC as only Bucket BC was equipped with the sensors to resolve all displacement components.

During periods of low excitation, the signal to noise ratio decreases and the stiffness cannot be estimated. Therefore, periods at low wind speeds or standstill were filtered out and not analysed. The plot is presented in terms of probability density which provides a relative indication of the number of occurrences of each normalised vertical stiffness value.

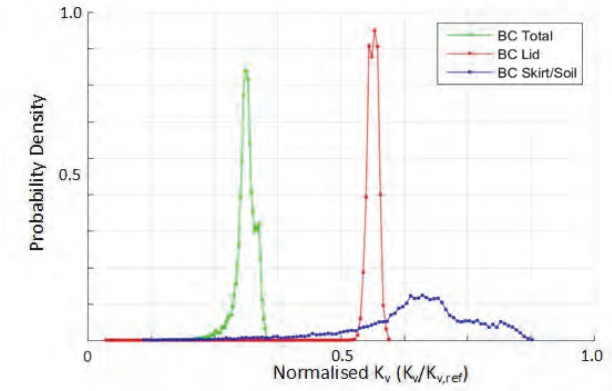

Figure 12. Total, lid and soil-skirt stiffnesses measured at Bucket BC

As expected, Figure 12 indicates that the suction bucket lid exhibits a relatively consistent linear stiffness response to loading which is independent of load level or load direction, as the normalised lid stiffnesses fall within a narrow band of values. The mean normalised vertical lid stiffness, $k_v/k_{v,ref}$, is approximately 0.56.

Conversely, the soil-skirt stiffness exhibits significant variability during the assessed monitoring period, with normalised vertical stiffnesses ranging from approximately 0.38 to approximately 0.88. This indicates that the soil-skirt stiffness is not constant as it is dependent on the load level, frequency and/or load direction, which is further described in Section 6.3.1 and Section 6.3.2. The mean normalised vertical soil-skirt stiffness is approximately 0.66. The mean stiffness of the suction bucket is greater than the mean stiffness of the lid potentially due to the large soil mass being mobilised during loading.

During design, the suction bucket's structural elements (bucket lid and soil-skirt response) are often idealised as a series of springs. When calculating the total bucket vertical stiffness, it is often assumed that the different components of the bucket can be combined as system of spring in series, such that:

$$\frac{1}{K_{total}} = \frac{1}{K_{lid}} + \frac{1}{K_{soil-skirt}} \quad (1)$$

Calculating the total stiffness using Eq. 1, with the mean stiffness values shown in Figure 12, a total normalised vertical stiffness of approximately 0.31 is found. This correlates well with the observed total bucket vertical stiffness shown in Figure 12. Therefore, observations from the BKR01 SBJ confirm the assumption that in terms of vertical stiffness, the suction bucket lid and soil response can be treated as pair of vertical springs in series.

6.3.1 Effect of load direction on bucket vertical load

The measured mean vertical load (F_z) at the 'clean section' for a series of nacelle positions and wind speeds is shown in Figure 13. There is a strong relationship between wind direction (indicated as a heading in bold above each sub plot) and the forces in the individual buckets. For example, for winds emanating from heading 232.5° to 262.5°, Bucket BC experiences a lower compressive load whilst Bucket AB and Bucket AC experiences a higher compressive load.

For some intermediate loading directions, the load appears to act around an axis perpendicular to the loading direction. For example, with winds emanating from heading 262.5° to 292.5°, very little force is observed in Bucket AC whilst 'push-pull' forces are observed to be acting on Bucket AB and Bucket BC respectively.

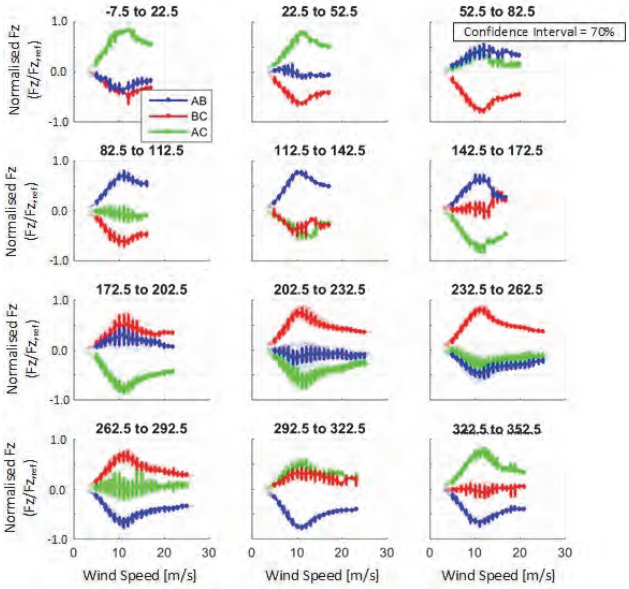

Figure 13. Mean vertical load on the three suction buckets as a function of wind speed and yaw direction

6.3.2 Effect of mean load level on bucket stiffness

A key observation from the BKR01 SBJ response to loading is that soil-skirt stiffness is dependent on the mean load level acting on the bucket. In Figure 14, the soil-skirt stiffness values binned by wind direction are shown for Bucket BC. This shows that Bucket BC behaves stiffer when subject to higher compression loads (winds generally from the north east with a heading of between -7.5° and 82.5°), as indicated by the blue series', and less stiff when subject to lower compression loads (winds generally from the south west with a heading of between 202.5° and 262.5°), as indicated by the yellow-orange series'.

This effect is studied by focusing on two wind direction bins which give the maximum and minimum compression loads on Bucket BC. Examining these two directional bins, the effect of static (mean) compressive loads on the bucket becomes more apparent. Orientation of these wind direction bins are shown in Figure 15 with the maximum compression load bin shown in red (wind from heading 37.5° to 97.5°) and the minimum compression load bin shown in blue (wind from heading 217.5° to 277.5°).

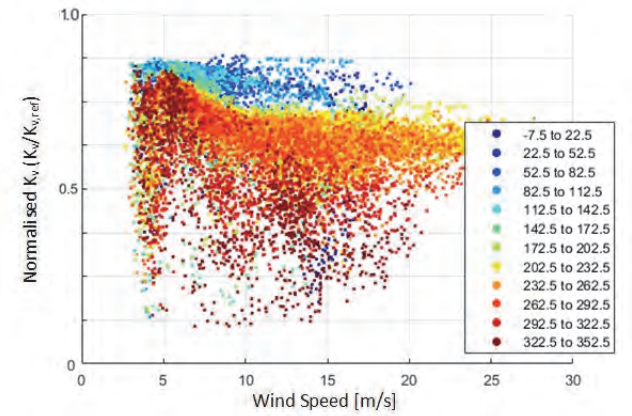

Figure 14. Bucket BC stiffness as a function of nacelle position and wind speed

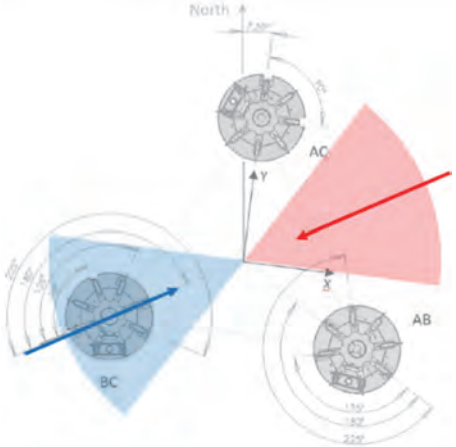

Figure 15. Two sectors aligned with Bucket BC

The resulting soil-skirt stiffness in these two load direction bins is shown in Figure 16a. When Bucket BC is experiencing compressive live loads (higher compression loads, shown in red), the normalised vertical stiffness is notably higher than when the bucket is experiencing tensile live loads (lower compression loads, shown in blue). This confirms that load level (which is a function of wind direction) has an effect on vertical stiffness.

Figure 16b shows two clear regions of distinct behaviour. When Bucket BC is experiencing compressive live loads, the foundation stiffness stays relatively constant. When the bucket is experiencing tensile live loads, the foundation stiffness tends to decrease linearly with decreasing compressive loads. This is particularly noticeable for the upper bound envelope of the data cloud where less scatter is observed.

These variations in stiffness may be a result of changes in the vertical effective stress regime under different loading conditions. An increase in the mean load level due to environmental loads (predominantly wind loading) will result in an increase of the mean vertical effective stress beneath the foundation. As the BKR01 SBJ is founded on predominantly sandy strata, this will increase the vertical capacity of the suction bucket as well as its stiffness response.

Wroth & Houlsby (1985) proposed a power function relationship between the shear stiffness and effective mean stress, p´. Aghakouchak (2015), in a set of recent laboratory tests on quartz sand, showed that increases in vertical effective stress caused an increase in the shear stiffness of sand. The relationship between effective stress and shear stiffness can be presented as:

$$\frac{G}{P_r} = f(e)C\left(\frac{\sigma'_v}{P_r}\right)^a \quad (2)$$

Where C is a material constant, *f(e)* is the void ratio normalisation function, P_r is the reference pressure and α varies from 0.5 to 0.6 at small strains and increases to 1 as higher shear strain levels are reached. Using the relationship in Eq. 2 with the methods proposed by Doherty *et al.* (2005) or Suryasentana *et al.* (2017) a prediction of the increase in bucket stiffness as a function of increase in vertical effective stress can be made. However, the increase in vertical effective stress beneath the suction bucket is unknown as the bucket skirt and the pore water (undrained behaviour) will take a portion of the load. By using the measured total bucket stiffness as a function of change in load level (Figure 16), the increase in vertical effective stress beneath the bucket as a proportion of the applied load (B) can be back-calculated to provide an estimate of the load distribution between lid and skirt.

Assuming a linear relationship between soil shear stiffness and foundation stiffness (Suryasentana *et al.*, 2017), the vertical effective stress under the foundation (σ'_2) after the application of environmental loads (F_z) can be calculated by assuming the initial vertical effective stress (σ'_1), the foundation stiffness prior to applying the load (K_1) and the new foundation stiffness value (K_2). This relationship is summarised by Eq 3.

$$\frac{K_2}{K_1} = \left(\frac{\sigma'_2}{\sigma'_1}\right)^a \quad (3a)$$

$$\sigma'_2 = \sigma'_1\left(\frac{K_2}{K_1}\right)^{\frac{1}{a}} \quad (3b)$$

$$\sigma'_2 = \sigma'_v + B\left(\frac{F_z}{A}\right) \quad (3c)$$

Where A is the area of the suction bucket and B is the proportion of the applied load which is observed beneath the suction bucket.

For the BKR01 SBJ, the initial stiffness (K_1) and initial vertical effective stress (σ'_1) are taken from the point where the maximum tensile live load is observed (approximately 3500 kN on Figure 16b). It is assumed at this point that the vertical effective stress is equal to the in situ vertical effective stress prior to installation of the SBJ such that $\sigma'_1 = \sigma'_v$.

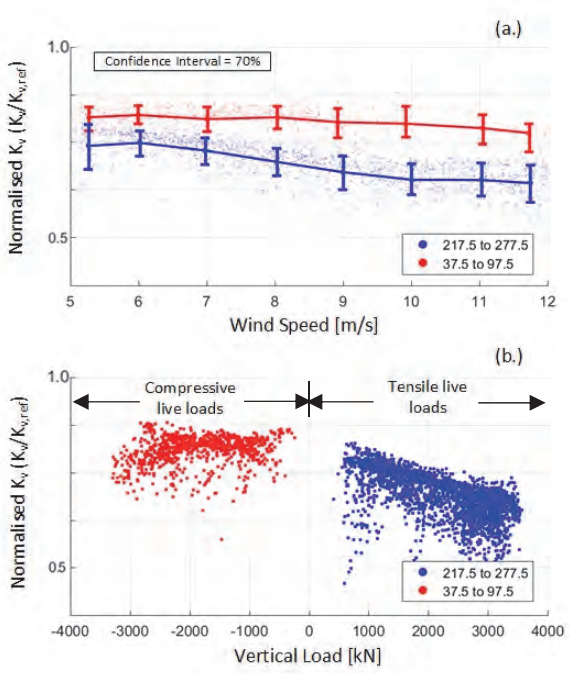

Figure 16. Vertical soil-skirt stiffness in two directional sectors of Bucket BC a) versus wind speed and b) versus vertical load

By using Eq. 3, the directional dependent stiffness observations from Bucket BC presented in Figure 16b for tensile live loads and taking K_2 at the structure's dead load level (0 kN on Figure 16b), the increase in effective stress in the soil mass back calculated from the stiffness variation is between 10% - 20% of the applied load. In other words, B is between about 0.1 and 0.2. The remainder of the increased load may be dissipated/resisted by the soil-skirt friction resistance or pore pressures.

Figure 16b shows that the trend of increasing stiffness with increasing load does not apply for compressive live loads, where it is observed that the stiffness is relatively constant and tends to reduce after a threshold value of approximately -2500 kN.

Figure 17a shows the suction bucket load-displacement response which is calculated for each data point by dividing the mean applied load by the measured secant stiffness values. It has been assumed that the highest tensile live load level corresponds to an absolute load of 0 kN. At high tensile live loads, the effect of soil stiffness on the load-displacement curve becomes apparent as the tangent slope of the curve reduces with reducing load. At compressive live load levels which are more than the deadweight of the structure, an initial linear load-displacement response is observed. At higher displacements, a non-linear response is observed. The overall shape of the load-displacement curve is similar to that observed from model tests reported by Byrne & Houlsby (2002). Of particular note, the 'banana shape' of the load-displacement curve as the load is reduced towards 0 kN net load is replicated in the BKR01 SBJ data. This is shown clearly in
Figure 17b where an indicative linear fit (in red) shows the data following a non-linear response as live tensile loads increase.

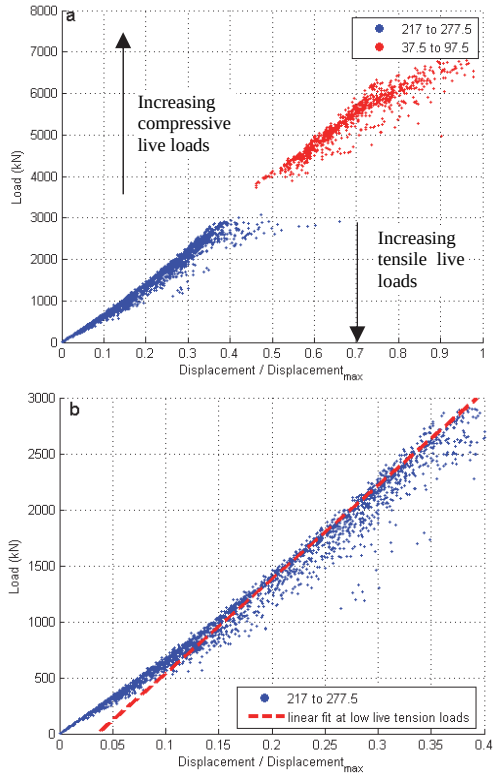

Figure 17. a) Load-displacement response of Bucket BC b) load-displacement response at maximum tensile live loads in which response becomes non-linear

6.4 Variation of stiffness between buckets

Figure 18 presents a comparison between the measured normalised vertical bucket stiffnesses for each bucket in terms of number of occurrences (probability density). It is clear that Bucket AB and Bucket BC have a similar mean normalised vertical stiffness which is lower than the mean normalised vertical stiffness of Bucket AC. This provides further evidence that the load level has a direct influence on the suction bucket vertical stiffness response with lower compressive loads leading to lower vertical stiffness. As Bucket AB and Bucket BC experience lower compressive forces under the prevailing wind direction (wind emanating from heading 200° to 300°) as shown in Figure 13, it would be expected that these buckets would exhibit lower vertical stiffnesses, as observed in Figure 18. Conversely, Bucket AC experiences higher compressive forces under these loading conditions and would therefore be expected to exhibit a higher vertical stiffness response, which is also observed in Figure 18. In general, the mean normalised vertical stiffness of Bucket AC is approximately 10% greater than the mean normalised vertical stiffnesses of Bucket AB and Bucket BC. This is consistent with the observations from Figure 16a, where it is shown that the vertical stiffness is approximately 10% – 20% higher for a bucket under higher compressive load levels.

Notably, a second normalised vertical stiffness 'peak' is observed for Bucket BC (normalised vertical stiffness of approximately 0.67) which may reflect the bucket behaviour under higher compressive loads (when the winds emanate from a more easterly heading).

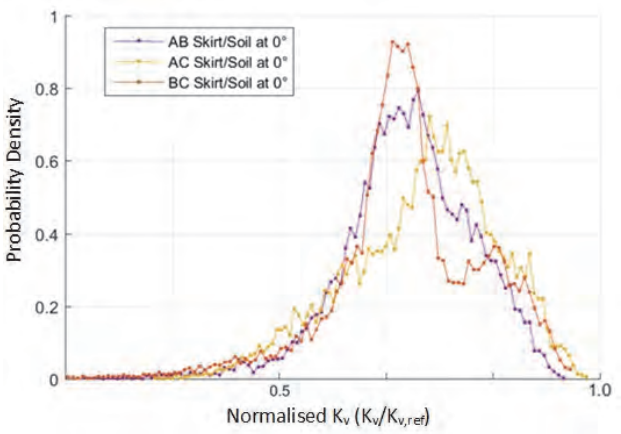

Figure 18. Soil-skirt vertical stiffness for each bucket

7 LOAD TRANSFER THROUGH THE SKIRT

The strain gauges installed along the bucket skirt (see Figure 5) can be used to measure forces in the skirt and therefore allow for the calculation of the shaft resistance over a small section of skirt length. The strain gauge readings can be used to estimate the shaft resistance during loading and the distribution of the load between the skirt and the lid during loading.

7.1 Unit shaft resistance

The shaft resistance was assessed by comparing the forces in the clean section with the change in force between the two strain gauge levels. By taking the 10 minute average skirt force for each strain gauge for all time points, the drained response of the bucket skirt can be assessed.

Figure 19 and Figure 20 show examples of the measured vertical force at the clean section against the calculated force in

the strain gauges for Bucket BC and Bucket AC. A mean of the data cloud is calculated for different load levels (blue line) and a best fit line (red dashed line) was fitted to this dataset. A slope of 1 (black dashed line) would indicate that the force measured at the clean section was equal to the force calculated at the strain gauge. A linear fit was generally observed up to load levels approaching the maximum compression load at which point the gradient is observed to reduce and exhibits nonlinear behaviour.

The 'slope' of the best fit line for each of the 9 strain gauges has been calculated and plotted against depth below lid level on Figure 21. Each data point shown on Figure 21 therefore represents the average proportion of load transferred from the clean section to each strain gauge. For example, for the strain gauge at 1 m below lid level on Bucket AC (0°) shown in Figure 20, an average slope of 0.88 was calculated, indicating that on average, the force measured at the strain gauge was 88% of the force measured at the clean section. As expected, Figure 21 shows that the force transferred to the strain gauges generally reduces with depth as force is transferred to the soil via friction between the soil and the skirt wall (shaft resistance).

By comparing the calculated slopes (load transferred to the strain gauges compared to the clean section) at the two different strain gauge levels (Figure 21), the unit shaft resistance of the skirt between the two strain gauge levels can be calculated. Using the upper bound envelope from Figure 21 as an example, the upper strain gauge level slope is 0.95 and the lower strain gauge level slope is 0.78. On average, this indicates that at the upper strain gauge level, 95% of the force measured in the clean section is measured at the strain gauge, but this value reduces to 78% at the lower strain gauge level. The force dissipated between the two strain gauge levels is therefore equal to the difference between the two levels, in this case, 17% of the force measured in the clean section.

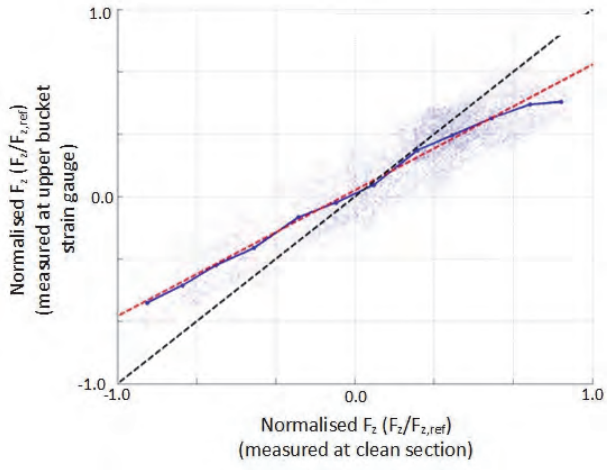

Figure 19. Bucket BC lower strain gauge response

As the surface area of the bucket skirt between the two strain gauge levels is approximately 69 m^2, a unit shaft resistance can be calculated by dividing the load dissipated between the two strain gauge levels by the relevant bucket surface area. Assuming a vertical force of 2500 kN measured at the clean section, which approximately corresponds to the predicted drained resistance of the suction bucket skirt, Table 3 provides an estimate of the unit shaft resistance based on the lower, mean and upper envelope of the measurements of forces at the strain gauges. Based on the back calculated unit shaft resistance values using the strain gauge measurements (Table 3), the unit shaft resistance is approximately 6 kPa. In the extreme case, taking readings from the Bucket BC 0° upper strain gauge and the Bucket AC 0° lower strain gauge, the unit shaft resistance is found to be approximately 16 kPa although this is considered unrealistically high based on the general trend observed.

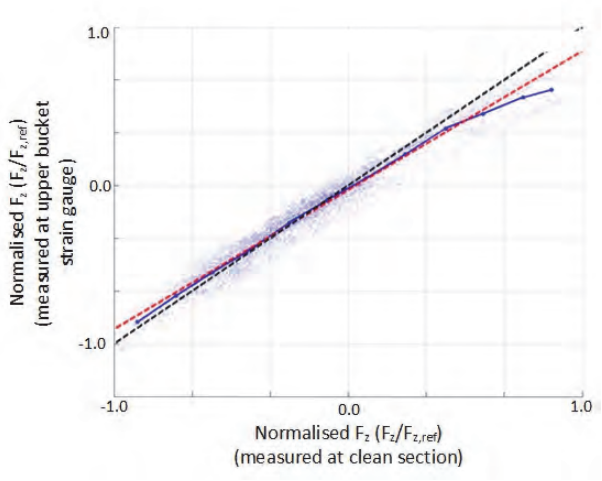

Figure 20. Bucket AC upper strain gauge response

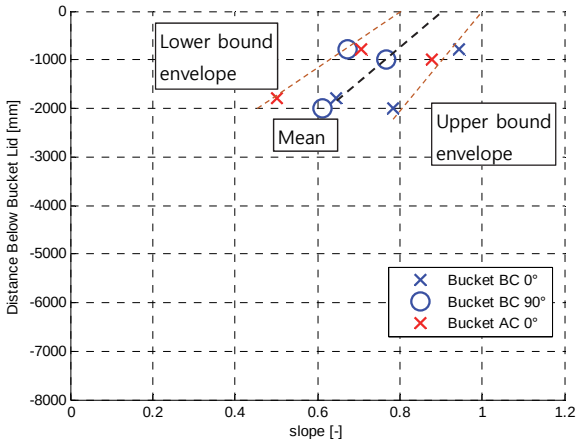

Figure 21. Slopes of skirt force versus vertical input force for all skirt strain gauges

For reference, the mean slope for the upper strain gauge level (at approximately 1m below the lid level) is 0.79 and the mean slope for the lower strain gauge level (at approximately 2 m below the lid level) is 0.64.

Table 3. Back calculated drained unit shaft resistances between strain gauge levels

Measurement value	Unit shaft resistance (kPa)
Lower envelope	5.9
Upper envelope	6.2
Mean	6.3

7.2 Comparison of measured values against calculated values

Assuming the fully drained conditions and the shaft capacity calculation method described by Tomlinson & Woodward (2008) for cohesionless soils, the unit shaft resistance for the BKR01 conditions can be estimated. Both sets of strain gauges are located within the shallowest soil unit identified (Table 2). Although this unit has a relatively high peak friction angle and relative density, the unit shaft resistance has been calculated using standard design approaches which takes the interface friction angle into account. Assuming an interface friction angle of 29° for sand with a mean particle size of 0.2 mm (Jardine et

al, 2005), a K_0 value of 0.8 (API, 2007) and an even distribution of shaft resistance between the inside and outside of the skirt, a drained unit shaft resistance of 6.9 kPa could be expected over the depth range being investigated. This is similar to that measured at BKR01 and indicates that drained unit shaft resistance values are likely to be appropriate on average. As the strain gauge measurements are taken close to the ground surface, OCR effects were not explicitly taken into account, although these have been used to justify a K_0 value considerably higher than the Jaky (1944) formulation.

7.3 Load distribution estimate using strain gauge measurements

Whilst the strain gauge measurements in Figure 21 show some degree of scatter, these provide a useful estimate of the general load distribution between the skirt and bearing under the suction bucket lid. Although extrapolation of the trends below the lower strain gauges is considered inappropriate, extrapolation of the data to the bucket lid is considered acceptable as the strain gauges are located relatively close to the lid. By extrapolating the upper and lower bound envelopes to the lid level, the data in Figure 21 indicates that the load transferred from the clean section to the skirt walls may be between approximately 80% (lower envelope) and 100% (upper envelope), the latter implying that the load from the structure is completely transferred to the skirt.

These values are generalised across the entire load spectrum and can therefore only be considered approximate and load independent. As the strain gauge measurements are based on 10 minute average values, individual load cycles are not considered.

8 COMPARISON BETWEEN A 'CALM' PERIOD AND A STORMY PERIOD

Observations for a 'calm' period with wind speeds at or below the rated wind speed of the WTG (
Figure 22) are compared to observations from a stormy period (Figure 23) to assess if there is any variation in behaviour during these two periods. In
Figure 22 and Figure 23, the 10 minute average wind speed, wave height, pore pressure beneath the bucket lid and vertical bucket stiffness are plotted for several days with periods of operation and non-operation. The green shading indicates times of high electricity production and the unshaded areas indicate times of low electricity production.

8.1 Observations from a 'calm' period

During electricity production on a standard operational day where wind speeds at or below the rated wind speed of the WTG, the stiffness is relatively consistent. The stiffness becomes more scattered and appears to reduce during periods of low production, which is likely due to the lower loads leading to a higher signal to noise ratio. The stiffness recovers to approximately its original value when load is re-applied (during operation) and no stiffness degradation is observed.

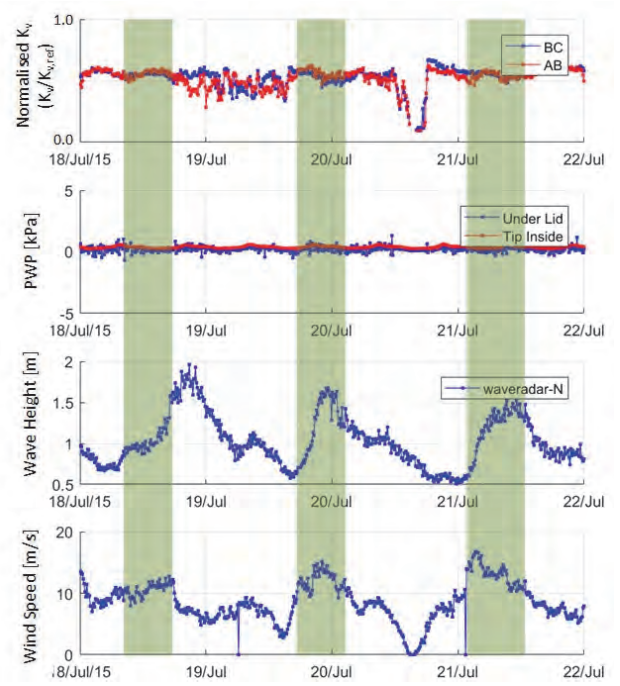

Figure 22. Observations from an average operational day

8.2 Observations from a stormy period

Similar patterns were observed for a 'stormy' day. During electricity production, the stiffness is relatively consistent and during periods of low production the stiffness becomes more scattered and typically appears to decrease. The stiffness recovers to its original value when load is reapplied (during operation) and no stiffness degradation is observed. In addition, no long term excess pore water pressures were generated during the storm. This result was expected as the long-term SBJ structural frequency has shown no measurable deviation since first power.

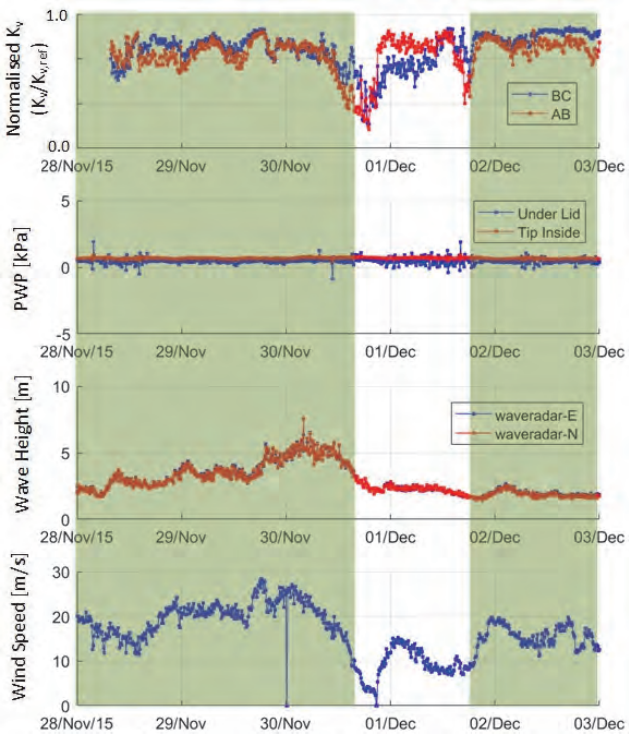

Figure 23. Observations from a stormy day

The correlation between vertical load and excess pore water pressure beneath the bucket lid is examined for a period during the peak of the storm (Figure 24). The dynamic component of the vertical pressure (vertical load minus mean load divided by bucket area) on the buckets is dominated by wave loads during the peak of the storm. The pore water pressure within the bucket (excess pore water pressure measured beneath the lid and at the inside of the skirt tip) takes a significant portion of the vertical pressure with a minimal phase shift. For fully undrained conditions, the excess pore water pressure response beneath the bucket lid and at the skirt tip (inside the bucket) should exactly match the vertical pressure applied to the bucket. However, Figure 24 shows that this is not always the case suggesting that some vertical pressure is unaccounted for, which as described in Section 7, may be due to the lid transferring some load to the bucket skirt or a number of other mechanisms. The excess pore water pressure is not completely be transferred between the lid and skirt tip levels. This might be due to the interaction between the bucket grout and skirt or due to the presence of the silt layer (described in Section 4) preventing the direct transfer of the excess pore water pressure down the skirt.

In addition, observations from Figure 24 indicate that the frequency and duration of the load has an effect on the excess pore water pressure response. For example, the response for the peak load at 29 s and 58 s can be compared. For the peak at 29 s, which applies a relatively sinusoidal force over approximately 5 s, the response of the excess porewater pressure is directly linked to the increase in vertical force giving an almost a fully undrained response. For the peak at 58s, where the peak wave load is applied over approximately 1s and is preceded by a time of chaotic force application, the response of the excess porewater pressure is not linked during application of the peak load. This indicates that the frequency and duration of the load clearly influences the excess pore water pressure response.

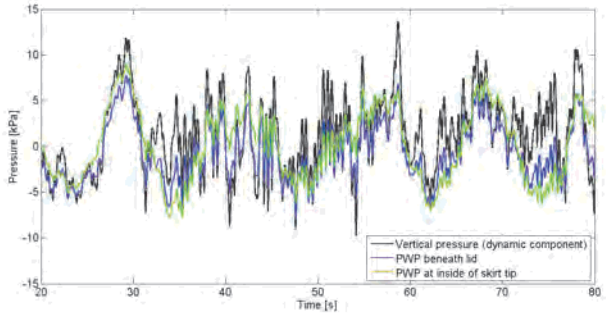

Figure 24. Time history of the vertical pressure and excess pore water pressure (denoted PWP) beneath the lid and at the inside of the skirt tip

To calculate the average amount of vertical pressure carried by the pore pressure for a select 10 minute period at the peak of the storm on 30 November, the area under the curve for each component was calculated using numerical integration. Over the 10 minute period, the pore pressure beneath the lid was estimated to carry 64% of the vertical pressure and the pore pressure at the skirt tip was estimated to carry 42% of the vertical pressure. These percentages would be considerably higher if the data was filtered to only include loads with a longer time period, such as those associated with large wave loads as observed at 29s in Figure 24.

9 DRAINAGE RESPONSE OF THE SUCTION BUCKET

If the variation in loading is sufficiently slow, the water beneath the bucket lid will have sufficient time to drain and the pressure inside and outside the bucket will equalise. Thus, no excess pore pressure will be generated and the vertical input force from the jacket leg will be taken by the soil-bucket interaction whereby the bucket is said to be responding in a drained manner. Conversely, if the loading on the bucket lid is sufficiently fast, the water beneath the bucket lid will not have sufficient time to drain. As the volume of water is constant and assumed incompressible, excess pore pressure will be generated creating a pressure difference across the bucket lid leading to undrained conditions and significant additional capacity.

A key assumption of suction bucket design for non-cohesive materials is that undrained conditions exist if the loading is sufficiently fast. For pull out capacity, this has been extensively investigated and shown to be significant (Tjelta, 1994; Houlsby *et al.*, 2005; Achmus & Thieken, 2014; Thieken *et al.* 2014).

In this section, the force transferred from the jacket leg (through the clean section) to the pore pressure inside the suction bucket is investigated for the entire data set to determine under what loading conditions the bucket behaves in a drained or undrained manner. The pore pressure beneath the lid acts on the bucket lid to resist the vertical input force from the jacket leg, however it is difficult to distinguish the portion of load acting through the lid due to the rigidity of the lid.

9.1 Typical examples of undrained responses

An example of bucket input force (F_z) compared to the excess pore water pressure (converted back to a force, denoted FWP) beneath the lid during a period of well correlated short term undrained behaviour is shown in Figure 25. The water beneath the lid takes a significant portion of the high frequency input load with a minimal phase shift. The mean load and the mean excess pore pressure are also approximately equal (near 0 kN). The force not resisted by the pore pressure is assumed to be distributed to other resistance mechanisms such as skirt friction, skirt tip resistance, lid plug contact and damping.

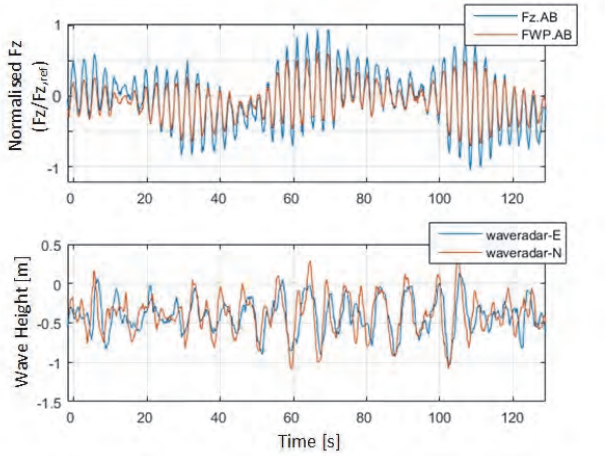

Figure 25. Example of bucket responding to loading in an undrained manner

Examining the time history in Figure 25, the cyclic loading frequency acting upon the bucket is approximately 0.3 Hz which is close to the 1P frequency of the structure (Harte et al., 2012), indicating that the loads presented in Figure 25 are dominated by the wind loads acting on the RNA (hence the zero mean) and not the wave loads which would be expected to have a lower frequency.

Figure 26 shows another example of bucket input force compared to the excess pore water pressure beneath the lid during a period with a non-zero mean input load. In Figure 26, the excess pore pressure reacts to each individual cycle in an undrained manner (the excess pore water pressure response and

the load response are aligned but at different absolute magnitudes) and the long term (steady state conditions) mean is zero. However, some excess pore water pressure is generated between 150 s and 250 s as the mean load shifts from a normalised mean load ($F_z/F_{z,ref}$) of 0.5 to -0.5 (also normalised to the mean dead load). Steady state pore pressure conditions are only re-established after approximately 100s. Thus, the drainage period for this example is approximately 1.5 minutes.

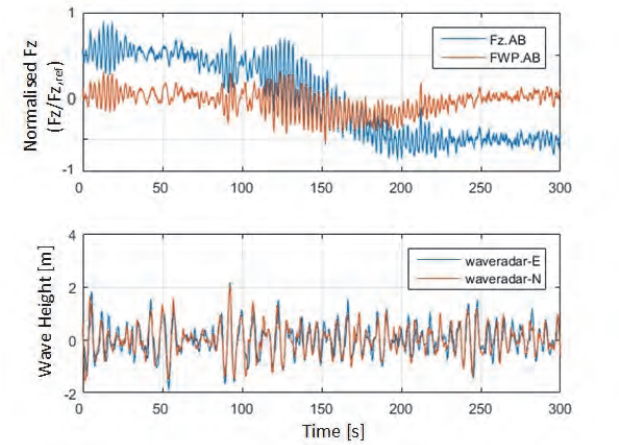

Figure 26. Example of bucket responding to loading in a drained manner

9.2 Drainage analysis

In order to estimate the suction bucket drainage response at different times during the monitored period, a more detailed analysis of the drainage conditions was required, which can be applied across the entire data set. To do this, the input force and excess pore water pressure (beneath the bucket lid) were converted from the time domain to the frequency domain and their coherence examined.

9.2.1 Drainage analysis methodology

For the undrained case, where there is assumed to be no flow in or out of the bucket, the pore pressure resistance force (F_{WP}) will take some proportion (K) of the bucket input load (F_z) as follows:

$$\dot{F}_{WP,undrained} = K \cdot \dot{F}_z \quad (4)$$

Where the first-time derivative is denoted by the dot. For the bucket to drain, water within the bucket must flow through the seabed into or out of the bucket, as idealised in Figure 27.

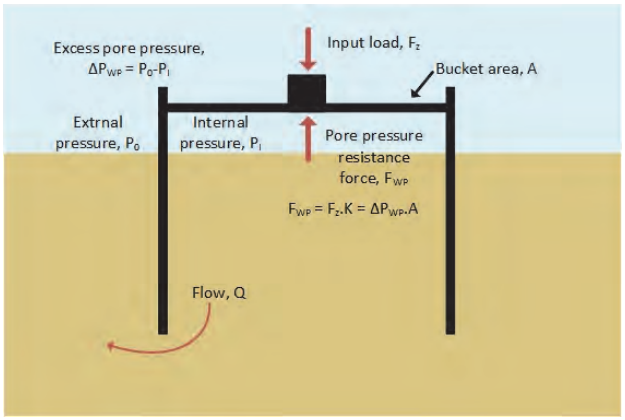

Figure 27. Model of flow around a bucket during loading

The proportion of load (K, also denoted as 'Gain' in Section 9.3) and drainage time affect the rate of resistance. This resistance is due to the generation of excess pore water pressure which can be combined in the following differential equation:

$$\dot{F}_{WP} = K \cdot \dot{F}_z - \frac{1}{\tau} \cdot F_{WP} \quad (5)$$

Where τ is a time coefficient and F_{WP} is the resistance force due to the generation of excess pore water pressure. The time scale on which the bucket's F_{WP} transitions between drained and undrained response can be gauged by plotting the transfer function between the input load and the bucket's F_{WP} as follows:

$$H(j\omega) = \frac{F_{WP}(j\omega)}{F_z(j\omega)} = \frac{j\omega \cdot K}{j\omega + 1/\tau} \quad (6)$$

The spectrum of the input load and the bucket's F_{WP} is estimated using a windowed fast Fourier transform (FFT) with a Hanning weighting function (Welch, 1967). The windows are taken with a 50% overlap and the resulting FFTs are averaged.

9.2.2 Drainage analysis for one day's data set

The data for a single day is given in Figure 28 and Figure 29. From Figure 28, it can be seen that the spectra of the vertical input load F_z and the pore pressure resistance force F_{WP}, are similar at high frequencies but diverge as the frequency drops. At short periods, lower than about 2 minutes, the excess pore water pressure resists a consistent proportion of the input load, showing the undrained response of the bucket. While at longer periods, the ratio between the spectra decays.

The transition between drained and undrained response is highlighted in grey. At very long periods, greater than about 20 minutes, the pressure force does not resist much of the input load, showing the drained response of the bucket. For periods around 5 s to 15 s (highlighted with blue shading), there appears to be a peak in the transfer function. As seen in the wave height spectrum (denoted 'eta' in Figure 28), this region contains wave energy. As the waves pass over the bucket, the static head pressure outside the bucket changes and the coherence between input load and excess pore water pressure decreases. This indicates that energy is being added to the excess pore water pressure response in this frequency range. The increased coherences between the excess pore water pressure and the wave height also indicates that energy is being added to the excess pore water pressure spectrum. Results from this frequency are considered unrealistic. Therefore, when trying to fit a transfer function between the input force and the excess pore water pressure, this portion of the transfer function should be excluded. This is shown in Figure 29 where it is clear that the fitted function does not take this frequency range into account.

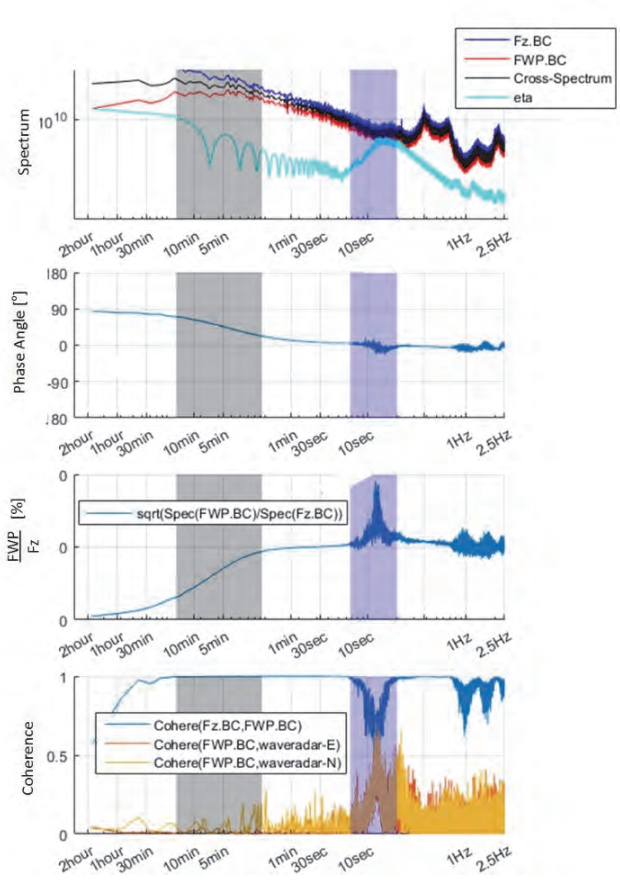

Figure 28. Spectrum of input load and excess pore water pressure beneath the lid for the analysed day

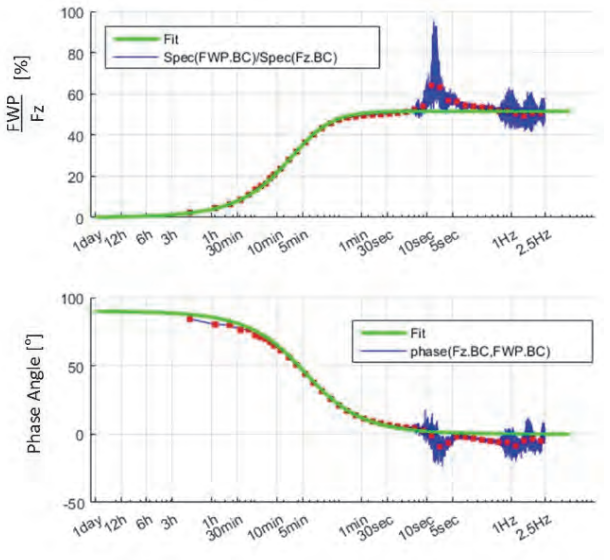

Figure 29. Best fit transfer function for the analysed day

The resulting model parameters for this period were K=0.516 and τ=45 s which is shown to fit the transfer function well (Figure 29). However, it should be noted that these values are only for one day of data.

9.3 Drainage analysis for the entire data set

The analysis described in Section 9.2 was repeated for all the available data to quantify time scales at which the transition between the drained and undrained response occurs. A histogram of the gain (K) and time constant (Eq. 5) for all the available data for Buckets AB and BC is given in
Figure 30.

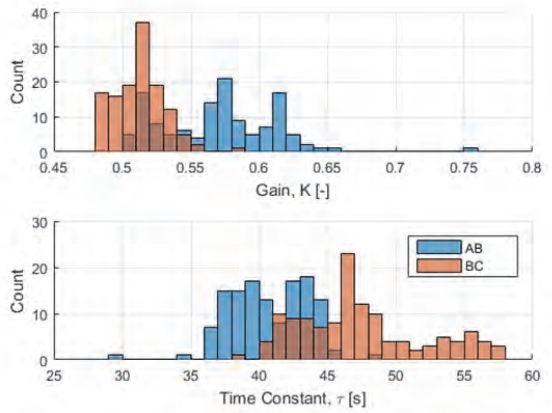

Figure 30. Model parameter fit results distribution

Figure 30 shows that the Buckets AB and BC exhibit different drainage characteristics, with the drainage at each bucket expected to be affected by the site specific soil conditions at each bucket and the bucket loading history. On average, Bucket AB experiences higher compressive loads than Bucket BC which may explain the higher gain observed. During undrained loading the gain for Buckets AB and BC varies from approximately 0.45-0.65, thus on average the pore pressure is carrying between 45-65% of the load transferred through the bucket clean section. A similar result was found for the November 30th 10 minute storm time history assessed in Section 8.2.

Examining the entire data set for both buckets, the determined average thresholds between the drained and undrained response are given in Table 4.

Table 4. Thresholds between drained and undrained regions

Drained	Partially Drained	Undrained
T > **46 min**	> T > **2.5 min**	> T

The undrained region is defined as the regions for which the transfer function is greater than 90% of the gain (K) and conversely the drained region is defined as the region for which the transfer function is less than 10% of the gain. The partially drained region is taken as the region where the transfer function is between the two thresholds. These results show that the buckets are undrained at relatively low frequencies compared to what is typically assumed in design of suction buckets in non-cohesive strata. This is most likely due to the site specific soil conditions, in particular, the silt layer described in Section 4.

10 CONCLUSION

The BKR01 SBJ, installed in 2014 in collaboration with Carbon Trust OWA program, is the first SBJ to support a WTG. An extensive monitoring system installed on the SBJ has provided an insight into the behaviour of the suction buckets during different loading conditions.

The vertical stiffness response of the buckets was shown to be dependent on the wind direction and the load level. The assumption that the average total bucket vertical stiffness response can be represented by a system of springs in series was confirmed, verifying an important design assumption. It was also

shown that the vertical stiffness response is influenced by mean load level with a distinct vertical stiffness increase of between 10 and 20% when the mean load was increased. The suction bucket response showed a typical non-linear response at low compressive load levels (high tensile live loads) confirming previous research in this area.

The strain gauge readings showed that the measured unit shaft resistance was within the expected range when compared with traditional shaft capacity hand calculations. The readings also indicated that the load transferred from the clean section to the skirt walls may be between approximately 80% and 100%, for drained loading conditions.

After comparing the results from a 'calm' period (wind speeds at or below the rated wind speed of the WTG) with a 'stormy' period, an investigation of the pore pressure response to loading was presented. Transforming the data to the frequency domain, it was found that on average, loading frequencies faster than 2.5 mins led to undrained behaviour, loading frequencies slower than 46 mins were fully drained and loading frequencies in between were partially drained. It was also found that the drainage characteristics varied from Bucket AB to Bucket BC most likely due to the site specific loading conditions and ground conditions at each bucket.

Overall, analysis of the data from the comprehensive monitoring system installed on the BKR01 SBJ has provided a significant insight to the behaviour of suction bucket jackets subjected to wind and wave loading in the North Sea. The in-situ observations from a world-first full scale monitoring system are likely to inform future offshore windfarm developments where SBJs are utilised as the foundation solution.

11 ACKNOWLEDGEMENTS

The authors would like to acknowledge the many contributions made by their colleagues at DONG Energy especially from Mrs Annelies Vanstraelen and Dr. J Schupp. The authors would also like to acknowledge the contributions made by Mr Stephen Suryasentana from the University of Oxford.

The BKR01 SBJ project was undertaken in collaboration with the Carbon Trust Offshore Wind Accelerator program and DONG Energy acknowledges the contributions made to the project by the entire Carbon Trust team.

12 REFERENCES

Achmus, M., and Thieken, K., 2014. Numerical Simulation of the Tensile Resistance of Suction Buckets in Sand. *Journal of Ocean and Wind Energy*, 1(4), pp. 231–239.

American Petroleum Institute, 2007. *API Recommended Practice for Planning, Designing and Constructing Fixed Offshore Platforms – Working Stress Design, API RP 2A WSD*. API Publishing Services, Washington DC, USA.

Aghakouchak, A., 2015. *Advanced laboratory studies to explore the axial cyclic behaviour of driven piles*. PhD thesis, Imperial College London, London, UK.

Bye, A., Erbrich, C., Rognlien, B. and Tjelta, T.I., 1995. Geotechnical design of bucket foundations. *Offshore Technology Conference*. Houston, Texas, USA, May 1-4.

Byrne, B.W. and Houlsby, G.T., 2002. Experimental investigations of response of suction caissons to transient vertical loading. *Journal of Geotechnical and Geoenvironmental Engineering*, 128(11), pp.926-939.

Dekker, M.J., 2014. *The Modelling of Suction Caisson Foundations for Multi-Footed Structures*. Norwegian University of Science and Technology.

Doherty, J.P., Houlsby, G.T. and Deeks, A.J., 2005. Stiffness of flexible caisson foundations embedded in nonhomogeneous elastic soil. *Journal of geotechnical and geoenvironmental engineering*, 131(12), pp.1498-1508.

Ehrmann, A., Penner, N., Gebhardt, C.G. and Rolfes, R., 2016. Offshore Support Structures with Suction Buckets: Parameter Fitting of a Simplified Foundation Model. *In The 26th International Ocean and Polar Engineering Conference. International Society of Offshore and Polar* Engineers. Rhodes, Greece, June 26–July 2 2016.

Erbrich, C.T. and Tjelta, T.I., 1999. Installation of bucket foundations and suction caissons in sand-geotechnical performance. *Offshore Technology Conference*. Houston, Texas, USA, May 3-6.

Harte, M., Basu, B. and Nielsen, S.R., 2012. Dynamic analysis of wind turbines including soil-structure interaction. *Engineering Structures*, *45*, pp.509-518.

Houlsby, G.T., Kelly, R.B. and Byrne, B.W., 2005. The tensile capacity of suction caissons in sand under rapid loading. *In Proceedings of the international symposium on frontiers in offshore geomechanics*, Perth (pp. 405-410).

Houlsby, G. T, 2014. "Interactions in Offshore Foundation Design." 54th Rankine Lecture. Imperial College London, UK. 19 March 2014.

Jaky, J., 1944. The coefficient of earth pressure at rest. *Journal of the Society of Hungarian Architects and Engineers*, 78(22), pp.355-358.

Jardine, R., Chow, F., Overy, R. and Standing, J., 2005. *ICP design methods for driven piles in sands and clays*. London: Thomas Telford.

Sparrevik, P. & Strout, J. M., 2015. Novel monitoring solutions solving geotechnical problems and offshore installation challenges. *In Proceedings of the international symposium on frontiers in offshore geomechanics*, Oslo (pp. 319-324).

Suryasentana S.K., Byrne B.W., Burd H.J., Shonberg A., 2017. Simplified model for the stiffness of suction caisson foundations under 6 dof loading. *Offshore Site Investigation & Geotechnics (OSIG) International Conference*, London, UK, Sept 12-14.

Sturm, H. 2017. Design aspects of suction Caissons for offshore wind turbine foundations. *In Proceedings of TC209 Workshop (Foundation design of offshore wind structures): 19th International Conference on Soil Mechanics and Geotechnical Engineering*, Seoul, South Korea, 20 September.

Thieken, K., Achmus, M. and Schröder, C., 2014. On the behavior of suction buckets in sand under tensile loads. *Computers and Geotechnics*, 60, pp.88-100.

Tjelta, T.L., 1994. Geotechnical aspects of bucket foundations replacing piles for the Europipe 16/11-E jacket. *Offshore Technology Conference*. Houston, Texas, USA, May 2-5.

Tjelta, T.I., 1995. Geotechnical experience from the installation of the Europipe jacket with bucket foundations. *Offshore Technology Conference*. Houston, Texas, USA, May 1-4.

Tomlinson, M.J. and Woodward, J. 2008. *Pile design & construction practice*. 5th ed. London: Taylor and Francis.

Welch, P., 1967. The use of fast Fourier transform for the estimation of power spectra: a method based on time averaging over short, modified periodograms. *IEEE Transactions on audio and electroacoustics*, 15(2), pp.70-73.

Wroth, C.P. and Houlsby, G.T., 1985. Soil mechanics-property characterization and analysis procedures. *Proceedings of the 11th International Conference on Soil Mechanics and Foundation Engineering*. San Francisco, USA. Vol. 1.